The University Of Sheffield.

Investigating Through Multiple Experimental Approaches How Early Visual Circuit Functions Affect *Drosophila* Behaviour

By:

Sidhartha Anil Dongre

A thesis submitted in partial fulfilment of the requirements for the degree of Doctor of Philosophy

The University of Sheffield
Faculty of Science
Department of Biomedical Science

30-June-2015

Acknowledgements

Firstly, I start with my parents – Dr's Anil & Shubha Dongre. Without their continuous support and advice during my life this would never have come to be. I am forever grateful. Congrats too, to my Brother Chetan and Sister-in-Law Alex, married two years ago and now with little baby Micah! I can't forget my little sister either, not so little anymore. Wishing you much fun with your brethren, i.e. those monkeys!

Also a special 'Thank You' to Sarah. For being with me through the gamut of experiences and emotions we have had together over the last, almost 4 years. It's your turn next!

Mikko, since the beginning your no-nonsense take on life has helped me to de-clutter. Thanks for your guidance and for the opportunity to embark upon this PhD. The almost-constant football chatter and speculation has been great procrastination; hopefully with a couple of signings we can be on an even footing again next season!

To my fellow lab members past and present; Florence, Diana, An, Xiaofeng, Zhuoyi, David, Olivier, Jouni & Uwe. Each of you has contributed positively to my life for the past four years, thanks for the help, the conversation and for easing the difficult times, of which there have been many over the years!

Thank you to my advisors, Professor David Grundy, Dr. Anton Nikolaev and to Professor Ian Meinertzhagen, Dorota Tarnorgoska and colleagues at Dalhousie in Halifax, Canada all of whom provided key assessment, training and advice.

And finally, thank you to my good friends Craig & Dom. Our rural, and sometimes urban, getaways have been a greatly appreciated escape from daily life; here's to many more!

My final thoughts go out for Professor Matti Weckström, who suddenly and sadly passed away prior to my final submission.

Abstract

Drosophila melanogaster has become a versatile model organism, with high genetic tractability and ease of manipulability, mixed with low cost and low space constraints. Genetic tools with which to modify flies in myriad ways are constantly developed and updated, whilst physical tools have also become more apt for access to various biological systems. In this thesis I have used several such tools, such as the Drosophila flight simulator, High Pressure Freezing and Transmission Electron Microscopy to test visual behaviour and synaptic function, respectively.

In *Drosophila's* early visual system, R1-R6 and R7/R8 information channels carry visual information to the visual brain. These channels have been thought separated on the basis of their structure and function, however it is our hypothesis that these channels can functionally inform each other and that this occurs at an early stage of the visual pathway. Here I have used the flight simulator to show that the absence of 'chromatic' photoreceptors adversely affects visually-driven optomotor behaviour. In conjunction with other electrophysiological data, I have helped to support the idea that this influence may result from functional connection between R1-R6 and R7/R8 photoreceptors.

Similarly, I have used the flight simulator to show that Ca^{2+}-activated K^{+} channel mutations in post-synaptic Large Monopolar Cells can affect visual behaviour, but that these effects are often managed by homeostatic mechanisms that serve to maintain biologically-relevant function. Additionally, I have shown that the absence of dietary Polyunsaturated Fatty Acids can influence visual behaviour.

Pre- and post-synaptic information at Drosophila photoreceptor synapses has been shown to adapt in accordance with changing visual conditions. I used programmes of light- and

dark-adaptation, along with High Pressure Freezing and Transmission Electron Microscopy to test how these adaptations are translated at the synapse.

All of these conclusions are discussed alongside electrophysiological findings acquired from the early visual system.

Contents

Acknowledgements ..... - 3 -

Abstract ..... - 4 -

List of Abbreviations ..... - 9 -

List of Figures ..... - 10 -

General Introduction ..... - 10 -

Chapter 2 ..... - 10 -

Chapter 3 ..... - 10 -

Chapter 4 ..... - 11 -

Chapter 5 ..... - 11 -

Chapter 6 ..... - 12 -

Supplementary Figures ..... - 12 -

Investigating Through Multiple Experimental Approaches How Early Visual Circuit Functions Affect *Drosophila* Behaviour ..... - 14 -

1 General Introduction ..... - 14 -

1.1 The *Drosophila* Visual System ..... - 14 -

1.1.1 Structure ..... - 14 -

1.1.2 Phototransduction ..... - 19 -

1.1.3 Synaptic Transmission ..... - 21 -

1.1.4 Adaptation ..... - 26 -

1.2 *Drosophila* Behaviour ..... - 31 -

1.2.1 The Drosophila Optomotor Response ..... - 31 -

2 General Methods ..... - 33 -

2.1.1 Genetics ..... - 33 -

2.1.2 Electrophysiology ..... - 35 -

2.1.3 The Drosophila Flight Simulator ..... - 36 -

3 Colour, Motion & Optomotor Behaviour ..... - 38 -

3.1 Introduction ..... - 38 -

3.2 Methods ..... - 40 -

3.2.1 Drosophila Genetics ..... - 40 -

3.2.2 Flight Simulator ..... - 43 -

3.2.3 Motion Stimulus ..... - 44 -

3.2.4 Light Stimulus ..... - 44 -

3.3 Results ..... - 45 -
3.3.1 Wild-type Drosophila Optomotor Response ..... - 45 -
3.3.2 ninaE Variants ..... - 47 -
3.3.3 norpA Rescue Lines ..... - 49 -
3.3.4 'Transitional' Stimulus ..... - 50 -
3.3.5 Painted Ocellus ..... - 53 -
3.4 Discussion ..... - 55 -
4 The Vesicle Hypothesis; Adaptation States and Quantal Dynamics ..... - 60 -
4.1 Introduction ..... - 60 -
4.2 Methods ..... - 62 -
4.2.1 Adaptation & Fixation (Conventional Aldehyde-based) ..... - 63 -
4.2.2 Sectioning & Staining ..... - 64 -
4.2.3 Terminal Selection, Microscopy & Image Encoding/Blinding and Analysis ..... - 65 -
4.2.4 Image Analysis & Vesicle Selection Criteria ..... - 66 -
4.2.5 High Pressure Freezing & Automatic Freeze Substitution ..... - 67 -
4.3 Results ..... - 68 -
4.3.1 Conventional, Aldehyde Fixation ..... - 68 -
4.3.2 Selection Optimisation ..... - 71 -
4.3.3 Indiscriminate, Internal Vesicle Selection ..... - 72 -
4.3.4 High Pressure Freezing & Automatic Freeze Substitution ..... - 75 -
4.4 Discussion ..... - 76 -
5 Ca^{2+}-activated K^{+} Ion Channels and the Behavioural Response ..... - 83 -
5.1 Introduction ..... - 83 -
5.2 Methods ..... - 85 -
5.2.1 Drosophila Genetics ..... - 85 -
5.3 Results ..... - 86 -
5.4 Discussion ..... - 90 -
6 Dietary Polyunsaturated Fatty Acids and the Optomotor Response ..... - 95 -
6.1 Introduction ..... - 95 -
6.2 Methods ..... - 96 -
6.2.1 Drosophila Genetics ..... - 96 -
6.2.2 Flight Simulator ..... - 97 -
6.3 Results ..... - 97 -

6.3.1 Wild-type Oregon Red ..... - 97 -
6.3.2 Slow 45°/s Grating Rotation ..... - 98 -
6.3.3 Fast 180°/s Grating Rotation ..... - 99 -
6.4 Discussion ..... - 101 -
7 Concluding Remarks: ..... - 105 -
Supplementary Figures ..... - 107 -
Bibliography ..... - 108 -
Appendix – Published Manuscripts ..... - 124 -

List of Abbreviations

EMS – Ethyl Methane Sulfonate

TRP – Transient Receptor Potential

ERG – Electroretinogram

Rh_x – Rhodopsin

LMC – Large Monopolar Cell

UV – Ultra Violet

PIP_2 – Phosphatidylinositol 4,5-bisphosphate

IP_3 – Inositol Triphosphate

DAG – Diacylglycerol

PUFA – Polyunsaturated Fatty Acid

DGK – DAG Kinase

M – Metarhododpsin

ninaE - neither inactivation nor afterpotential E

norpA - no receptor potential A

PLC – Phospholipase C

GPCR – G-Protein Coupled Receptor

RNAi – RNA Interference

AC – Amacrine Cell

HPF – High Pressure Freezing

AFS – Automatic Freeze Substitiution

TEM – Transmission Electron Microscopy

GABA – Gamma-Aminobutyric Acid

NMDA – N-Methyl-D-Aspartate

ROR – Red-eyed Oregon Red

LNA – Linolenic Acid

List of Figures

General Introduction

Fig. 1.1 – Structure & function of the *Drosophila* eye.

Fig. 1.2 – Components and arrangement of Drosophila photoreceptors.

Fig. 1.3 – Organisation of *Drosophila's* visual pathways.

Fig. 1.4 – Overview of synaptic transmission.

Fig. 1.5 – Schematic models of synaptic transmission and modes of vesicle recycling.

Fig. 1.6 – Importance of gain regulation.

Fig. 1.7 – Photoreceptor voltage and quantum bump response characteristics at different mean background illumination levels.

Fig. 1.8 – LMC voltage and Histamine bump response characteristics at different stages of adaptation under repetitive naturalistic stimulation.

Fig. 1.9 - Photograph of a wild-type Drosophila, prepared for use in a traditional 'flight simulator'.

Chapter 2

Fig. 2.1 - Schematic representation of a traditional 'flight simulator'.

Chapter 3

Fig. 3.1 – Optomotor responses of Canton-S (green) and UV-Flies (purple), to 45^{o}/s grating rotation, illuminated by UV light (≈350-405nm).

Fig. 3.2 – Optomotor responses of UV-Flies lacking R7 & R8 (green) and flies with only R7 & R8 function remaining (purple). 45^{o}/s grating rotation, illuminated by UV light (≈350-405nm).

Fig. 3.3:

a) Optomotor responses of flies with only R1-R6 function, compared against Canton-S, UV-Flies and flies with only R7/R8 function remaining. 45 ^{o}/s grating rotation, illuminated by UV light (≈350-405 nm).

b) Optomotor responses of all norpA rescue flies, compared against Canton-S, flies with only R7/R8 function remaining and the summed responses of all norpA rescue flies. 45 ^{o}/s grating rotation, illuminated by UV light (≈350-405 nm).

Fig. 3.4 – UV-Fly optomotor responses to 45 ^{o}/s grating rotations are significantly larger than UV-Flies lacking R7/R8. Mean variance +/- SD.

Fig. 3.5 – Transitional optomotor response string of UV-Flies responding to UV light (≈350-405 nm, 4 s duration), followed by dimming UV light (6 s duration), followed by a period of amber illumination (≈560-620 nm, 4 s duration), then back to UV (4 s duration). 45 ^{o}/s grating rotation. Grey shading – SEM.

Fig. 3.6 – Transitional optomotor response string of Canton-S responding to UV light (≈350-405 nm, 3 s duration), followed by dimming UV light (4 s duration), followed by a period of amber illumination (≈560-620 nm, 6 s duration), then back to UV (3 s duration). 45 ^{o}/s grating rotation. Grey shading – SEM.

Fig. 3.7 – Means comparison for Transitional stimulus data in Figs 5 & 6. Means +/- SD.

Chapter 4

Fig. 4.1 - Example dark- & light-adapted photoreceptor terminals.

Fig. 4.2 - Comparison of stringent and indiscriminate selection process for conventionally-processed dark- & light-adapted photoreceptor terminals and associated vesicles.

Fig. 4.3 – Stringent test criteria. Data selected using very defined standards, e.g. high sphericity or contrast and non-overlapping profiles.

Fig. 4.4 – Indiscriminate test criteria. Data selected using looser standards, e.g. non-sphericity, lower contrast and overlapping profiles.

Fig. 4.5 – Final dataset. Vesicles selected using a more indiscriminate approach, resulting in the separation of two distinct groupings based around vesicle area and number.

Fig. 4.6 – Final dataset. Histogram of data in Fig. 3 showing distinct population means and distributions (df = 172, n = 174).

Fig. 4.7 - Example test images from initial HPF/AFS trials without light control.

Chapter 5

Fig. 5.1 - Wild-type, Canton-S optomotor responses to fast and slow grating rotations.

Fig. 5.2 - dSK;;dslo^{4} double mutant optomotor responses to fast and slow grating rotations.

Fig. 5.3:

a) dslo^{4} mutant optomotor responses to fast and slow grating rotations.

b) dslo^{18} mutant optomotor responses to fast and slow grating rotations.

Chapter 6

Fig. 6.1 - Wild-type ROR optomotor responses to fast and slow grating rotation with broadband illumination.

Fig. 6.2 – Optomotor responses to slow grating rotation with broadband illumination; from ROR, LNA-Diet and YF-Diet flies.

Fig. 6.3 – Optomotor responses to fast grating rotation with broadband illumination; from ROR, LNA-Diet and YF-Diet flies.

Fig. 6.4 – Mean optomotor responses to fast and slow grating rotation with broadband illumination, for the period 2.5-3 s, with SD; from ROR, LNA-Diet and YF-Diet flies:

a) Compared against themselves.

b) Compared against each other.

Supplementary Figures

Supp. Fig. 1 – Optomotor responses of Rh1, Rh3, Rh4 & Rh6 norpA rescue flies, each with painted ocelli. 45 ^{o}/s grating rotation, illuminated by broadband light (≈380-900nm).

Supp. Fig. 2 – Optomotor responses of Rh1 and Rh3 norpA rescue flies, compared against flies with only R7 & R8 function remaining, all with painted ocelli. 45 ^{o}/s grating rotation, illuminated by UV light (≈350-405nm).

Supp. Fig. 3 – Optomotor responses of Rh1 and Rh6 norpA rescue flies, each with painted ocelli. 45 ^{o}/s grating rotation, illuminated by amber light (≈560-620nm).

Supp. Fig. 4 – Optomotor responses of Rh1 and Rh6 norpA rescue flies, compared against Canton-S flies, all with painted ocelli. 45 ^{o}/s grating rotation, illuminated by red light (≈590-670nm).

Investigating Through Multiple Experimental Approaches How Early Visual Circuit Functions Affect *Drosophila* Behaviour

1 General Introduction

Organisms that navigate the world require sensory-neural systems to provide information regarding the state of the external environment, as it is relative to the navigator. As the world is often in a state of flux and an organism's priorities may change, these systems must be flexible to capture dynamic information. Through genetic evolution organisms can accrue optimal neural processing mechanisms that possess a direct relevance to their respective environmental niche, which Heisenberg & Wolf (1984) call "phylogenetic information". However, the collaboration between the environment and an organism's genes is indirect and is usually temporally remote. Therefore, such intermediate neural circuitry and resulting processing must be able to reflect the diversity present in the outside world and be subject to short-term changes that allow dynamic interaction with external phenomena.

1.1 The *Drosophila* Visual System

1.1.1 Structure

Dipteran vision is predicated upon the function of an externally arrayed set of optical facets, or ommatidia (**Fig. 1-1a**). Each is composed of a subset of 8 photoreceptors which project in neural superposition (Kirschfeld, 1967). Both the ommatidia and comprising photoreceptors are asymmetrically arranged in a fashion that allows the dissemination of

spatially similar visual information to common synaptic targets in the early visual brain (**Fig. 1-1b, c & d**). Such an arrangement enables the summation of photoreceptor responses for a specific stimulus, thus enhancing sensitivity without hindering spatial resolution.

The photoreceptors themselves are arrayed in stereotypical fashion across the eye, each unit based upon an outer ring of 6 photoreceptors (**Fig. 1-2a**), known as R1-R6 (Braitenberg, 1967), which express a single photopigment, and an inner pair of photoreceptors with tiered rhabdomeres, i.e. R7 &R8 (Trujillo-Cenóz, 1965). The latter pair express different subsets of photopigments, giving rise to a subset of photoreceptors (R7 yellow/pale & R8 yellow/pale) with a 70:30, yellow to pale ratio (Franceschini et al., 1981). R1-R6 photoreceptors express the Rh1 photopigment, which possesses a dual-peaked spectral sensitivity (Horridge and Mimura, 1975; McCann, 1972). R7 and R8 photoreceptors express combinations of Rh3 and Rh4 (Fryxell and Meyerowitz, 1987; Montell et al., 1987; Zuker et al., 1987), or Rh5 and Rh6 (Chou et al., 1996; Huber et al., 1997; Papatsenko et al., 1997), respectively.

Each photoreceptor possesses a distal, brush-like membrane specialisation that expresses the photo-sensitive pigments (**Fig. 1-2b**). There are approximately 30,000 of such microvilli, each thought to contain a unitary instance of the phototransduction machinery (Howard et al., 1987), which effectively forms a photon sampling unit (Song et al., 2012). Microvilli comprise highly folded structures known as rhabdomeres that in *Drosophila*, are 'open' and composed of separated structures. The open rhabdom structure serves to best exploit the amount of available photo-sensitive membrane, allowing each individual photoreceptor maximal exposure to light with the rhabdom acting like a light guide (Kirschfeld and Snyder, 1976), channelling light along its length and insulating adjacent ommatidia to enhance resolution.

In addition to the aforementioned photo-instable opsins, i.e. those whose structure and function are modified by interaction with light and that confer specific spectral sensitivities, there are also photo-stable screening pigments (**Fig. 1-2d**) whose structures are not altered but whose function is to 'insulate' individual ommatidia and the eye as a whole from the effects of extraneous, reflected light (Tomlinson, 2012). These pigments, stored in granules, migrate from the ommatidial periphery towards the rhabdomere in a light-dependent fashion (Kirschfeld and Franceschini, 1969), generating a 'pupillary' reflex and serving as an inaugural mode of light adaptation.

Further to these protective pigments, evidence suggested that a second class of modifying pigment may exist (Goldsmith et al. 1964; Kirschfeld et al. 1977; Vogt 1983), and that such pigments may act as dichroic filters, blue-shifting the spectral sensitivities of associated Rhodopsin photopigments. In fact, the short wavelength, U.V. sensitivity peak of Rh1 arises due to the co-expression of such an "accessory" sensitising pigment (Hamdorf et al., 1992; Kirschfeld et al., 1983), which can absorb light quanta, biophysically transferring energy to the opsin component, thus extending its functional range. R7 photoreceptors are also associated with a sensitising pigment that due to its positioning, affects both R7 and R8 function (Hardie and Kirschfeld, 1983; Hardie, 1977; Kirschfeld, 1979; Kirschfeld et al., 1978).

In parallel to the aforementioned specialisations, these subsets of photoreceptors are segregated not only on the basis of their relative photopigment expression and resulting variance in spectral sensitivity, but also in terms of their synaptic targets. Outer, R1-R6 photoreceptors project to Large Monopolar Cell (LMC 1-3) targets situated in the *lamina ganglionaris* (optic lamina), whilst the central R7 and R8 associate with multiple targets in the *medulla* **(Fig. 1-3c)**. The specific trajectories of these cells and their associated target areas have been systematically and intimately defined using serial electron microscopy, see

Meinertzhagen & O'Neil (1991) and Takemura et al. (2008). These studies elucidate a dense interconnectivity that allows for complex feed-forward, feedback and sometimes re-entrant information communication.

a)

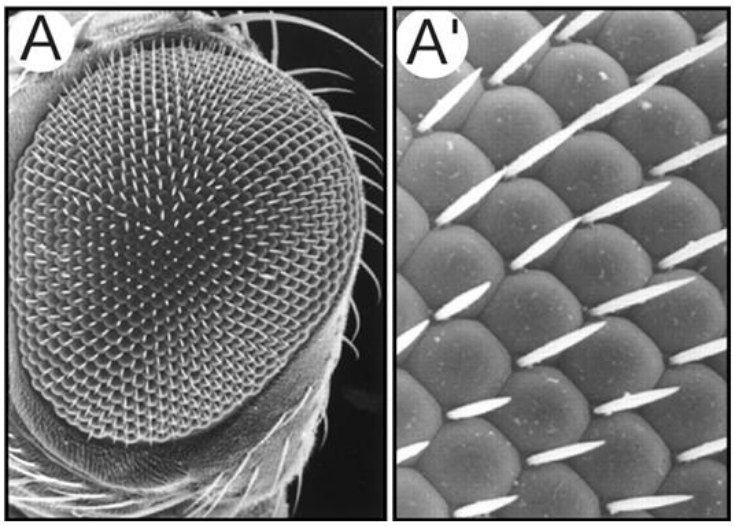

Adapted from Grzeschik & Knust (2005)

b)

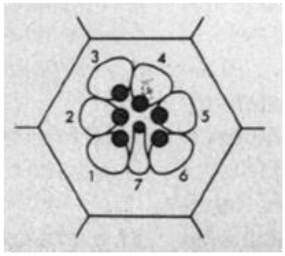

c)

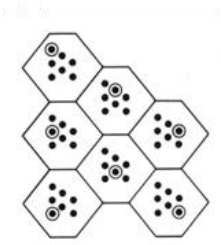

Adapted from Franceschini et al. (1981) and Kirschfeld (1967)

d)

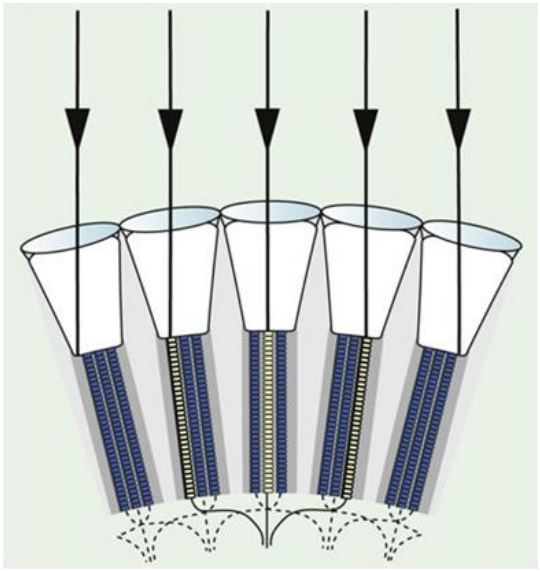

Adapted from Borst (2009)

Fig. 1-1 – Structure & function of the *Drosophila* eye:

a) Scanning electron micrograph of a wild-type *Drosophila* eye, A' shows and enlargement of the external surface, highlighting bristles and hexagonal ommatidia.

b) Schematic arrangement of R1-R7 photoreceptors and rhabdomeres. R8 will occur below R7.

c) Schematic showing asymmetrical arrangement of both adjacent ommatidia and photoreceptors. Circled photoreceptors receive spatially similar information and pool their respective outputs.

d) Schematic outlining the neural superposition principle, where information is pooled from photoreceptors receiving spatially-similar information.

a)

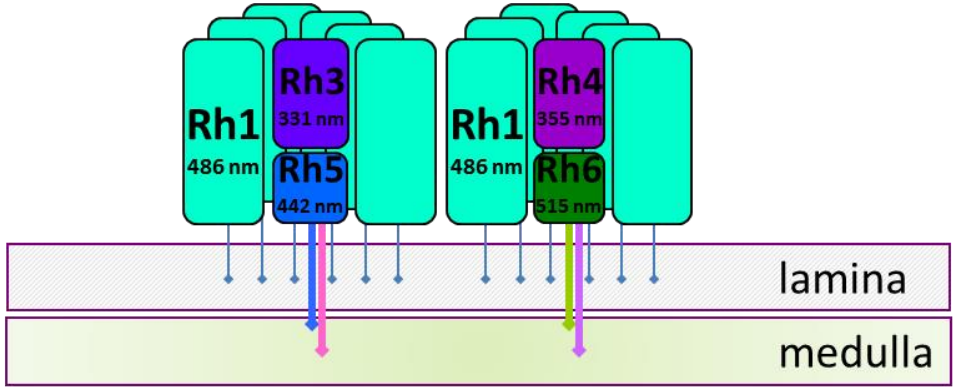

Adapted from Jackowska *et al.* (2007)

b)

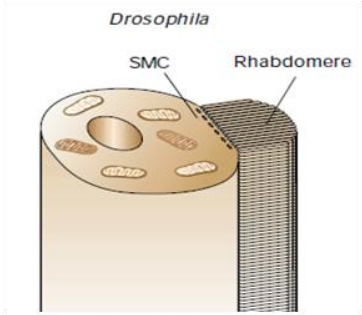

c)

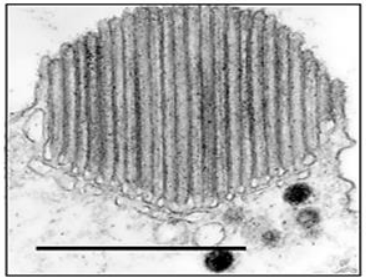

Adapted from Hardie & Raghu (2001)

d)

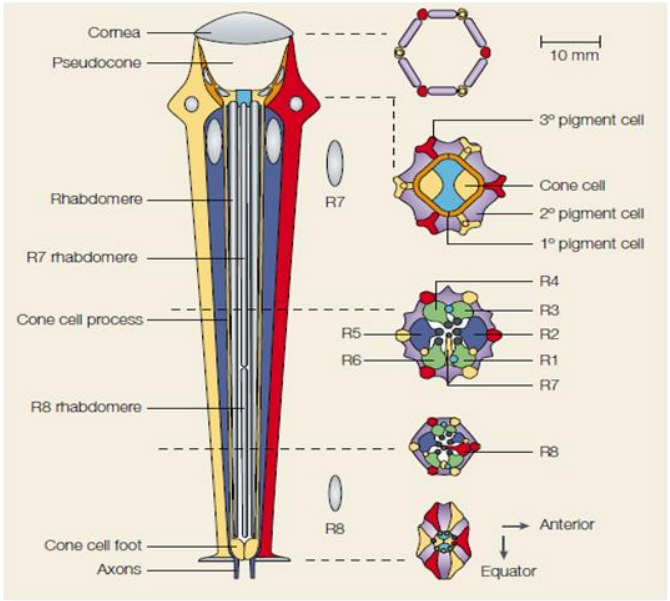

Adapted from Kumar (2001)

Fig. 1-2 – Components and arrangement of Drosophila photoreceptors:

a) Schematic outlining the concentric arrangement of R1-6 and pale-type and yellow-type R7/R8 photoreceptors, and their respective spectral sensitivities.

b) Schematic of the light-sensitive *Drosophila* photoreceptor rhabdomere. Sub-microvillar Cisternae (SMC) may subserve photopigment turnover.

c) Transmission electron micrograph of a photoreceptor rhabdomere. Stratified microvillar structure corresponds to the rhabdomere of a single photoreceptor. Scale bar = 1 µm.

d) Schematic showing an ommatidial profile and component cell types. Light entering at the cornea, is channelled down through the rhabdomere using the light-responsive pigment cells, interspersed between the photoreceptors.

Such apparent structural segregation and functional specialisation has fuelled the notion that fly motion and colour vision are conducted by separate channels (Strausfeld and Lee, 2009). Agreeing with this view are other solely functional studies on visual mutants such as Heisenberg & Buchner (1977) or Yamaguchi et al. (2008). Despite this long-standing ideology, there have been several relatively recent studies suggesting that this is not a "black and white" story (Gegenfurtner and Hawken, 1996; Schnaitmann et al., 2013).

In Wardill et al. (2012), using various techniques including intracellular electrophysiology, 2-photon Ca^{2+} imaging, modelling and behavioural assay, each of the photoreceptor classes and relevant sub-classes were tested to determine their relative contribution to motion vision. The paper conclusively showed that prior assumptions about the functional segregation of R1-R6 and R7/R8 channels were incorrect and that in fact, the two photoreceptor subsets share functionally- and behaviourally-relevant information at an early stage of vision. Some key findings of this paper are outlined and discussed in Chapter 1.

1.1.2 Phototransduction

Drosophila phototransduction (**Fig. 1-4a**) is initiated by receipt of a photon of light occurring with a relevant wavelength range at a corresponding photosensitive, G-protein linked Rhodopsin pigment molecule (Cowman et al., 1986; Zuker et al., 1985). This interaction leads to Rhodopsin photoisomerisation, a conformational change that produces an active, meta-Rhodopsin intermediate (M). The M configuration activates a subsequent $G\alpha_q$/Transducin-driven chemical cascade (Stryer et al., 1981), that eventually culminates in the activation of TRP and TRPL cation channels (Niemeyer et al., 1996; Reuss et al., 1997).

Downstream of Transducin, the phototransduction pathway progresses via the activation of Phospholipase C, which in turn cleaves the membrane-bound phospholipid PIP_2. Such a metabolic event generates two main products, IP_3 and DAG, but also results in the release of a proton thus producing a local acidification. These cleavage products possess a number of roles, i.e. IP_3 is known to facilitate the release of intracellular calcium from stores within the Endoplasmic Reticulum, whilst DAG has been shown to affect the activation of *Drosophila* eye Protein Kinase C (PKC – *inaC* gene), response inactivation and adaptation (Hardie et al., 1993; Smith et al., 1991).

Despite the mechanism of activation up to this point being relatively well characterised, the exact mechanism of TRP/TRPL channel activation is not fully understood. Both IP_3 and DAG are potential candidates for such a role. However, IP_3 mutants do not lack phototransduction (P Raghu et al., 2000), nor is IP_3 sufficient to activate TRPL channels in cell culture (Hardie and Raghu, 1998), whilst the involvement of DAG and its associated proteins has become a confusing and convoluted topic.

DAG is well known to activate *inaC*/PKC, though recent evidence has highlighted another role in phospholipid metabolism. DAG levels are regulated through phosphorylation by the action of DAG Kinase (DGK), encoded by the *rdgA* gene (Masai et al., 1993). Such phosphorylation, producing Phosphatidic Acid, allows DAG to be used as a substrate for re-generating PIP_2. Moreover, DAG may also be metabolised by the action of DAG Lipase, whose action upon DAG can produce Polyunsaturated Fatty Acid metabolites (PUFAs).

PIP_2 hydrolysis and DAG were implicated in TRPL channel activation (Estacion et al., 2001), and at the same time, a role for DGK function was also postulated (Raghu et al. 2000), as was the potency of certain DAG metabolites (Chyb et al., 1999). The effects of DAG and its metabolites have since been further implicated by using patch-clamp studies (Delgado and Bacigalupo, 2009; Delgado et al., 2014) with the latter study suggesting that DAG Lipase

inhibition does not affect TRP/TRPL channel activation, thus potentially ruling out the action of PUFAs.

As previously outlined, the immediate consequences of PIP_2 cleavage are PIP_2 depletion, the generation of IP_3 and DAG and acidification, of which depletion and acidification have been shown to activate TRP channels in patch configuration (Huang et al., 2010). Hardie & Franze (2012) explored such an avenue further by using atomic force microscopy and electrophysiology. They showed that photoreceptors generate light intensity-dependent contractions that are able to gate mechano-sensitive channels when ectopically expressed in dissociated photoreceptors that simultaneously lack light-sensitive channels. These findings stoked further the burgeoning idea that membrane contractility may be involved in channel gating and that PIP_2 depletion may play a role in such a phenomenon.

Taking these findings, and coupling them with techniques gleaned from other lipidomic investigations (Carvalho et al., 2012), Randall et al. (2015) reported on a multi-pronged approach showing that dietary PUFA restriction indeed results in reduced photoreceptor contractility, and that this is accompanied by a slowing of photoreceptor voltage responses and of visual perception also. Some of the findings of this paper are further outlined and discussed in Chapter 4.

1.1.3 Synaptic Transmission

Completion of the phototransduction cascade results in the generation of graded voltage potentials that themselves drive synaptic transmission, or the activity/voltage-dependent release and receipt of chemical signals across the synaptic cleft.

a)

b)

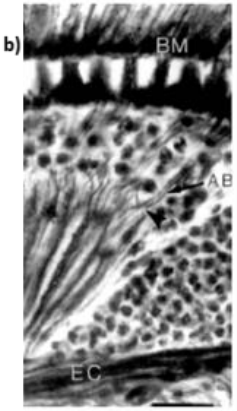

Adapted from Meinertzhagen & O'Neill (1991)

c)

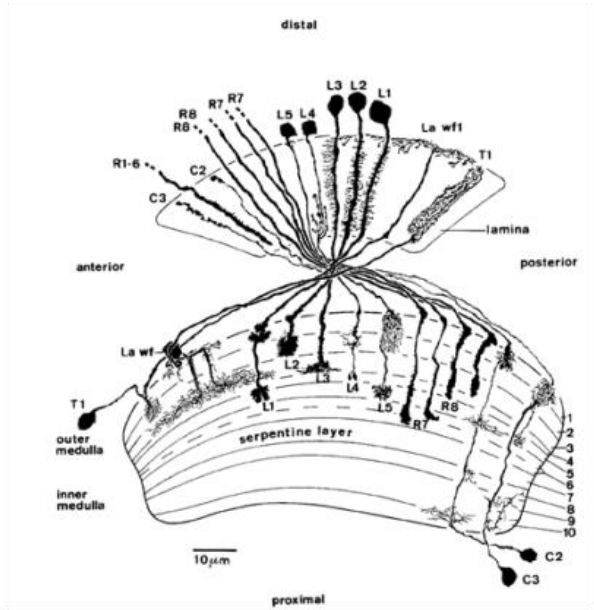

Adapted from Fischback & Dittrich (1989)

Fig. 1-3 – Organisation of *Drosophila's* visual pathways:

a) Scanning electron micrograph of a wild-type *Drosophila* optic lobe. R-retina, L – optic lamina, EC – external chiasm, M – medulla, IC – internal chiasm, LO – lobula, LP - lobula plate, AN – antennal nerve. Scale bar = 100 µm.

b) Inset enlargement through the optic lamina from a). BM – basement membrane, AB – axon bundles, EC – external chiasm. Scale bar = 10 µm.

c) Tracings of lamina and medulla cell types and their terminal strata, derived from Golgi staining. Also shown are the trajectories and terminii of R1-8 photoreceptors.

Histamine (Gengs et al., 2002) is released from vesicles in the pre-synaptic terminals of *dipteran* R1-R6 photoreceptors in a tonic (Uusitalo et al., 1995) and Ca^{2+}-dependent fashion. Histamine molecules diffuse across the cleft and interface with receptors at the post-synapse, ultimately producing a graded voltage response in L1-L3 LMC target cells (Jarvilehto and Zettler, 1971; Zheng et al., 2006) in the *Drosophila* visual lamina (Strausfeld, 1971).

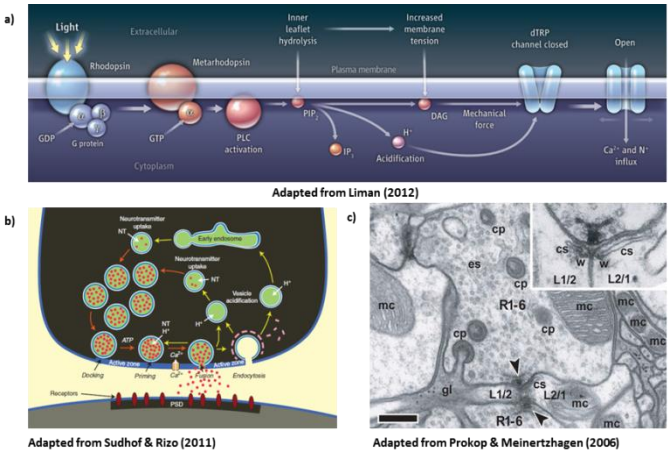

Fig. 1-4:

a) Schematic showing the basic events occurring during *Drosophila* phototransduction, with emphasis on the hypothesis that mechanical forces, generated during PIP_2 hydrolysis, may be responsible for TRP channel gating.

b) Generic pre-synaptic stages of synaptic transmission. Showing vesicle filling after budding from the early endosome, docking at the synaptic active zone, priming for release, then Ca^{2+}-dependent fusion and endocytic vesicle retrieval via an endosome.

c) Transmission electron micrograph showing connections between two R1-6 photoreceptors and the same L1/L2 LMC targets in the optic lamina (arrowheads). Inset shows detailed T-Bar synapse, which are optimised for high rates of synaptic transmission. Gl – glia, mc – mitochondria, es – endosome, cp – capitate projection, w – whiskers, cs – postsynaptic cisternae. Scale bar = 320 nm (150 nm for inset).

Synaptic transmission (**Fig. 1-4b**) is a highly regulated process, consisting of multiple phases that are co-ordinated by intracellular Ca^{2+} dynamics, see Südhof & Rizo (2011) for a review. Rates of exocytosis (vesicle release) and endocytosis (vesicle re-capture/generation) must be optimised to best reflect the input signal, but also to allow for its ongoing representation. Traditional theories of synaptic release have outlined a Clathrin-dependent exocytic process (**Fig. 1-5b**), where synaptic vesicles fully fuse with the plasma membrane, discharging their contents in their entirety (Heuser, 1973). Due to apparent constraints governing membrane depletion and the timing of vesicle recycling, this process had initially been deemed too slow (Ceccarelli et al., 1972). In this view, the traditional process would be unable to support the high rates of information transfer that the *Drosophila* retina is known to be capable of (Juusola et al., 1995b, 1996; Zheng et al., 2006).

This perceived need for optimisation of membrane retrieval has led to the proposition of several theories of synaptic vesicle exo-/endocytosis, one such theory being “kiss-and-run” (Ceccarelli et al. 1973; review - Harata et al. 2006). In parallel to full-fusion exocytosis, kiss-and-run employs partial vesicle fusion (**Fig. 1-5a**); where vesicle content can be retained, as can the vesicle membrane and its bound signalling structures, thus facilitating its re-use when needed. There have been reports of multiple modes of kiss-and-run (Gandhi and Stevens, 2003), using techniques ranging from conventional Transmission Electron Microscopy (Bartolomé-Martín et al., 2012), electrophysiological recording (Klyachko and Jackson, 2002), to live confocal microscopy with quantum dot-loaded vesicles (Zhang et al., 2009).

Despite the glut of supportive data, there have also been many dissenting voices. Examples include experimental discrepancies found to relate to the time course of endocytosis (Ryan et al., 1996). Questions have been raised considering the physical characteristics of the dyes and markers used for visualising fast membrane dynamics (Granseth et al., 2009), suggested to impinge upon normal vesicular fusion. And most recently, an innovative stimulation and fixation paradigm was developed by Watanabe et al. (2013), where they reveal a novel form of Clathrin-independent ‘ultrafast’ endocytosis in mouse hippocampal cells that can occur at speeds that far outstrip those of kiss-and-run (**Fig. 1-5c**). They went on to show the same process in *C. elegans* (Watanabe et al., 2013a), and also clarified the existence of an intermediate, large synaptic endosome, where Clathrin-coated vesicles can be regenerated after bulk endocytosis (Watanabe et al., 2014). Given these findings it is reasonable to explore alternative explanations as to how synaptic transmission can support high-rates of information exchange and the communication of highly-dynamic changes in photoreceptor voltage across the synapse. One such idea is that synaptic vesicle size may also be dynamically altered in response to varying environmental light conditions and that pre- and post-synaptic mechanisms may modify such communication.

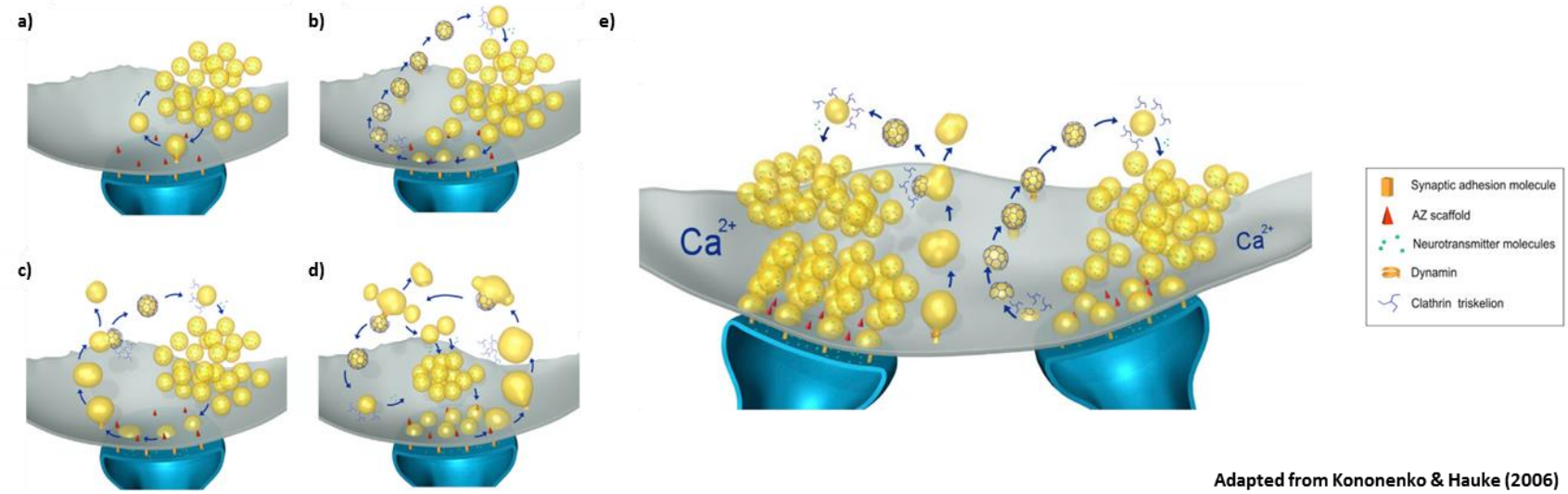

Adapted from Kononenko & Hauke (2006)

Fig. 1-5 – Schematic models of synaptic transmission and modes of vesicle recycling:

a) Kiss-and-run. Vesicles fuse and partially expel their contents in an activity-dependent fashion. Semi-filled vesicles recycle to the reserve pool before further incomplete fusion and release is initiated when necessary.

b) Clathrin-mediated endocytosis (CME). Vesicles fuse with the membrane and 'fully collapse', releasing all stored transmitter. Recycling occurs in a Clathrin-dependent fashion, returning coated vesicles to the pool for re-filling and re-use after vesicle uncoating.

c) Ultrafast endocytosis. Vesicles fully fuse with the membrane and recycle via the formation of a large endosome-like-vacuole (ELV). In a Clathrin-dependent fashion, vesicles bud from here to join the reserve vesicle pool after uncoating.

d) High-frequency stimulation can result in the generation of large endosomes, resulting from bulk endocytosis. From these, new vesicles are formed by both Clathrin-dependent and Clathrin-independent mechanisms.

e) Model based upon current flash-and-freeze data. Left - Vesicles fully fuse during high input rates. Vesicles recycle via ELV formation and re-generate in a Clathrin-dependent fashion. Right – Vesicles fully fuse and recycling occurs via a normal CME.

1.1.4 Adaptation

Sensory-neural apparatus are tuned to detect changes in the environment, however the range of possible detectable states can theoretically surpass the physical capabilities of the encoding machinery, leading to response saturation (Williams and Noble, 2007). The nervous system has evolved many adaptive mechanisms in an attempt to avoid this loss of information and reconcile the changing world with an intrinsic need for reliability (Nelson and Turrigiano, 2008).

Drosophila photoreceptor responses show a ≈50 mV range. Therefore, adaptive mechanisms must modulate their response gain, scaling mean activity levels in accordance with input levels so that extreme inputs do not become saturating (**Fig. 1-6**). Both the *Drosophila* photoreceptor and their LMC targets generate graded, macroscopic voltage responses (Juusola et al., 1995a). These integrated and adaptive (Juusola et al., 1995c) responses arise due to the summation of unitary voltage responses (quantum bumps) occurring at the rhabdomere (Henderson et al., 2000) and histamine-evoked voltage responses at the LMC post-synapse (Li, 2011).

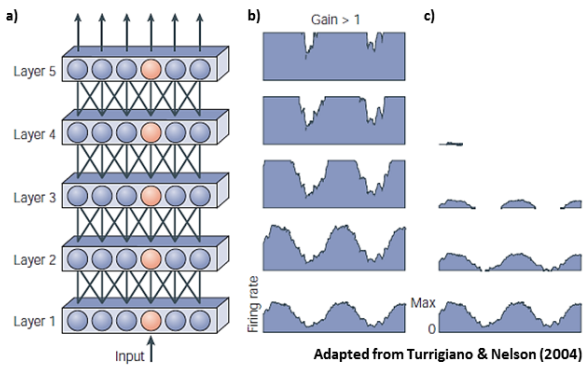

Fig. 1-6 – The importance of gain regulation:

a) Schematic, hypothetical feed-forward network, where input follows the 'red' pathway.

b) Red neuron firing rates in the corresponding layer, where gain is >1. Communicated signals are amplified to saturation with increasing propagation through each node, thus high frequency and low amplitude signal components will eventually be masked.

c) Corresponding red neuron firing rates where gain is <1. Communicated signals diminish with subsequent propagation events, ultimately resulting in failed transmission and loss of the signal.

Juusola & Hardie (2001a) studied adaptation in photoreceptor voltage responses and the unitary events of which they are comprised (**Fig. 1-7**). They systematically characterised the effects of dynamic broadband ("white-noise") stimulation at varying background light

intensities. These data indicated that photoreceptor voltage signals adapt positively with incremental light intensity, whilst signal noise appears inversely correlated. This illustrates the idea that *Drosophila* photoreceptors must find a way of elevating the representation of actual inputs above the level of system noise at low light levels. They also show that quantum bump size and latency reduce with increases in light levels. Conversely, on average quantum bump information content is least in dim conditions, however it is likely that the information per quantum bump may be higher at lower light intensities as more light means there are less available sampling units overall, thus a mid-level light stimulus may better allow faithful representation of highly dynamic input information.

Further to this, with increasing background illumination photoreceptor voltage responses appeared more closely tied to the timing of the stimulus, they lasted less long and response dynamics could modulate more often. The latter data together imply that visual information is potentially best encoded by smaller, shorter bumps, as these can usefully inform voltage-based representations at higher frequencies during bright conditions. A sister paper, Juusola & Hardie (2001b), elaborated upon these findings and showed that photoreceptor voltage responses can be further refined by the physiological temperature of the organism.

Nikolaev et al. (2009) and Zheng et al. (2009) went on to demonstrate the sign-inverted effects of persistent stimulation upon the voltage responses of LMCs (**Fig. 1-8**). Together these papers show that both *Drosophila* photoreceptors and LMCs dynamically reduce their response latencies, and that this aids temporal encoding at varying mean light levels. These data also help support the premise that adaptation in these visual components is necessary to overcome basal noise and that such cells can modify their dynamic voltage range to better represent persistent and temporally varying information.

In Li (2011), analysis of LMC voltage noise afforded further insight into the existence of quantum bumps at the *Calliphora* LMC post-synapse. By exposing preparations to a prolonged, saturating light pulse (6s), one can induce the compensatory activation of Na^+/K^+-exchange pumps that attempt to re-balance the now-heavily skewed ionic equilibria. This process results in a large hyperpolarisation of the photoreceptor voltage; thus negating tonic synaptic transmission and indicating a period of synaptic silence that is also reflected in the voltage response of LMCs (Uusitalo and Weckström, 2000; Uusitalo et al., 1995). The remaining voltage dynamics are thought to correspond to intrinsic synaptic noise and that arising due to the experimental set-up. This can then be subtracted from measurements taken in dark conditions; a process which is thought to reveal the minimal average voltage responses (possibly composed from responses to individual vesicle release from tens of histamine receptor openings), i.e. postsynaptic histamine bumps. Analysis of these proposed LMC bumps has exposed adaptational trends which show similar characteristics to microvillar quantum bumps in photoreceptors, i.e. responses get smaller and shorter with increasing light levels (**Fig. 1-8e**).

Given that macroscopic photoreceptor/LMC voltage responses and the summed quantum/histamine-induced bumps upon which they are founded, both adapt in the face of changing light intensities, it is therefore natural to conclude that co-ordination of these phenomena must be communicated through the synapse. In Chapter 2 I use light- and dark-adaptation protocols, in conjunction with conventional Transmission Electron Microscopy, in order to ascertain whether activity influences synaptic vesicle size in the *Drosophila* retina. These analyses were conducted on slices obtained from the visual laminae of wild-type flies that were raised as normal, but subjected to either saturating light or complete darkness prior to fixation.

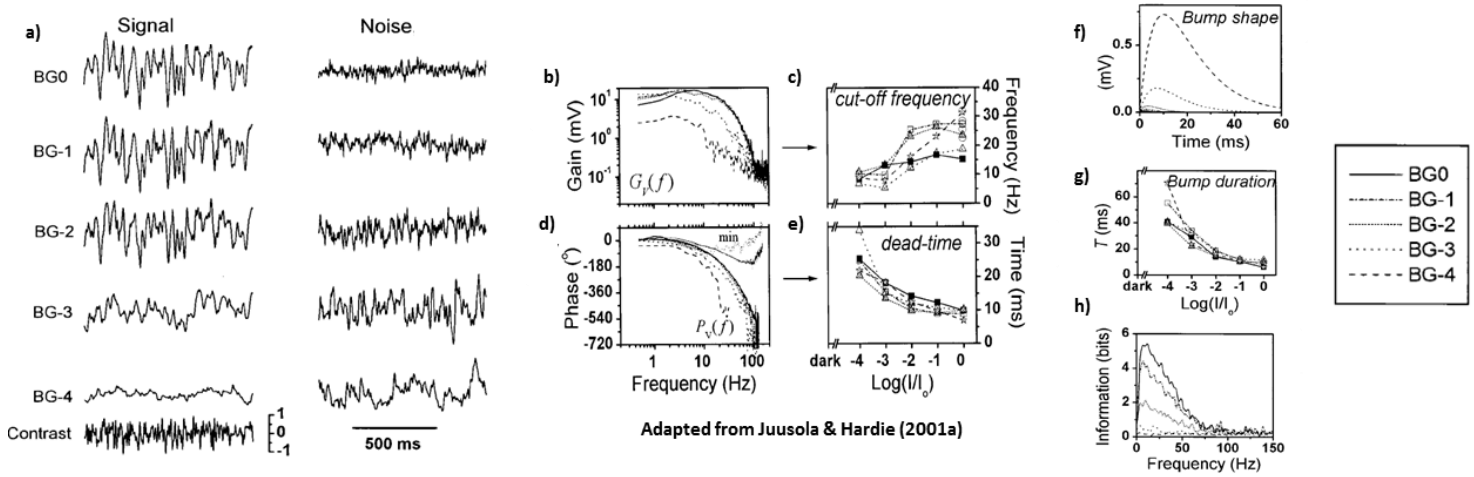

Fig. 1-7 – Photoreceptor voltage and quantum bump response characteristics at different mean background illumination levels:

a) Average intracellular photoreceptor signal and voltage noise comparison at 4 different mean backgrounds (green LED, each ~1 log unit apart, reducing in intensity from BG0 to BG-4). Average photoreceptor voltage responses are larger and voltage noise is comparatively less at high mean light intensities, the converse is true at low mean light levels.

b) Voltage signal gain increases in size with increasing mean light backgrounds.

c) The cut-off frequency is higher at higher mean light backgrounds, though at lower background light levels it is possible to support higher rates of communication as reduced numbers of photons mean there are more microvilli available for use.

d) The temporal difference between stimulus and response (phase difference) is reduced at higher, non-saturating mean light backgrounds, suggesting that voltage responses become better correlated with the stimulus when more photons are available.

e) Response dead-time is less at higher mean light backgrounds, indicating that the ability to generate new responses is enhanced where more photons are available.

f) Quantum bumps, the unitary voltage responses generated by individual microvilli, reduce in size at higher mean light backgrounds.

g) Quantum bump duration reduces with increased mean light backgrounds, revealing a mode of light adaptation.

h) The information content of bumps is least at lower mean light backgrounds, suggesting that photoreceptors respond faster when there is more available light information.

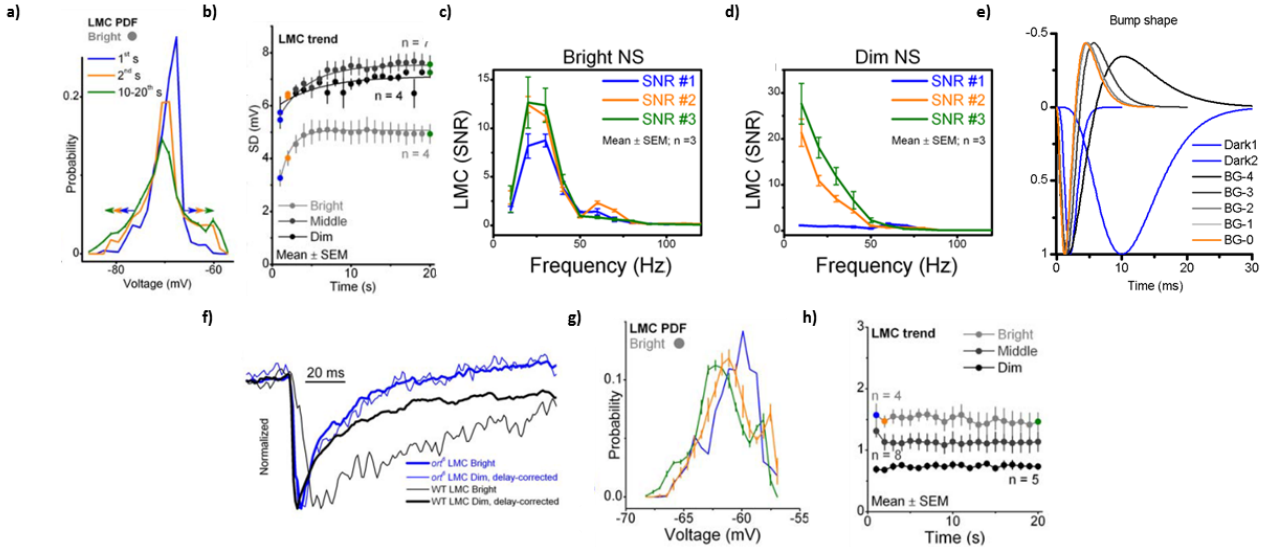

Adapted from Li (2011), Zheng et al. (2009) and Nikolaev et al. (2009)

Fig. 1-8 – LMC voltage and Histamine bump response characteristics at different stages of adaptation under repetitive naturalistic stimulation:

a) LMC Probability Density Functions (PDFs) indicate that LMC responses reduce in size and 'flatten', distributing responses over more of their voltage range. Blue – Responses at 1st second of repeated naturalistic stimulation, Orange – responses at 2nd second and Green – responses between the 10-20th seconds.

b) Mean LMC adaptational trends for different light backgrounds. Shows that LMCs become increasingly sensitised to photoreceptor outputs at low light levels.

c) LMC signal to noise ratios (SNR) are enhanced after prolonged stimulation and adaptation in bright conditions.

d) Higher LMC SNR after prolonged stimulation and adaptation in dim conditions.

e) Estimated histamine bumps (unitary responses to histamine occurring at the LMC post-synapse) show reducing latencies in brightening conditions. May also occur during dark adaptation.

f) Comparing LMC voltage responses in wild-type flies and *Ort^{P306}* mutants. In the mutant, voltage responses appear to lack light adaptation, remaining similar in bright and dim light conditions.

***g)* *Ort^{P306}* LMC PDFs do not flatten with prolonged stimulation, thus these receptor mutants fail to use their bandwidth efficiently.**

***h)* *Ort^{P306}* LMC response sensitisation to prolonged stimulation is not evident in their adaptational trends, confirming the lack of light adaptation shown in f).**

1.2 *Drosophila* Behaviour

1.2.1 The Drosophila Optomotor Response

From the eye to the brain, its musculature and back again, *Drosophila* flight requires the co-operation of multiple modalities of fly biology. Such co-ordination enables the visuo-motor coupling required to fine tune and match the fly's behaviour with relevant environmental cues. With advances in genetic tractability and the ease of physical manipulation afforded by *Drosophila*, it has become increasingly simple to affect, mis-express and modify the specific biological components that govern such behaviours.

The term optic flow refers to the perceived motion of environmental visual features that occur relative to the motion of the organism. For example, stationary elements in the visual field or those moving more slowly than the fly, will move from front to back (expansion) if the organism is moving forwards. This relative motion reverses for organisms moving in the opposite direction (contraction) and is similar for movement of the organism around other body axes (Blondeau and Heisenberg, 1982). Visual elements with their own agency may produce other unwanted diversions from normal, motion trajectories. Flies attempt to mitigate the effects of such visual deflections and exploit optic flow; updating their own sense of position within the world and generating the optomotor response.

The optomotor response is composed of the syn-directional turning response of a moving fly when faced with a directional stimulus, i.e. the fly will turn in the same direction as the perceived motion (Heisenberg and Wolf, 1979).

Fig. 1-9 - Photograph of a wild-type Drosophila, prepared for use in a traditional 'flight simulator'.

Shows a tethered and flying fly at the preparation bench, elucidating the position of the head, body and the location of the pre-formed and super-glued copper wire tether – located between the head and torso.

of the changing environmental visual signal upon the fly's behaviour (Heisenberg and Wolf, 1988a; Holst and Mittelstaedt, 1971). The optomotor response correlates with alterations to wing-beat frequency and amplitude (Theobald et al., 2010), which form the basis for manoeuvrability during flight, thus the optomotor response requires sensorimotor integration to match muscular output with visual input (Heide and Götz, 1996).

2 General Methods

2.1.1 Genetics

The fruit fly, *Drosophila melanogaster*, has been used as a biological model for over 100 years, having been proposed as a useful organism for genetic analysis. Here, particularly favourable is their ability to generate large numbers of progeny that require little space, upkeep and resources. Seymour Benzer (1967) kick-started the neurogenetic study of behaviour in *Drosophila*, showing that Canton-S flies are robustly phototactic. When disturbed into a period of action, flies will migrate towards a light source. Benzer tested around a hundred individuals at a time, using dual-chambered fly tubes and an external lamp. The study also incorporated several mutant fly strains, generated using the novel technique of Ethyl Methane Sulfonate (EMS) mutagenesis (Alderson 1965), used to ethylate DNA bases, resulting in their hydrolysis from the backbone thus causing weakness and strand breakage. This experimental protocol and many others like it, illustrate the level of simplicity that has helped elevate *Drosophila* to its ubiquity as a model organism.

EMS was used to successfully induce mutation at high rates in bacteria in Loveless (1958), though its use in *Drosophila* was first recorded in the 1950's (Bird, 1951). Until then, mutagenesis techniques had taken much time to evolve, beginning from observations of naturally occurring mutations, to the use of irradiation (Muller, 1927), and then the use of other chemical mutagens (review - Auerbach 1949). Since these initial investigations, a plethora of genetic techniques and assays have been developed, allowing its use for the study of a vast number of biological processes.

Key genetic discoveries relating to gene sequencing, cloning and amplification notwithstanding; the ability to introduce exogenous genetic material into the nuclei of cells, and have the introduced genetic material induce inheritable phenotypic effects

(Graham and van der Eb, 1973; Pellicer et al., 1980; Schaffner, 1980), was another major leap forward in genetic modification techniques. Though due to chromosomal re-arrangements, these procedures initially generated unstable results.

Rubin & Spradling (1982) went on to develop the P-element transformation system. This constituted a hi-jacking of the abilities of transposable genetic elements discovered in laboratory strains of *Drosophila* (Kidwell et al., 1977). P-elements are free to move around a genome due to the co-expression of a transposase enzyme that possesses the ability to remove and insert itself and associated DNA at specific genetic sequences. However, this ability is normally repressed in somatic cells (Laski et al., 1986). Montell et al. (1985) co-injected a P-element engineered to contain the TRP channel gene sequence into functionally-null trp^{CM} mutants; they also inserted an active transposase and a marker gene for transformation. Using this novel technique, they mated transformants successfully to give rise to flies with normal wild-type electroretinograms (ERGs). This technique conferred a lasting advantage, eventually contributing to the deciphering of the *Drosophila* genome. In addition to the ability to rescue function in loss-of-function genetic mutants, P-elements also showed aptitude for the disruption of gene function (Spradling et al., 1995).

Suffice it to say that a panoply of techniques has paved the way and facilitated the genetic dissection of *Drosophila* biology and behaviour. However, this is only a compressed history of the genetic tools relevant to this thesis. Nevertheless, current research and effort continues to produce novel and innovative methods by which to specify particular biological components in a spatio-temporally controlled fashion.

2.1.2 Electrophysiology

The eye, as an electrical organ, has been studied since the mid-1800s and since then a plethora of techniques have been developed and realised. The ERG was the first technique to be used across several species throughout the early 20th century. In Nobel prize-winning work, the ERG was thoroughly characterised and shown to consist of multiple electrical components originating from various sources (Granit, 1938). Several components comprise the ERG, on and off transient potentials that derive from stimulus-dependent LMC hyperpolarisation and depolarisation respectively, and the receptor component which originates from the light-dependent voltage change occurring in the photoreceptors. The ERG is therefore, an extracellular, polyphasic and composite signal and is therefore an indirect but informative measure of overall electrical activity in the distal visual system.

The development and use of microelectrodes (Curtis and Cole, 1940; Graham and Gerard, 1946; Ling and Gerard, 1949; Nastuk and Hodgkin, 1950) afforded a direct approach, as individual cells of interest are 'impaled' and current or voltage can be simultaneously measured. Voltage clamp techniques allow the injection of current into a cell, whilst simultaneously measuring the electrical properties of an associated membrane. This technique allows electrophysiological assay whilst the membrane is held at a particular potential. These early intracellular works helped to deduce the dynamic electrical properties of many biological systems, and have given rise to several variants (Ogden, 1994).

Single-electrode techniques are such a variation; they negate the necessity for dual clamp and stimulation electrodes, which are often inappropriate for measuring currents in *in vivo* preparations. Current clamp recordings differ from voltage clamp techniques in that the membrane voltage is not controlled, so dynamic, stimulus-specific membrane properties

can be recorded (Juusola, 1994; Weckström et al., 1992). Juusola & Hardie (2001) further refined a single-electrode current clamp technique for studying *Drosophila* photoreceptors *in vivo*, providing a thorough analysis and further insight in to mechanisms of light adaptation at the level of 'quantum bumps' and photoreceptor voltage. These modern techniques are boosting the quality of recorded data and are bolstered by innovative analysis and modelling.

2.1.3 The Drosophila Flight Simulator

With fly behaviour being a veritable black box, it is necessary to possess simple and highly controllable stimulation and detection methods that impinge minimally upon the fly's experience of the world. The study of *Drosophila* flight behaviour was facilitated by the invention of the flight simulator, as described in Götz (1964). This device, through exploitation of the optomotor response, allowed observation of the effects of the environment upon the flight of the organism.

In the flight simulator (**Fig. 2-1**), flies are tethered to a torque meter and are presented with a rotating visual stimulus. The fly's relative optomotor turning responses are transduced by the torque meter and converted into an electrical signal that can be read out and analysed. The stimulus pattern can be pre-specified, the illumination of the environment can be precisely controlled, as can the speed and directionality of the stimulus. Stimulus rotation can be generated in different directions relative to the mounted fly, thus allowing the detection of stimulus-specific torque outputs, i.e. yaw, pitch and roll.

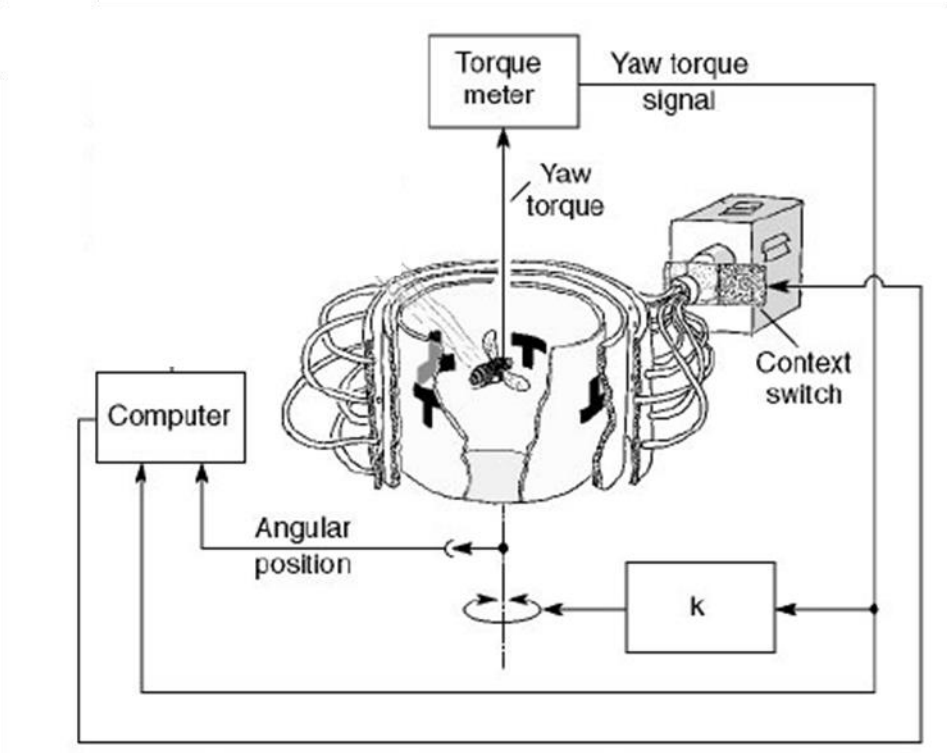

Fig. 2-1 - Schematic representation of a traditional 'flight simulator'.

Shows a fly attached in a traditional flight simulator in a 'closed-loop' configuration. In flight and during and rotational stimulation, the fly's optomotor yaw torque responses may be used to control the position of the stimulus pattern, thus providing environmental feedback to the fly's nervous system.

Adapted from Liu et al. (1999).

Furthermore, the device can be used in either an open- or closed-loop configuration, where either the experimenter or the fly itself has control over the visual environment, respectively. Thus these variant paradigms can be very useful for studying visual behaviour and visual learning in a controlled fashion.

3 Colour, Motion & Optomotor Behaviour

3.1 Introduction

Dipteran vision is limited by the function of its compound eye, across which stereotypical ommatidia are arranged in hexagonal fashion. Each ommatidium is composed of an outer ring of six photoreceptors, the achromatic R1-R6 (Braitenberg, 1967); and a central, tiered and multi-class pair, R7 and R8 (Trujillo-Cenóz, 1965). R1-R6 photoreceptors express the dual-peaked Rh1 photopigment, giving rise to their supposed achromaticity and the belief that they subserve motion vision, whereas R7 and R8 photoreceptors subdivide into classes defined by the differential expression of several photopigments, Rh3-Rh6 (see Hardie 1979 for a comparative functional characterisation), thus being thought to subserve colour vision. In conjunction with this differential expression of photopigments is the fact that each 'channel' terminates within a different layer of the optic lobe. R1-R6 photoreceptors synapse with Large Monopolar Cells (LMC's) in the optic lamina, and R7/R8 with intrinsic and trans-medullary targets in the medulla (Bausenwein et al., 1992; Strausfeld, 1971; Takemura et al., 2008).

The UV-Fly, developed by the Juusola laboratory (Wardill et al. 2012), provides a means through which to functionally segregate these visual channels. In these flies, Rh1 function has been annulled in R1-R6 photoreceptors, using *ninaE*^{8} or *ninaE*^{P334} mutations (Johnson and Pak, 1986), and has been replaced with the UV-sensitive Rh3, expressed under control of the Rh1 promotor. Using this system, R1-R6 photoreceptors can be stimulated using UV light, whilst R8 can be excited by longer wavelength light such as green, or in this case amber, thus affording a degree of photoreceptor channel-directed stimulus separation that was not available beforehand.

In contrast to previous assumptions (Yamaguchi et al., 2008), electrophysiological and imaging data upon such UV-Flies and other visual mutants (Wardill et al. 2012), has shown that motion-relevant colour information is reflected in the voltage responses of photoreceptor LMC targets, and that this information is absent in flies lacking R7 and R8 photoreceptors. This study went on to show that this information likely comes from R8 cell types (R8p or R8y), and their potential contacts with R6 (Shaw et al., 1989). This is because the relative contributions of Rh5 and Rh6 photopigments to the overall spectral sensitivity, approximately match the second peak of the bi-phasic LMC responses to blue or yellow-green light flashes, respectively.

A fly's head and body reorients to maintain straight flight by reducing the retinal slip of optic flow signals that naturally occur due to environmental motion (Götz, 1968). This classic *Drosophila* optomotor response results from the integration of sensorimotor information and serves to stabilise a fly's gaze during flight through an involuntary displacement from a straight course. This behaviour is re-afferent (Heisenberg & Wolf 1988), conditionable (Brembs and Heisenberg, 2001), and spontaneous (Wolf and Heisenberg, 1990).

In this chapter, I exploit the classic optomotor response by using open-loop experiments in the traditional, *Drosophila* flight simulator (Götz, 1964). I set out to characterise the behavioural consequences of manipulating the colour and motion visual channels by observing optomotor responses to predominantly monochromatic, horizontal grating rotation, and testing the limits of the fly's coloured motion vision. I utilised flies of differing visual phenotypes, derived from various photopigment knock-outs and rescues. These methods allowed me to isolate the colour and motion channels and to assess the relative inputs of each photopigment, thus allowing identification of the specific spectral influences upon the behavioural response.

My experiments ultimately confirm that, rather than being solely achromatic, coloured motion can be used to evoke *Drosophila* optomotor behaviour. Thus, it appears to be driven by combined, additive and spectrally-variant inputs from R1-R6 and R7 + R8 photoreceptor subsets. Akin to the electrophysiology (Wardill et al., 2012), the behavioural data suggests a role for R8y and R8p in sharing colour information with R1-R6 photoreceptors and also reflects the way that *Drosophila's* visual function is tuned to its natural environment.

3.2 Methods

3.2.1 Drosophila Genetics

3.2.1.1 Stocks

Most of the flies used in this study were generated in-house by Dr. Trevor Wardill and Dr. Olivier List, though some original lines used for these crossings were acquired from external sources; $norpA^{36/P24}$ from Roger Hardie (University of Cambridge), $ninaE^{8/P334}$ from William Pak (Purdue University), UAS-GCaMP3.0 from Vivek Jayaraman (HHMI Janelia Farm) and *3A*-Gal4 from Martin Heisenberg (University of Würzburg). UV-fly R1-R6 rescue lines were derived from *Rh1+3 norpA* mutants from Charles Zuker (Columbia University), and *Rh1+norpA* R1-R6 rescue constructs from Steve Britt (University of Colorado).

Line	Genotype
Canton S	WT
UV-fly	w[+]; +; Rh3[4303], ninaE[8]/TM6b
UV-fly lacking R7/R8	w[+],norpA[P24]; +; P{w+,Rh1:norpA},Rh3,ninaE[8]
UV R1-R6 rescue (with inactive R7/R8)	w[+] norpA[P24]; +; Rh3-ninaE[8](666-1)/TM6b
R7/R8 Only	w[+]; +; ninaE[8]
Rh1 in R1-6 Rescue	w[+]; norpA; Rh1-norpA[12]/th1
Rh3 in R7p Rescue	norpA[36].CS; Rh3-norpA[1]
Rh4 in R7y Rescue	norpA[36].CS; Rh4-norpA[12]/(cyo)
Rh5 in R8p Rescue	norpA[36].CS; Rh5-norpA[20pa]/(cyo)
Rh6 in R8y Rescue	norpA[36].CS; Rh6-norpA[5a1]/(cyo)

Table 3-1 – Table of lines used and their specific genotypes.

3.2.1.2 Crosses & Optimisation

Many neurally-directed mutations have unwanted, secondary effects upon an organism's biology, thus these ancillary phenotypes must be minimised and controlled for. In this study, all crosses and genotypic optimisation were carried out by Dr. Trevor Wardill and Dr. Olivier List.

3.2.1.2.1 ninaE

The *ninaE* gene encodes for the Rhodopsin-1 opsin, expressed in R1-R6 photoreceptors (O'Tousa et al., 1985; Zuker et al., 1985), conferring a dual-peaked spectral sensitivity (Hardie, 1979). To achieve silencing of R1-R6 photoreceptors, this study initially employed the *ninaE*^{17} mutation, due to its aberrant optomotor response (Strauss et al., 2001), and

impaired ERG function. However, in accordance with previous reports (Kumar and Ready, 1995), using electron microscopy it was confirmed that R1-R6 structure was catastrophically damaged; thus function could not be separated from the developmental effects of the mutation upon rhabdomere structure. *ninaE*^{8} was shown to possess similarly impaired ERG and optomotor responses. These flies also displayed a wild type-like rhabdomeric and overall ommatidial morphology (T. J. Wardill et al., 2012), thus *ninaE*^{8} was used instead. Taking flies with a *ninaE*^{8} background, UV rescue flies were generated by introducing a P-element containing Rh1+3 (functional Rh3 under control of an Rh1 promotor, for technique see Feiler et al. 1992).

3.2.1.2.2 P-elements

P-elements are a form of transposable genetic element, specific to *Drosophila*, that are able to move around a genome (for review see Castro & Carareto 2004). Though such motility is normally repressed in somatic cells (Laski et al., 1986; Misra et al., 1993). Experimentally this repression can be circumvented through the simultaneous use of fly lines, which are engineered to lack P-elements or their repressors and the incorporation of an active form of P-element. This allows their inherent function to be exploited for the further generation of transgenic *Drosophila* strains. P-element motility is enabled by the expression of a transposase enzyme (Kaufman and Rio, 1992); a type of restriction endonuclease which cuts DNA at specific sequences of base pairs, allowing a P-element containing the relevant, complementary 3' and 5' sequences, to insert under control of host genetic machinery (Rio et al., 1986). Both the transposase and P-element can be engineered to show specificity for any target gene, and can be used to insert coding DNA sequences into the control region of an endogenous gene of interest, thus placing the construct's expression under control of the host organism's promotor (Karess and Rubin, 1984).

3.2.1.2.3 norpA

The *norpA* gene encodes for Phospholipase C (Bloomquist et al., 1988), a critical component of the phototransduction cascade in *Drosophila* (Hardie et al., 2002). PLC, in response to activation by Rhodopsin's $G\alpha_q$ GPCR subunit, is responsible for metabolism of the membrane phospholipid PIP_2, resulting in the generation of the DAG and IP_3 secondary messengers. PLC-null mutants lack normal phototransduction in all photoreceptors (Pearn et al., 1996). Specifically $norpA^{36/P24}$ is associated with normal synaptic structure (Hiesinger et al., 2006), so it can be used without fear of impact from structural aberrancy. The $norpA^{36/P24}$ mutation was used to produce several, selective photopigment rescue lines, i.e. lines expressing only individually functional photopigments. The same mutation was also used to generate UV-flies that lacked functional R7 + R8 photoreceptors (*norpA* Rh1 rescue via P-element insertion).

3.2.1.2.4 UV-Flies

We also used UV-flies that contained a Genetically Encoded Calcium Indicator (Palmer et al., 2011), expressed in the Vertical System cells (VS cells) of the Lobula Plate. Using two-photon microscopy, Wardill et al. (2012) studied changes in VS cell Ca^{2+} flux occurring as a result of the vertical motion of a black & white striped grating lit by UV (385±30 nm) or amber light (590±40 nm) for details see Wardill et al. (2012) supplementary materials.

3.2.2 Flight Simulator

Experiments were carried out in open loop fashion using a traditional *Drosophila* flight simulator. To maximise body and response size, large, virgin female flies of 3-5 days old were selected for experiments and kept in large ICRF-type bottles, the latter to provide

increased flight space. Flies were raised at 25^{o}C on a 12hr:12hr day/night light cycle and were fed on a standard, plant-based diet. During preparation, single flies were cold-anaesthetised and tethered using a micro-manipulator to manoeuvre a triangular, copper-wire hook. This was superglued between the head and thorax; so as to remove head movements relative to the direction of turning.

3.2.3 Motion Stimulus

The motion stimulus, programmed using an in-house developed MATLAB script, consisted of a cylindrical arena comprising a black grating of vertical elements with a 14^{o} distribution. Via the use of a stepping motor, the arena was bi-directionally rotatable in the horizontal plane. Preceded and concluded by a 1 second pause, the arena was rotated anti-clockwise then clockwise at 45^{o}/s, separated by a 2 second cessation of motion. For each fly, this stimulus was repeated 10 times and the yaw torque responses that made up each set of 10, sampled at 1 kHz, were averaged to make one recording and the process was then repeated for a number of flies per genotype. Individual flies were tested for a best of 10 and average responses were selected if the traces in each recording were consistent in characteristic. For a given trace, periods of cessation of flight, turning or other severe behavioural erraticism were cause for rejection of the averaged response.

3.2.4 Light Stimulus

To illuminate the motion stimuli, the grating was either backlit by a broadband, external ring light (Philips, ≈380-900nm) or with the use of LED's with relatively specific wavelength ranges, controlled and driven using a Cairn Research OptoLED light source. Using the latter, in conjunction with a silver, reflective acetate insert, meant that the arena could be lit from

above, producing simple, uniformly illuminated coloured motion of various types (UV: ≈350-405nm, amber: ≈560-620nm, green: ≈460-580nm, red: ≈590-670nm). The spectral characteristics of the stimulus were calibrated using a Hamamatsu spectrometer and were shown to be attenuated with respect to the LED output specifications, due to the indirect, reflected nature of the stimulus set-up. The Cairn LED driver also enabled a degree of real-time, manual control over the light stimulus. This became useful to employ a 'transitional' stimulus, where continuous rotation of the grating could be coupled with a manually dimmable and switchable light stimulus.Different protocols were designed to test whether R7/R8 photoreceptors could modify behaviour by taking over the ongoing processing of motion information when the background illumination of the scene changed, i.e. upon a gradual switch from a UV-lit arena, to one lit with an Amber hue.

3.3 Results

3.3.1 Wild-type Drosophila Optomotor Response

I acquired torque responses of Canton-S Isoline flies in a traditional, *Drosophila* flight simulator. Torque responses were pooled and averaged for a particular fly in open-loop configuration. See methods for stimulus parameters.

The *Drosophila* optomotor response shown here, manifests as a syn-directional, bi-phasic yaw torque turning response, peaking first at the point of termination of the anti-clockwise grating rotation. For each individual fly, the time taken for the complete decay of the optomotor response can vary taking up to 20 s (pg. 45 - Heisenberg and Wolf, 1984), as such when the rotation stops the torque response tends towards zero, but never reaches abolition, as insufficient time is given in which to do so. Upon clockwise grating rotation,

the yaw torque turning response resumes, but in the opposite direction, i.e. responses are always syn-directional to the new stimulus program, and due to the aforementioned time discrepancy, the response appears to be of reduced amplitude.

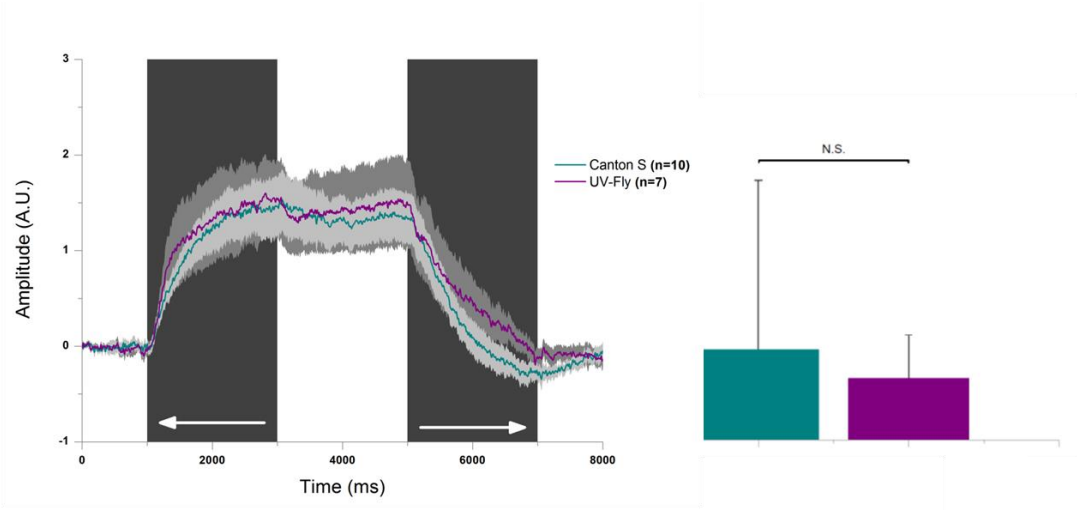

Fig. 3-1 – Mean optomotor responses of Canton-S (teal) and UV-Flies (purple), to 45°/s grating rotation, illuminated by UV light (≈350-405nm). Grey areas show the SEM. Right-hand panel shows the mean optomotor response for each line. Means comparisons showed no significant difference, which is congruent with the visual inseparability of the mean traces.

The ability of this study to successfully stimulate R1-R6 and R7/R8 visual channels separately hinged directly on the fidelity of the UV-Fly. With R1-R6 photoreceptors allegedly being responsible for motion vision through Rh1 functionality, the UV-fly; with its replacement of Rh1 with Rh3, required testing under open-loop flight simulator conditions and its performance was then compared against wild-type responses (**Fig. 3-1**).

Because of the UV-sensitising pigment expressed in wild-type R1-R6 photoreceptors (Hamdorf et al., 1992; Kirschfeld et al., 1983), wild-type Canton-S flies performed similarly to UV-Flies when responding to UV-illuminated 45°/s arena rotation. T-test on mean variances shows a lack of statistical significance (p=0.671), thus helping to validate the use of UV-flies for the purpose of this study (**Fig. 3-1 inset**).

3.3.2 ninaE Variants

The *ninaE* gene encodes Rh1. Thus *ninaE*^{8} mutant flies formed not only the basis for functional isolation of the R7/R8 channel, but also for the generation of UV-flies and associated variants.

ninaE^{8} mutants completely lack R1-R6 function, as shown by separate intracellular electrophysiological experiments, but these flies show a sizeable optomotor response in accordance with a 45^{o}/s, broadband light stimulus (**Fig. 3-2**). Surprisingly, the magnitude of this response approached that of the otherwise blind flies, whose R1-R6 functions were rescued by expressing Rh1 or Rh3 visual pigments (**Fig. 3-3a**).

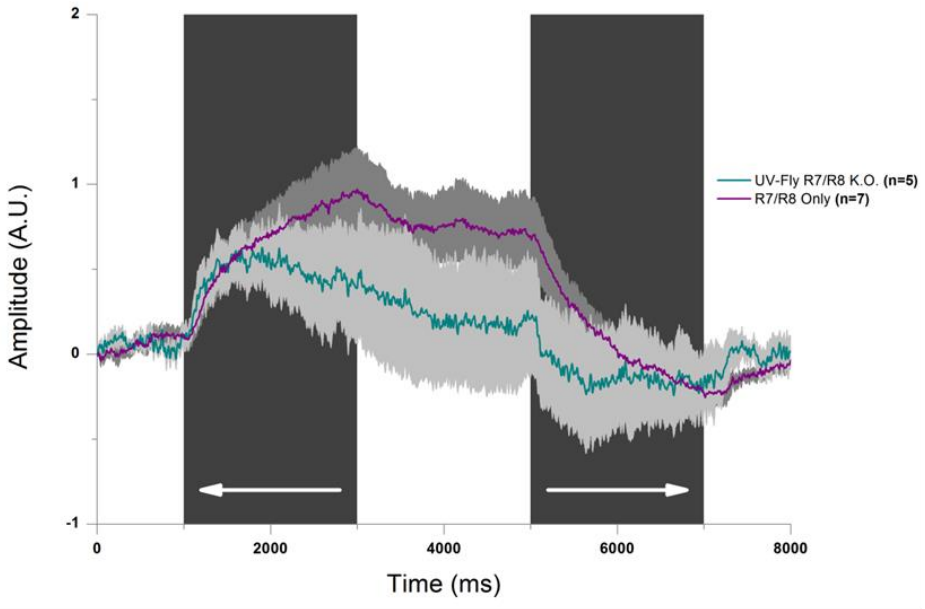

Fig. 3-2 – Mean optomotor responses of UV-Flies lacking R7 & R8 (teal trace) and flies with only R7 & R8 function remaining (purple trace). Flies retaining only R7/R8 photoreceptor function perform better than UV-Flies that lack them. 45^{o}/s grating rotation, illuminated by UV light (≈350-405nm).

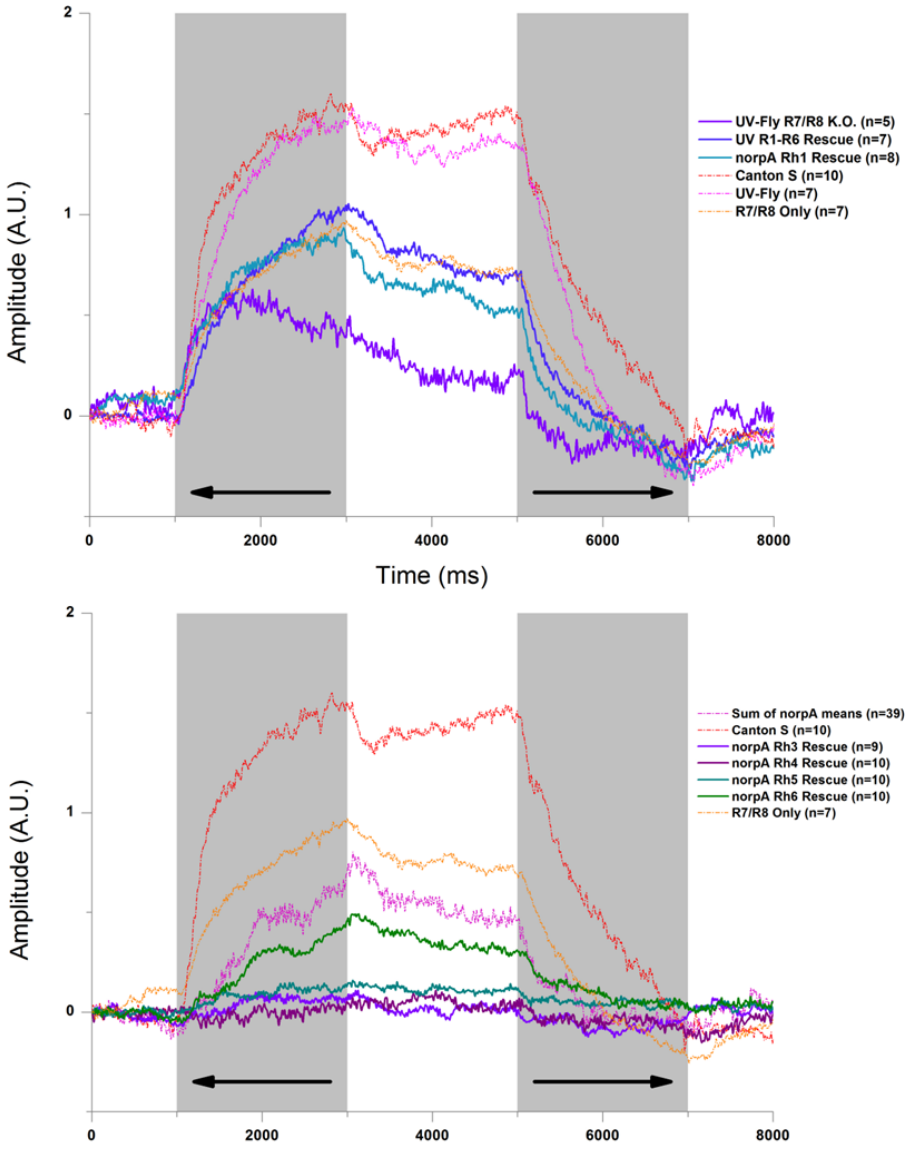

Fig. 3-3. Comparison of mean optomotor responses across all lines used:

a) Mean optomotor responses of flies with only R1-R6 function (purple, violet and blue traces), compared against Canton-S (red trace), UV-Flies (pink trace) and flies with only R7 & R8 function remaining (gold trace). Data show the similarities in optomotor function between; Canton-S and UV-Flies, whilst elucidating the behavioural impairments associated with removal of either the colour or motion information channels. 45°/s grating rotation, illuminated by UV light (≈350-405nm).

b) Mean optomotor responses of all norpA rescue flies, compared against Canton-S (red), flies with only R7 & R8 function remaining (gold) and the summed mean optomotor responses of all norpA rescue flies (pink). Rh3 (violet), Rh4 (burgundy) and Rh5 (teal), do not contribute much of an optomotor response. Rh6 expression alone can produce relatively large responses. Due to variance in data selection, the summed response does not equal that of flies with only R7/R8 function as per Wardill et al. (2012). 45°/s grating rotation, illuminated by UV light (≈350-405nm).

3.3.3 norpA Rescue Lines

norpA gene expression gives rise to the Phospholipase C enzyme in *Drosophila*, essential for the production of critical downstream signallers of phototransduction. Its mutation results in an abnormal phototransduction cascade, thus impairing vision in general. To test the relative contributions of individually expressed photopigments, *norpA*[36] mutant lines were created, and individual photopigment expression was re-instated by expressing *norpA* cDNA contained in various P-elements, alongside specific Rhodopsin photopigment promotor sequences.

Driven by a broadband light stimulus, some *norpA* rescue lines showed some ability to produce stimulus driven motor behaviour in the flight simulator, though with considerably different relative contributions.

Rh1 in R1-6 rescue flies, with inherent UV sensitivity, displayed substantial but incomplete rescue of the optomotor response (**Fig. 3-3a**). This was also true for *norpA* R1-R6 rescue flies, whose R1-R6 function was rescued using Rh3, making them purely UV-sensitive rescue flies. In contrast (**Figs 3-2** & **3-3a**), UV-Flies that lacked R7/R8 function performed less well than standard UV-Flies (**Fig. 3-4;** T-test on mean variances, p=0.04).

Flies in which Rh3, Rh4 and Rh5 were expressed alone in R7-pale, R7-yellow and R8-pale photoreceptor subtypes respectively, contributed little to the optomotor behaviour (**Fig. 3-3b**). Contrastingly, flies whose Rh6 photopigment was rescued (expressed in R8-yellow), showed a higher efficacy, generating much larger optomotor responses than their rescue counterparts.

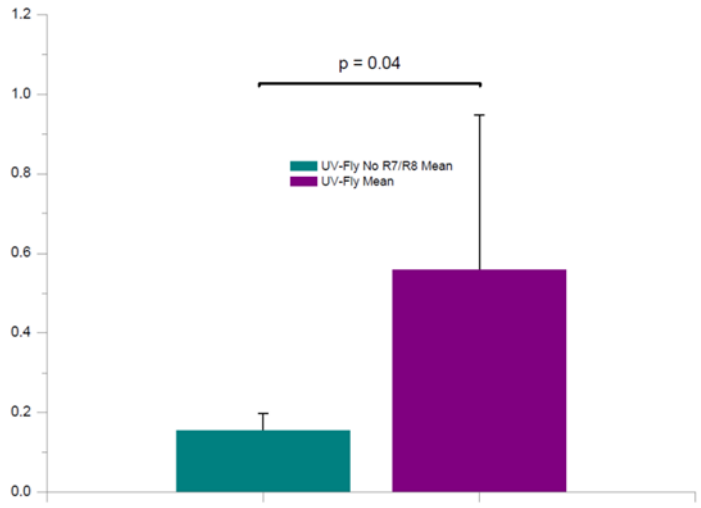

Fig. 3-4 – UV-Fly optomotor responses to 45 °/s grating rotations are significantly larger than UV-Flies that lack R7/R8. UV-Flies express Rh3 instead of Rh1 in R1-R6, but have normal and intact R7/R8 function. Mean variance +/- SD.

3.3.4 'Transitional' Stimulus

The transitional stimulus was designed to test whether the R7/R8 channel could assume responsibility for R1-R6 derived motion vision when flies were subjected to a change in the chromatic background illumination during field rotation stimulation. Here tethered, flying flies were exposed to a UV-motion stimulus and their subsequent behavioural responses were monitored. The rotational stimulus was continuous, thus traces appear in the style of a response string, rather than an averaged single trace.

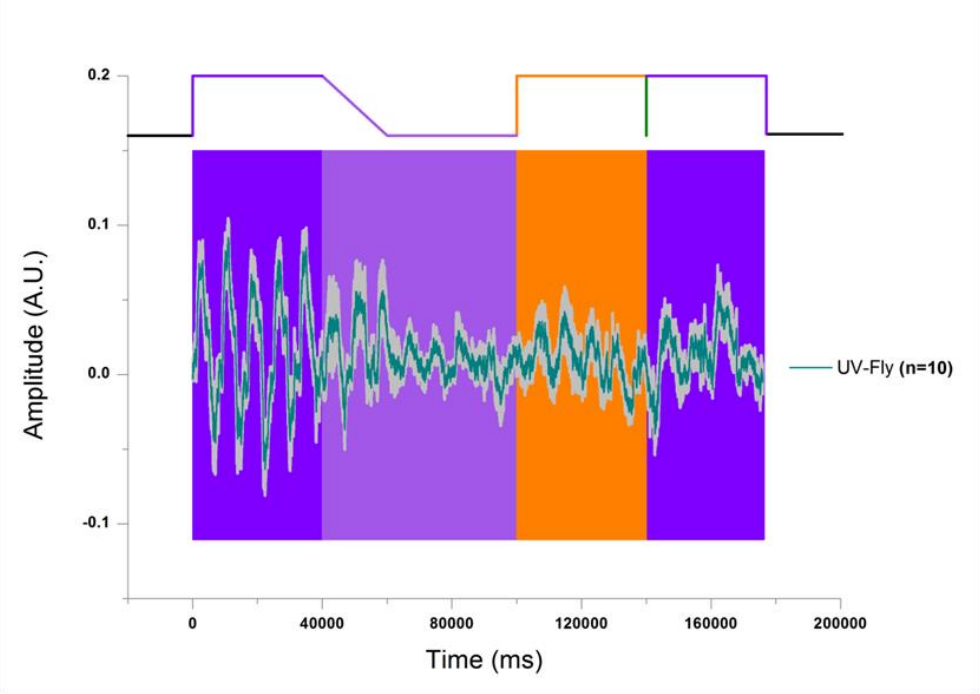

Fig. 3-5 – Transitional mean optomotor response string of UV-Flies responding to UV light (≈350-405nm, 4s duration), followed by dimming UV light (6s duration), followed by a period of amber illumination (≈560-620nm, 4s duration), then back to UV (4s duration). Full optomotor responses can be seen in response to the initial UV illumination. These reduce as the UV light is dimmed, as indicated on the upper schematic. Responses appear increasingly inconsistent and approach nullification as UV illumination is reduced to a negligible value. Introduction of amber illumination results in a re-instatement of a small but consistent optomotor response. Finally, re-introduction of a bright UV illumination further enhances the optomotor response. Continuous 45°/s grating rotation used throughout.

In real time and during recording, the UV illumination was gradually dimmed, until optomotor responses had ceased, as confirmed by eye. Upon confirmation of cessation of motion behaviour, longer wavelength, amber illumination was swiftly introduced and its contribution to motion behaviour was observed.

Whilst the exact stimulus paradigms vary on the basis of illumination duration (not intentionally controlled for), the patterns of behaviour appear very similar in UV- (**Fig. 3-5**) and Canton-S flies (**Fig. 3-6**). The flies' optomotor responses were executed synchronously with the stimulus program. Larger optomotor responses to initial UV stimulation, diminished to an approximate halt in accordance with the dimming illumination.

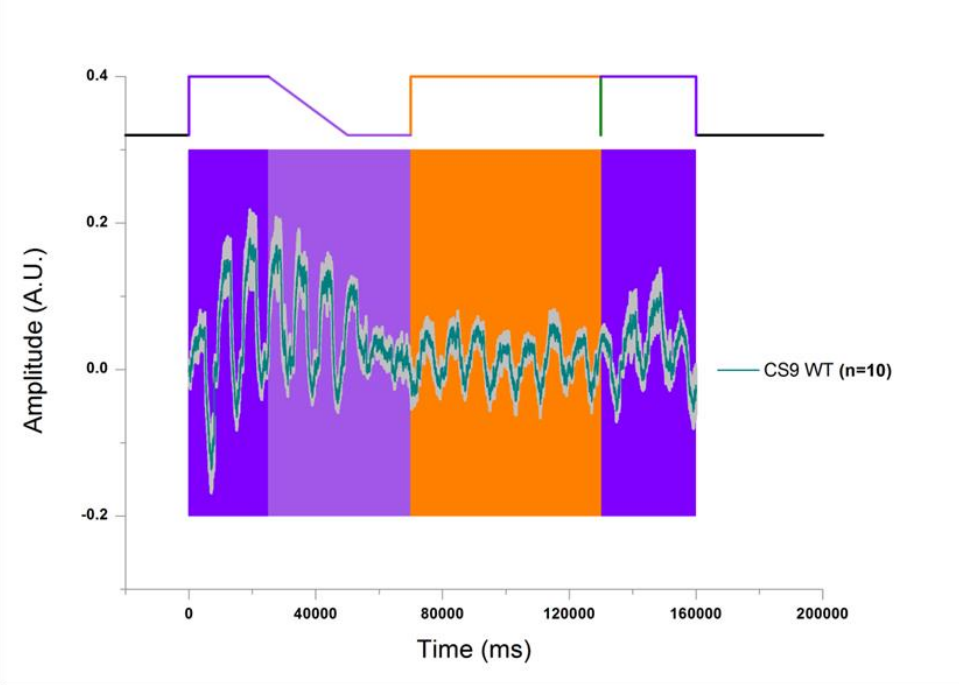

Fig. 3-6 – Transitional optomotor response string of Canton-S flies, responding to UV light (≈350-405nm, 3s duration), followed by dimming UV light (4s duration), followed by a period of amber illumination (≈560-620nm, 6s duration), then back to UV (3s duration). As in Fig. 5, full optomotor responses can be seen in response to the initial UV illumination. These reduce as the UV light is dimmed, as indicated on the upper schematic. Responses appear increasingly inconsistent and approach nullification as UV illumination is reduced to a negligible value. Introduction of amber illumination results in a re-instatement of a small but consistent optomotor response. Finally, re-introduction of a bright UV illumination further enhances the optomotor response. Continuous 45°/s grating rotation used throughout.

Responses were partially rescued by replacing UV illumination with bright Amber illumination that was further enhanced by a return to the initial UV stimulus setting. Doubling in size, responses were on the whole larger in Canton-S flies, as was the level of amber-mediated rescue (**Fig. 3-7**).

For individual UV-Flies, the variance for periods of the total response, corresponding with either dim UV or amber stimulus illumination, was compared; the inter-period variance for periods 40-100 s and 100-140 s respectively, were significantly different when compared by one-way, repeated measures ANOVA (**Fig. 3-7**; n=10, p=0.05). Values for the first 20 s, corresponding to the UV-dimming stage, were removed from the dim UV dataset for all UV-Flies.

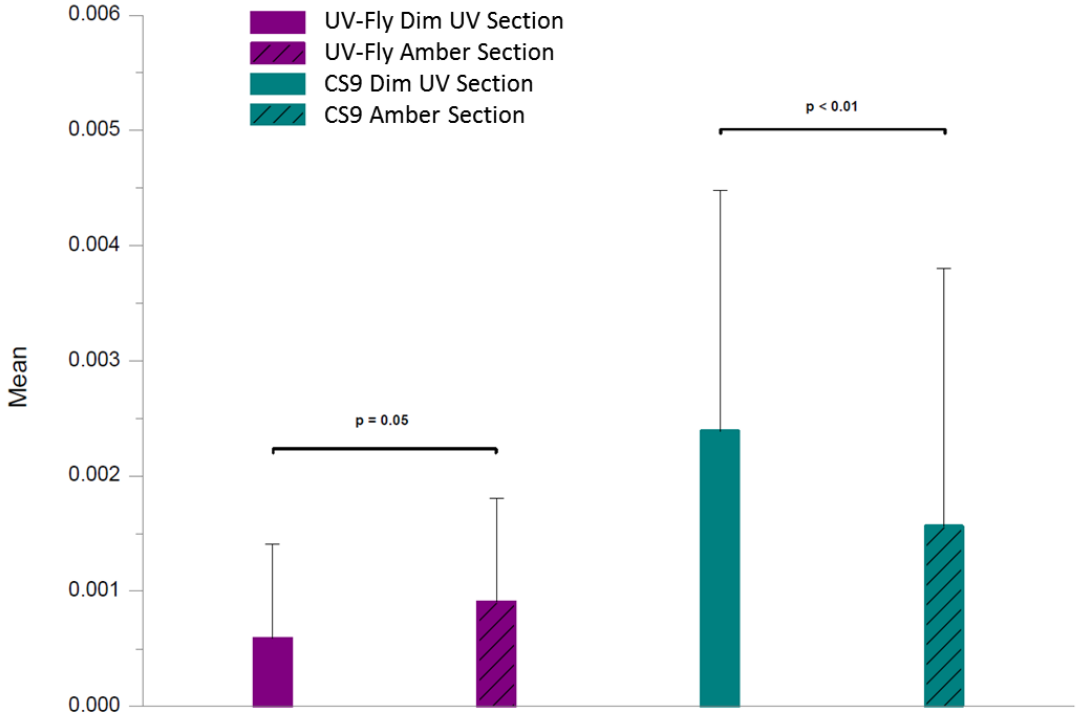

Fig. 3-7 – Mean and mean variance comparison for Transitional stimulus optomotor response data (Figs 5 & 6). Means +/- SD. P-statistics relate to the mean variance for the assigned periods and confirm the presence of illumination-dependent differences in optomotor performance, whilst the mean data reflects the inconsistency in using the mean value in this particular case (as can be seen visually in Figs 5 and 6) and shows the inherent inter-subject variability in the respective populations.

Likewise, this was also the case for Canton-S flies (ANOVA, n=10, p=<0.01) albeit for the following timings; variances were compared for dim UV (25-70 s) and Amber sections (70-130 s) though due to the aforementioned duration inconsistencies, only the last 20 s of values, corresponding to the UV-dimmed and late-amber stages, were used from each period for this comparison.

3.3.5 Painted Ocellus

The *Drosophila* ocelli are a tripartite, light sensitive organ, located centrally on the dorsal aspect of the head casing. Each ocellus uniquely expresses the Rh2 photopigment, and their functional characteristics and facilitatory role in phototactic behaviour have been reasonably well characterised (Hu and Stark, 1980; Miller et al., 1981). Additionally, ocelli

have been shown to feed rotational information to lobula plate tangential cells (Parsons et al., 2010) which drive optomotor responses (Krapp and Hengstenberg, 1996). Given that ocelli are known to contribute to visual behaviours, and that this role is thought dependent upon R7/R8 function, it was prudent to test whether their occlusion would alter the responses of some of our key lines. To do so I applied a non-toxic, all-natural and opaque, charcoal-based black paint (Winsor & Newton, Winton Oil Colour, Ivory Black -1414331) covering the ocelli *in situ* whilst flies were tethered at the torque meter.

Both painted *norpA* Rh1 in R1-6 rescue flies (**Supp. Fig. 1**), responding to 45^{o}/s spectrally broadband (380-900 nm) field rotation and painted *ninaE*$^{[8]}$ flies responding to the same stimulus (**Supp. Fig. 2**), appeared to show similar response characteristics to each other. Comparable responses were absent in other, relevant rescue flies. Also of interest here is the suggestion that such *ninaE*$^{[8]}$ flies display a comparable behavioural response to the broadband stimulus than was shown by Rh1 in R1-6 rescue flies (**Supp. Fig. 2**). This is possibly due to the lack of a functional connection between R1-6 and R7/R8 photoreceptors in the Rh1 in R1-6 rescue flies, a pre-requisite which I will discuss later.

The latter Rh1 in R1-6 rescue flies however, showed larger and approximately equivalent responses to UV and amber stimuli (**Supp. Fig. 1 & 3**) both of which appear relatively absent in Rh6 in R8y rescue flies.

The ability of wild-type Canton-S flies to show very small, but appropriately shaped responses to red stimulus illumination (≈590-670nm) is noteworthy. This is further reflected in the responses of Rh1 in R1-6 rescue flies (**Supp. Fig. 4**). These findings reflect the prolonged long-wavelength tail of Rh1 pigments which, once integrated over the whole eye, seem to provide sufficient sensitivity to detect very bright red field motion.

3.4 Discussion

In accordance with the electrophysiological and Ca^{2+} imaging results (Trevor J Wardill et al., 2012), the data outlined here confirm the validity of the use of UV-Flies as a means to study visual behaviour (**Fig's 3-1**, **3-5** & **3-6**).

Line	UV-fly
Canton S	p=0.671
UV-fly lacking R7/R8	p=0.04

Table 3-2 – Table showing WT/UV-Fly similarity and the difference in response when R7/R8 are missing.

But more importantly, they are fully supportive of the finding that the separate 'colour' vision information channel can drive the *Drosophila* optomotor response in isolation (**Fig's 3-2** & **3-3a**), and that its normal function is shaped by additive inputs from individual photoreceptors (**Fig. 3-3b**). Also supported here is the suggestion that such colour-motion integration depends upon connectivity between R1-R6 and R7/R8 photoreceptors (**Fig's 3-3b, 3-5, 3-6** & **Supp. Fig. 1**) and these data implicate the Rh6-expressing R8y in this role (**Fig. 3-3b**).

The finding that flies lacking any R1-6 function produced optomotor responses comparable to those of *norpA* Rh1 in R1-6 rescue flies (**Fig. 3-3a**) became central to the hypothesis that there is transfer of functional information between the colour- and motion-information channels. Moreover, genetic dissection of the relative contributions of distinct

photopigment classes helped shed light on how this may originate. Aside from previous morphological data (Shaw et al., 1989), such a hypothesis has been supported more recently with behavioural (Schnaitmann et al., 2013), and structural experiments (Jagadish et al., 2014), which respectively suggest that R1-R6 photoreceptors can contribute to colour discrimination, whilst R7/R8 synaptic targets may also connect with downstream R1-R6 targets in the lobula plate.

norpA Rh1 in R1-6 rescue flies showed slightly different responses to broadband and UV grating rotations (**Fig's 3-3a** & **Supp. Fig. 1**). This is likely to reflect changes in the collective capacity of their available photoreceptors to see these stimuli. UV-sensitive Rh3, whilst capable of driving the optomotor response when expressed in place of Rh1 in R1-6 photoreceptors (UV-Flies and UV R1-R6 rescue), when re-expressed alone, the *norpA* Rh3 in R7p rescue line was incapable of doing so in any meaningful way (**Fig. 3-3b**, **Supp. Fig's 1** & **2**). *norpA* Rh4 in R7y rescue flies, and *norpA* Rh5 in R8p rescue flies, also showed such impotence. Only the green-sensitive Rh6, expressed in *norpA* R8y rescue photoreceptors, showed any ability to modify the optomotor response (**Fig. 3-3b**). Given these findings, it is reasonable to infer that the Rh6-expressing R8y photoreceptor, above others, is responsible for conveying motion-relevant colour behaviour for the enhancement of optomotor responses in relevant environs.

Electrophysiologically, each photoreceptor class in isolation may contribute a wavelength and stimulus intensity-dependent voltage response (Wardill et al. 2012 - Fig. 2c and supplementary fig's S4 & S5). However, in the real world this response will be shaped and tempered by a plethora of environmental factors. For example, *Drosophila's* neural superposition eye pools spatially-similar photoreceptor information into a single lamina cartridge (Kirschfeld, 1967), whilst information acquisition is temporally controlled by their biophysical state (Song et al., 2012). Such pooling appears to be reflected in the summatory

behavioural responses of flies expressing single photopigments (Wardill et al. 2012 - Fig. 4). **Figure 3-3b** here likewise compares optomotor responses driven by individual photoreceptors contrasted against; wild-type flies, flies lacking R7/R8 function and the summed behaviour of the contributions from individual photoreceptors. The latter however, is not fully identical to the data shown in Wardill et al. (2012). This lack of correlation is down to the data selection process, with all data shown here being based on averages of 10 responses per individual fly, which sometimes included traces showing saccadic noise, or traces with instrumental and other external noise in the individual traces. Such noise and other artefacts can mask the true shape and magnitude of the response skewing subsequent analyses, thus in the published work, such distracting individual traces were excluded from the data before averaging. Despite these differences in selection, both Wardill et al. (Fig. 4) and the current datasets clearly indicate that the relative spectral sensitivities of each photoreceptor class sum up to approximately match estimates based upon real optomotor measurements.

The *norpA* Rh6 in R8y rescue line showed small, but well-correlated responses to 45^{o}/s, UV-illuminated grating rotations (**Fig. 3-3b**). This is interesting as it corroborates the electrophysiological findings, in which R1-6 voltage responses are modified by R8y input before synaptic transmission to lamina targets (Wardill et al. 2012 - Fig. 3). Certainly, UV-Flies lacking the dual-peaked spectral sensitivity of Rh1 can effectively respond to ≈560-620nm amber light (**Fig. 3-5**) and recover a failing optomotor response to an ongoing stimulus paradigm with an alternating illumination pattern. The same recovery was shown by Canton-S flies (**Fig. 3-6**), though to a slightly different stimulation protocol and with an apparent increase in response consistency and amplitude.

norpA-mutant photoreceptors lack any phototransduction due to the functional knock-out of PLC. These findings show that alone, *norpA* Rh6 in R8y rescue flies lack an optomotor

response during amber grating rotations, but that *norpA* Rh1 in R1-6 rescue flies show such a response (**Supp. Fig. 3**). These data therefore help to contest the idea that R1-R6 are achromatic and further add weight to the proposition that communication of such colour information should come from a pre-laminar, activity-dependent connection between R1-R6 and R7/8.

Ephaptic coupling, a non-synaptic method by which adjacent neurons can influence the synaptic output of their neighbours, has been suggested as a means of communication within nervous systems since the 1960's (Ruck, 1962). The process has been reasonably well characterised in the vertebrate retina (Byzov and Shura-Bura, 1986; Kamermans and Fahrenfort, 2004; Vroman et al., 2013), where such communication is mediated by mutual, intercellular ion exchange afforded by Connexin hemichannels (Kamermans et al., 2001) that occur between vertebrate cones and lateral horizontal cell dendrites.

In *Drosophila* there is no Connexin homologue. However, through misexpression in *Xenopus* oocytes, the Innexin, *shaking B*, was found to compose *Drosophila* gap junctions (Phelan et al., 1998). The *shaking B* gene is differentially processed in *Drosophila*, generating different functional alleles (Crompton et al., 1992; Krishnan et al., 1995, 1993). Moreover, the *shakB*^{2} mutant has been shown to have structural defects in the *Drosophila* retina, affecting the close apposition of R1-R6 photoreceptor terminals in the lamina. Using electron microscopy, Shaw et al. (1989) conclusively showed the presence of gap junctions between R1-R6 and R7/8 photoreceptor in the distal lamina of both *Musca domestica* and *Lucilia cuprina*, two alternative *Dipteran* species, thus lending further support to this argument.

The exact mechanism of information transfer between R1-6 and R7/R8 is as yet unknown, though this work, in conjunction with Wardill et al (2012), and other structural data, suggests that communication may well occur via gap junctions, prior to response

summation in the Large Monopolar Cells. As s*hakB*^{2} is widely expressed across the Dipteran nervous system, it will be necessary to find some way of targeting it for future experiments. Its expression could be knocked-down specifically in photoreceptors in a temporally controlled fashion, e.g. by using a Gal-4/80 coupled RNAi or temperature-sensitive mutation. Coupling such a genetically-targeted knock-down with structural, electrophysiological and behavioural assay may help further elucidation and consolidation of this view, though it is not a given that such techniques are technically feasible.

Alternatively, perhaps *shakB*^{2} gap junctions may not be the sole source of the proposed lateral connectivity. There are descending medullary feedback from R7/R8 through C2/C3 fibers, whose profiles can be seen in electron micrographs of cartridges, adjacent to R1, R6 and other LMC's (Meinertzhagen and O'Neil, 1991). In this case, visualisation of cell targets during electrophysiological study with the concomitant use of injected dyes may elucidate target specificity. Or perhaps the use of flash-and-freeze electron microscopy (Watanabe et al., 2013b) may allow the tight, temporal control of optogenetic uncaging of an RNAi construct, coupled with simultaneous light stimulation and high pressure freezing, thus allowing imaging of synaptic changes occurring as a result of gap junction ablation.

Irrespective of the mode of communication, as multi-pronged experimental protocols are honed and new techniques are developed or adapted, the ability to simultaneously control several variables will only help achieve better certainty in currently ambiguous experimental results.

4 The Vesicle Hypothesis; Adaptation States and Quantal Dynamics

4.1 Introduction

Drosophila R1-R6 and R7/R8 photoreceptors transmit visual information to the visual brain via Large Monopolar Cell (LMC 1-3) and Amacrine Cell (AC) interneurons in the Optic lamina (Strausfeld, 1971) and multiple potential cell targets in Medulla layers M1-M6 (Fischbach and Dittrich, 1989; Morante and Desplan, 2008; Takemura et al., 2008), respectively. Phototransduction occurs via a G-Protein Coupled Receptor (GPCR) mediated signalling cascade (Hardie, 2001), resulting in pre-synaptic voltage changes. These in turn, lead to vesicular quanta release in the form of histaminergic discharge from active zones (Gengs et al., 2002). Acting at the post-synapse through Histamine-gated Cl^- channels (*Ort/HisCL-α1/hclA*), Histamine serves a summatory and inhibitory effect upon LMC targets (Pantazis et al. 2008), thus affecting a hyperpolarisation of the LMC voltage in a graded fashion (Zheng et al., 2006).

Through these components, the *Drosophila* visual system has acquired the ability to resolve and adapt to environmental light patterns at wildly varying intensities, from individual photons (Henderson et al., 2000) to bright daylight (Juusola & Hardie 2001). These data show that graded photoreceptor voltage responses and the unitary microvillar responses to single photons of which they are composed, adapt in response to changes in ambient light levels. Such adaptation optimises their temporal resolution and information carrying capabilities for varying lifestyles (Gonzalez-Bellido et al., 2011) and light levels (Song et al., 2012), respectively.

Further work from the Juusola laboratory has shown that post-synaptic, macroscopic LMC voltage responses also adapt to variance in ambient illumination (Zheng et al., 2009) and

that this is also reflected in the estimated, bump-like responses to histamine vesicle receipt (Li, 2011). The latter data indicate that for increases in light intensity, estimated bump responses are reduced with respect to both their latency and amplitude and become more numerous. Similarly, LMC macroscopic voltage responses across Diptera become more transient and develop an improved resolution when faced with ongoing light incrementation (Laughlin et al., 1987; Juusola et al., 1995b; Nikolaev et al., 2009).

Relevant literature has reported the possibility of context-dependent variations in synaptic vesicle size. These include unexplained differences between R1-R6 (≈31nm) and R7/R8 terminals (44.45nm) (Takemura et al., 2008), increases in quantal size due to compound vesicle fusion in mammalian Calyx of Held synapses (He et al., 2009), and activity-dependent increases in synaptic vesicle size in the *Drosophila* neuromuscular junction (Steinert et al., 2006).

Such quantal bump adaptation can be observed in both rhabdomeric and LMC post-synaptic responses, with each subset of events being translated into macroscopic voltages, which themselves are inextricably linked (Li, 2011). Given this and the fact that differences in synaptic vesicle size have been observed before, it is reasonable to speculate that these adaptations may be similarly expressed in the quantal release and capture of neurotransmitter across the photoreceptor-LMC synapse. It is hence our hypothesis that, in line with the aforementioned photoreceptor and LMC data, synaptic vesicle size/volume/area will change in accordance with light intensity; decreasing in response to light increment, leading to reductions in LMC bump characteristics, whilst the converse should be true for light decrements (Juusola et al. 1995).

Here I explore such a possibility in the *Drosophila* retina. I initially employed transmission electron microscopy to visualise changes in synaptic vesicle area occurring at R1-R6 photoreceptor terminals, in accordance with variations in ambient light levels. I used a

conventional, aldehyde-based fixation protocol (similar to Meinertzhagen & O'Neil 1991), in tandem with a program of either light or dark adaptation. I used semi-thin and ultra-thin microtomy techniques to expose synaptic terminals of the first visual synapse in resin-embedded, half-head specimens of *Drosophila*.

Initial experiments using conventional fixation yielded suggestive, preliminary data implying that both synaptic vesicle area and number change during periods of light or dark adaptation. However, images acquired using this technique; whilst able to provide a proof of principle, were poor in contrast and plagued by non-seriality and common fixation artefacts, making them difficult to standardise or interpret with fidelity. For this reason I decided to undertake further experiments, utilising High Pressure Freezing and Automatic Freeze Substitution to fix and infiltrate the specimens. These methods remove fixation artefacts associated with aldehyde-based techniques, (Smith and Reese, 1980), and sample dehydration (Grace and Llinás, 1985) and also enable simultaneous fixation and light stimulation, as per Erik Jorgnsen's work on Ultrafast Endocytosis (Watanabe et al., 2014, 2013a, 2013b). This latter investigation is still ongoing.

4.2 Methods

All initial experiments were carried out on wild-type, Canton-S Isoline flies; 3-5 day old, female virgin flies were raised at 25^{o}C, on a standard, plant based medium in standard vials and selected for size.

4.2.1 Adaptation & Fixation (Conventional Aldehyde-based)

For experiments, flies were cold anaesthetised on ice, whilst being simultaneously pre-exposed to a given, 2-3 minute adaptation paradigm; either being enclosed in a uniformly reflective vial and subjected to light stimulation using a Cairn, broadband LED (range ≈410-740 nm) or being enclosed in an aluminium foil-covered vial also attached to the aforementioned LED, but without power.

Light-adapted subjects were transferred to a drop of pre-fixative (modified Karnovsky's fixative; 2.5% glutaraldehyde, 2.5% paraformaldehyde in 0.1 M sodium cacodylate buffered to pH 7.3 - as per Shaw et al. 1989) on a transparent agar dissection dish and were lit from above by a second, gooseneck, broadband light source (Luxeon Star/O, p/n: LXHL-NWE8, ≈410-740 nm range). Dark-adapted subjects were dissected in a dark, windowless room, lit using a Kodak Beehive darkroom safelight with Kodak 1 Safelight Filter attached.

Dissection was performed using a shard of Feather S razor blade, held in a blade holder. Flies were transferred onto their backs and insect pins, inserted into the lower abdomen and distal proboscis, were used to restrain them. The proboscis was first excised from the head, and then the head was removed from the body and halved. Left half half-heads were collected in fresh pre-fixative and kept for two hours at room temperature under relevant lighting conditions, in accordance with their adaptation paradigm.

After pre-fixation samples were subjected to two, 15 minute washes in 0.1 M Cacodylate buffer, and then transferred to a 4 ^{o}C, 1 hour post-fixative step in the fridge, comprising Veronal Acetate buffer and 4% Osmium Tetroxide. Flies were moved back to room temperature and after a nine minute wash in 1:1 Veronal Acetate and ddH2O, samples were serially dehydrated in multi-well plates; using subsequent, nine minute washes in 50%, 70%, 80%, 90%, 95% and 2x 100% ethanol.

Post-dehydration, samples were then transferred to small, glass vials for infiltration. Fixed half-heads were covered in Propylene Oxide (PPO) for two, nine minute washes, then transferred into a 1:1 PPO:Epoxy resin mix (*Poly/Bed® 812*) and left overnight. The following morning fly heads were placed in freshly made, pure resin for four hours, then again into the oven in fresh resin for a further 72 hours at 60 ^{o}C.

Fixation protocol was kindly provided by Professor Ian Meinertzhagen at Dalhousie University, Halifax, Nova Scotia.

4.2.2 Sectioning & Staining

Embedded samples were first subjected to semi-thin sectioning (1 µm section thickness) using a glass knife mounted in a Leica Ultracut UCT microtome. Samples were sectioned, collected on glass slides, stained using Toluidine Blue and then observed under a light microscope. This process was repeated and the cutting angle continuously optimised, until the correct orientation and sample depth was achieved; stopping when a dense spot of pigment, comprising the distal lamina, was discernible. Semi-thin sectioning was continued until approximately 40 lamina cartridges were visible, the block was then trimmed and shaped for ultra-thin sectioning. The latter preparation becomes necessary to reduce cutting pressure on the sample block, thus helping to prevent 'chattering' artefacts in the sections.

Ultra-thin (60 nm section thickness) sections were taken using a DiATOME Ultra 45 ^{o} diamond cutting knife, mounted and controlled using the Leica Ultracut. The knife edge was first cleaned using a special polystyrol rod, to ensure integrity of the samples block face upon cutting, cutting angles were aligned and automatic approach and return speeds set

on the microtome. Sectioning was automatic and samples were collected in the knife water boat.

Sections were collected on Formvar-coated, mesh grids and were then stained for imaging; ten minutes in Uranyl Acetate, wash in ddH2O, then five minutes in Reynolds' Lead Citrate, (Reynolds 1963), with a final ddH2O wash.

Cutting for the conventional methodology was performed by Zhiyuan Lu at Dalhousie University, Halifax, Nova Scotia.

4.2.3 Terminal Selection, Microscopy & Image Encoding/Blinding and Analysis

4.2.3.1 Selection

For each condition (dark and light adaptation), three flies were selected and from these flies, 30 cartridges were imaged, of which a single terminal was chosen for analysis. Lamina cartridges were selected from sections at random, throughout the depth of the Optic Lamina and were chosen based on the stipulate that six photoreceptors, without cutting blemish or fixation artefact, must be observable.

4.2.3.2 Encoding

To afford a blind analysis of the data all images were given a coded name by Dorota Tarnogorska at Dalhousie University, Halifax, Nova Scotia. Sections from each fly were mounted on separate grids and each grid was assigned a letter (K, N, & O for the light condition, L, M, & P for the dark condition). Each imaged terminal was given an encoded

name. This contained a randomised 4 digit prefix and a suffix, containing the latter grid assignation and an additional two randomised letters. The central pair of prefix digits were used to further distinguish between light and dark terminals, with light adapted sample codes containing digits that add up to an even value, and dark codes containing an uneven central digit pair, thus producing an image name such as the following:

Light – 8221QKg

Dark – 3251CWm

4.2.4 Image Analysis & Vesicle Selection Criteria

Images were analysed using ImageJ v1.46r software. Images were analysed so that the 200 nm scale bars for each image were standardised to 261 pixels in length (1 nm = 1.305 pixels). Photoreceptor synaptic terminals were identified by the presence of capitate projections, i.e. stalk-like epithelial glia connections occurring at photoreceptor synapses (Trujillo-Cenóz, 1965; Stark and Carlson, 1986). Histaminergic synaptic vesicles were identified by their electron dense outer boundary and clear inner core (dense core vesicles are electron dense throughout).

To begin with, a subset of images were analysed in two different ways to ascertain the optimal selection strategy. Images were firstly subjected to a traditional, stringent selection process, in which vesicles were selected and analysed based upon the uniformity of planar profiles, the perceived/apparent 'roundness' of vesicles, their distinguishability based upon their relative contrast and measurement of their external vesicle diameter.

A less restrictive strategy was trialled next. Here vesicles were selected based upon accommodating vesicular diameter variance, allowing elliptical vesicle profiles and the use of less well defined subjects and a perceived/apparent adherence to the internal diameter of the vesicle membrane.

4.2.5 High Pressure Freezing & Automatic Freeze Substitution

The practicalities of using this process require that dissection and adaptation be carried out in a slightly different manner. Additionally, due to its novel application, the process was subject to considerable troubleshooting and ongoing optimisation.

In similar fashion to that employed during conventional fixation, flies were pre-adapted whilst being kept in either; uniformly reflective fly vials and lit using a broadband, Cairn Research LED (light condition) or in aluminium foil-covered vials and unpowered LED. Flies were, one-by-one, transferred to a transparent Sylgard®-covered dissection dish, pinned and dissected. Upon dissection, left-half fly half-heads were placed into gold-plated, Leica specimen carriers (0.6 mm thickness, 1.2 mm diameter, 400 µm depth) then inserted into a manual, Leica bayonet sample holder. Before insertion, any remaining, 'empty' space in the carrier basin was filled using Hexadecene, an hydrophobic and inert cryoprotectant that helps prevent the ingress of ice crystals into the sample. Later iterations of the protocol utilised Heptane, as per Thijssen et al. (1998). The bayonet system was loaded into the Leica EM PACT2 High Pressure Freezer system and was exposed to broadband light stimulation, from an LED fastened onto the loading corridor wall; the LED was positioned to maximise illumination of the preparation whilst awaiting proper loading in situ. Illumination was continued until the specimen was fired into the freezer proper.

Upon freezing, which typically takes around 60 ms at between 2040-2100 bar, specimens were retained in their pods in a liquid nitrogen chamber, cooled to -96 ^{o}C, until ready for transfer into a Leica EM AFS2 for semi-automated Freeze Substitution (AFS). Samples were transferred from liquid nitrogen into the AFS cocktail (Acetone dried over $CaCl_2$, 1% OsO_4, 0.25% glutaraldehyde, 1% Uranyl Acetate) and kept at -90 ^{o}C for 30 hours. From then fly heads were brought up to -60 ^{o}C, heating at a rate of 5 ^{o}C/hour. Heads were held at -60 ^{o}C for eight hours, then brought up to -30 ^{o}C, heating at a rate of 5 ^{o}C/hour. After holding the samples at -30 ^{o}C for another 8 hours, they were put on ice at 0 ^{o}C for one hour, and then were subjected to three, one hour washes in fresh Acetone. Fly heads were then moved to a mix of Acetone and Poly/Bed 812 resin (2:1 or 50:50) for three hours at +4 ^{o}C, following which heads were moved into fresh Acetone:Poly/Bed mix over night at room temperature on a rotor to aid infiltraton. The next morning samples were twice placed in fresh Poly/Bed for seven hours per change, again on a rotor, after which they were ready for embedding.

After infiltration, specimens were transferred into moulds containing fresh Poly/Bed resin for embedding. Heads were oriented using a toothpick and then placed in the oven, at 60 ^{o}C for 72 hours. Sectioning occurred in the aforementioned fashion.

4.3 Results

4.3.1 Conventional, Aldehyde Fixation

Using conventional fixation and infiltration techniques, it was possible to produce electron micrographs of photoreceptor terminals in the *Drosophila* Optic Lamina for analysis (using

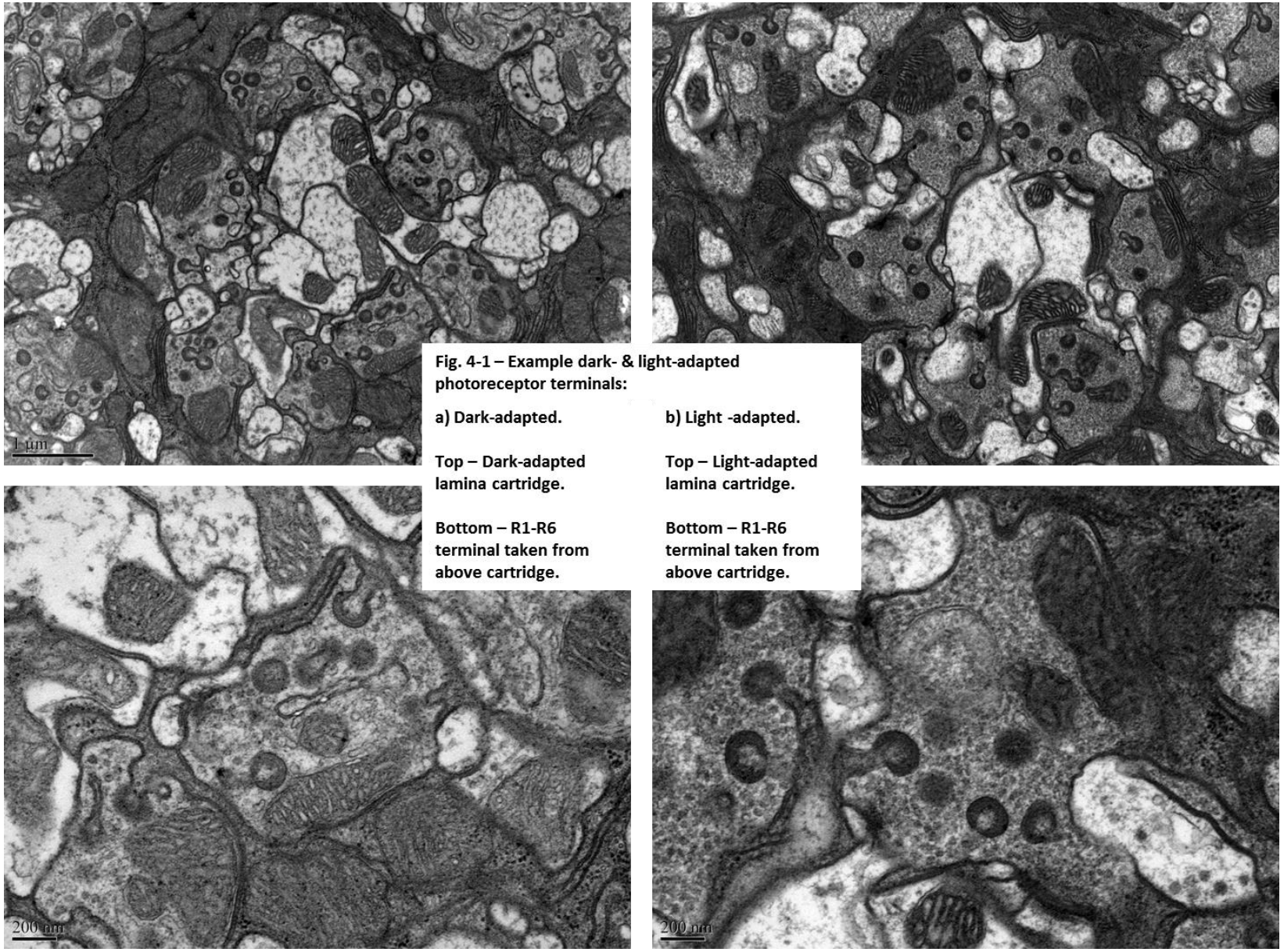

Fig. 4-1 – Example dark- & light-adapted photoreceptor terminals:

a) Dark-adapted.

Top – Dark-adapted lamina cartridge.

Bottom – R1-R6 terminal taken from above cartridge.

b) Light -adapted.

Top – Light-adapted lamina cartridge.

Bottom – R1-R6 terminal taken from above cartridge.

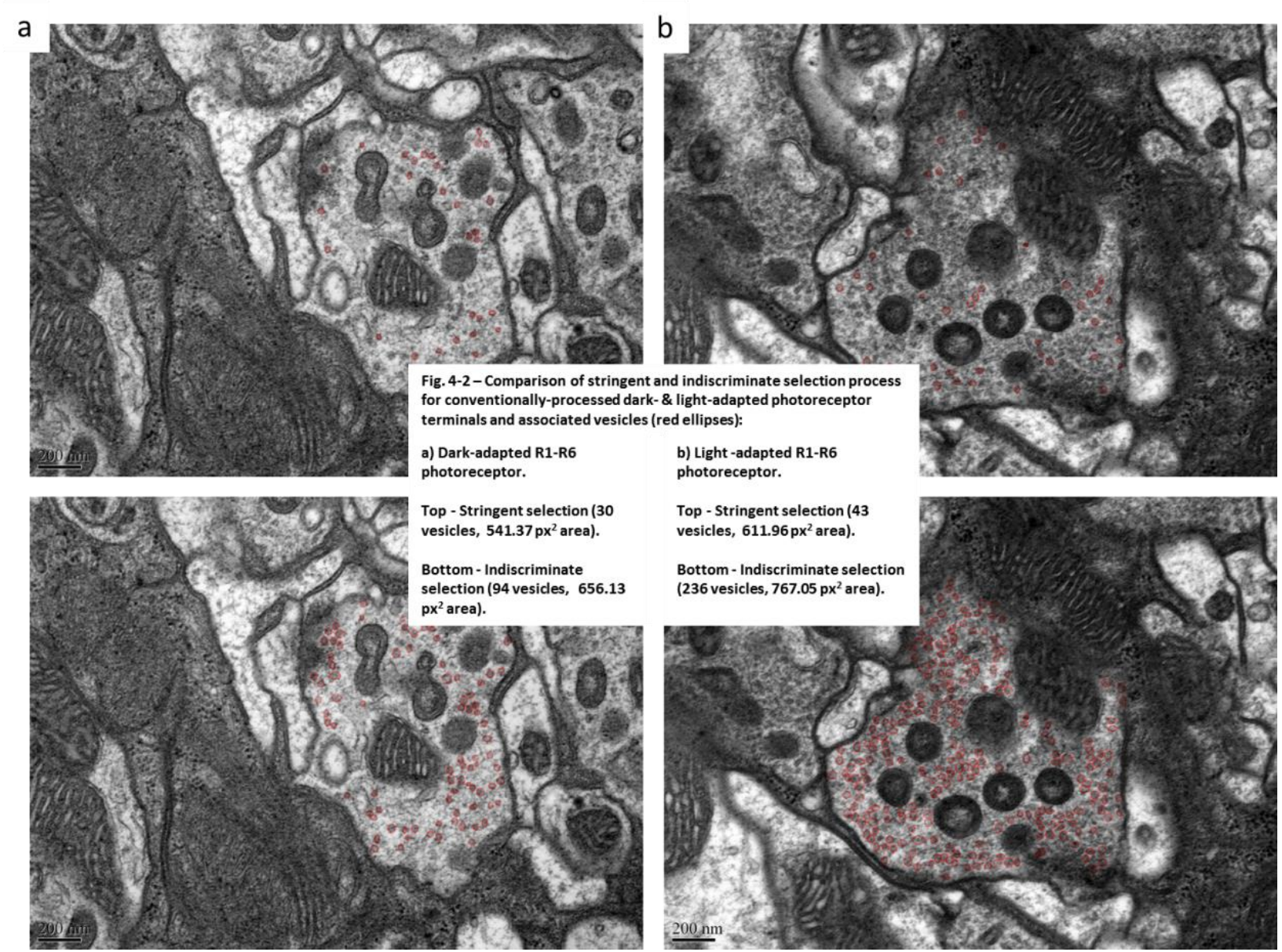

Fig. 4-2 – Comparison of stringent and indiscriminate selection process for conventionally-processed dark- & light-adapted photoreceptor terminals and associated vesicles (red ellipses):

a) Dark-adapted R1-R6 photoreceptor.

Top - Stringent selection (30 vesicles, 541.37 px^2 area).

Bottom - Indiscriminate selection (94 vesicles, 656.13 px^2 area).

b) Light -adapted R1-R6 photoreceptor.

Top - Stringent selection (43 vesicles, 611.96 px^2 area).

Bottom - Indiscriminate selection (236 vesicles, 767.05 px^2 area).

the open-source ImageJ v1.46r software). This approach allowed me to record and analyse the number and area, in pixels, of apparent synaptic vesicles.

4.3.2 Selection Optimisation

Vesicle selection methods were compared and criteria were optimised to not restrict the range of possible vesicle shapes and sizes available for selection (see methods section 4.2.4 for details). Stringent selection criteria produced undifferentiated, shotgun-type scatter of vesicle area vs. number data plots (**Fig. 4-3**).

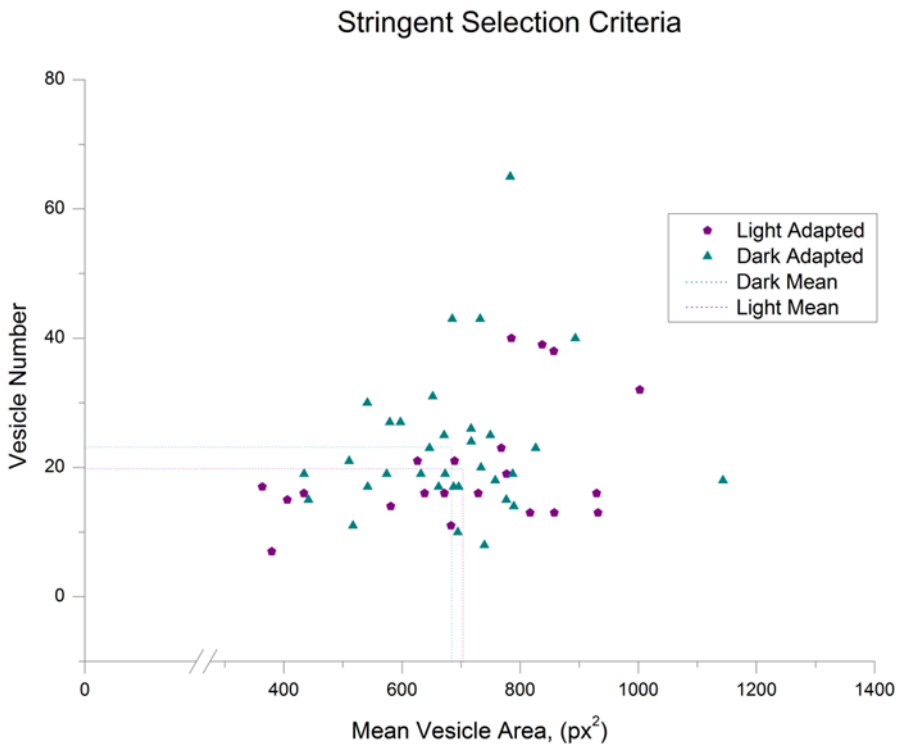

Fig. 4-3 – Stringent test criteria employed during vesicle selection. Data were selected using very defined standards, e.g. population uniformity, high sphericity or contrast, non-overlapping vesicle profiles and use of the external diameter as a means to determine vesicle area. Such a selection process gives rise to a shotgun-like scatter of total vesicle number per terminal, over mean vesicle pixel area for each terminal.

Conversely, using relatively indiscriminate selection criteria gave rise to distinct vesicle population plots which were distinguishable based upon both their pixel area and their numbers (**Fig. 4-4**).

4.3.3 Indiscriminate, Internal Vesicle Selection

Based upon the aforementioned selection criteria optimisation, vesicle selection was undertaken using the relatively indiscriminate selection criteria and measurement of the internal vesicle diameter. Using this methodology, I was able to record many more vesicles per electron micrograph (**Figs 4-2** & **4-5**) ultimately resulting in the finding that light and dark adapted vesicle populations separated on the basis of vesicle area and number (n=174).

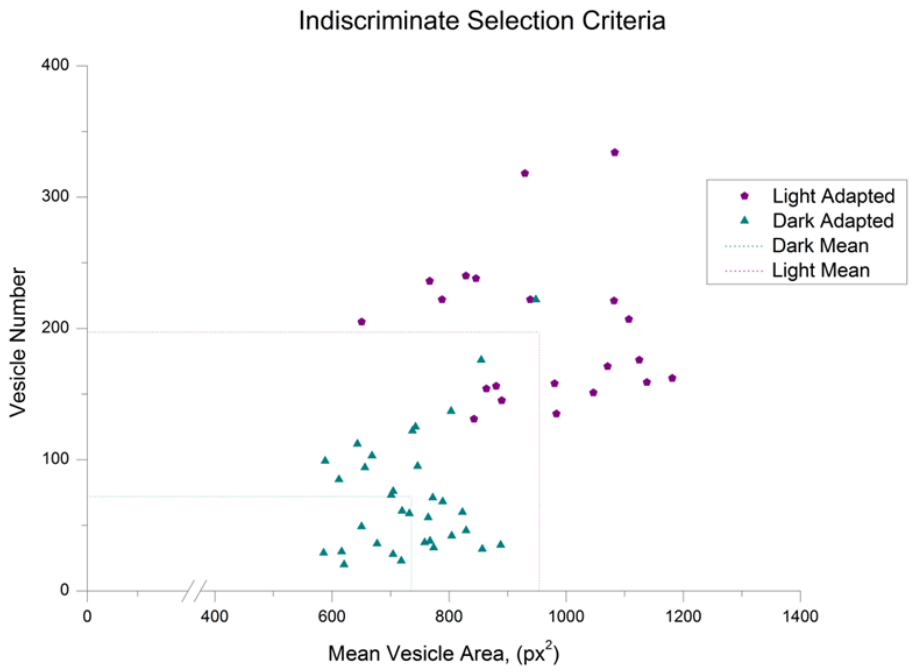

Fig. 4-4 – Indiscriminate test criteria employed during vesicle selection. Vesicles were selected using looser standards, allowing for vesicular non-sphericity, lower contrast vesicle boundaries , overlapping vesicle profiles and by the use of the internal diameter as a means to determine vesicle area. This selection process gave rise to distinct vesicle populations based upon both total vesicle number per terminal, over mean vesicle pixel area for each terminal.

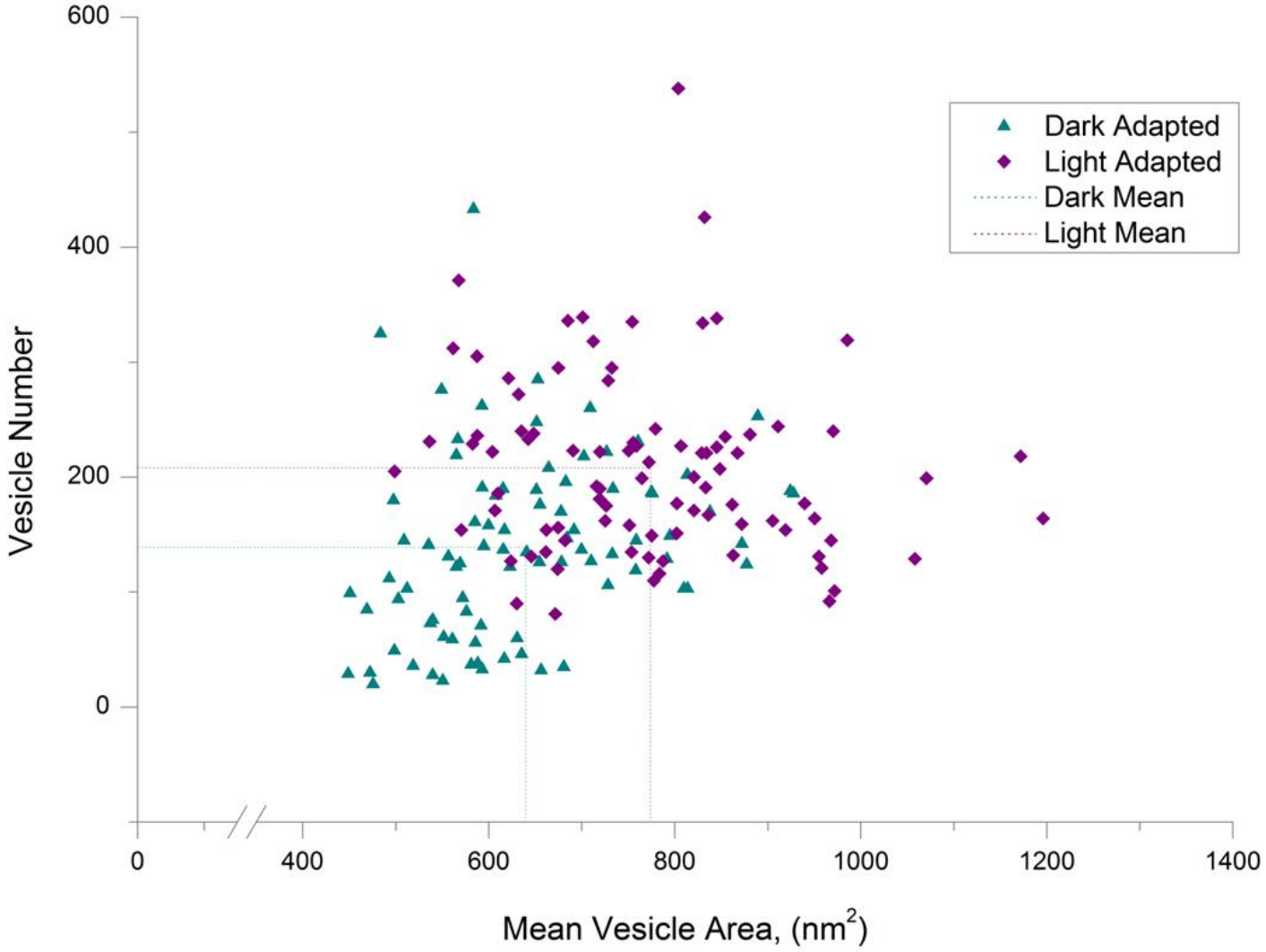

Fig. 4-5 – Final dataset. Synaptic vesicles were selected using an indiscriminate approach outlined in section 4.2.4 and Fig. 4-2, resulting in the separation of two distinct groupings of vesicles based around mean vesicle pixel area per terminal, over total vesicle number per terminal. These groupings were derived from fly populations exposed to saturating light or prolonged darkness, prior to and during fixation.

From 174 electron micrographs 30355 synaptic vesicles were recorded in total, 11804 dark adapted and 18551 from the light condition. Vesicle areas were measured in pixels and converted into nm, with dark adapted vesicles averaging 834.551 px^2/640.940 nm^2 and light adapted vesicles averaging 1010.041 px^2/772.486 nm^2.

Due to the inherent subjectivity in the vesicle selection process and the resulting necessity for third-party verification, 10 random electron micrographs per condition were sent to Dorota Tarnogorska at Dalhousie University, Halifax, Nova Scotia. Only vesicle areas were recorded and analysed, and more stringent selection criteria were employed. In concordance with the full dataset analysed previously, light and dark adapted vesicle populations significantly showed respectively bigger and smaller synaptic vesicle areas (n = 20, p = 0.01).

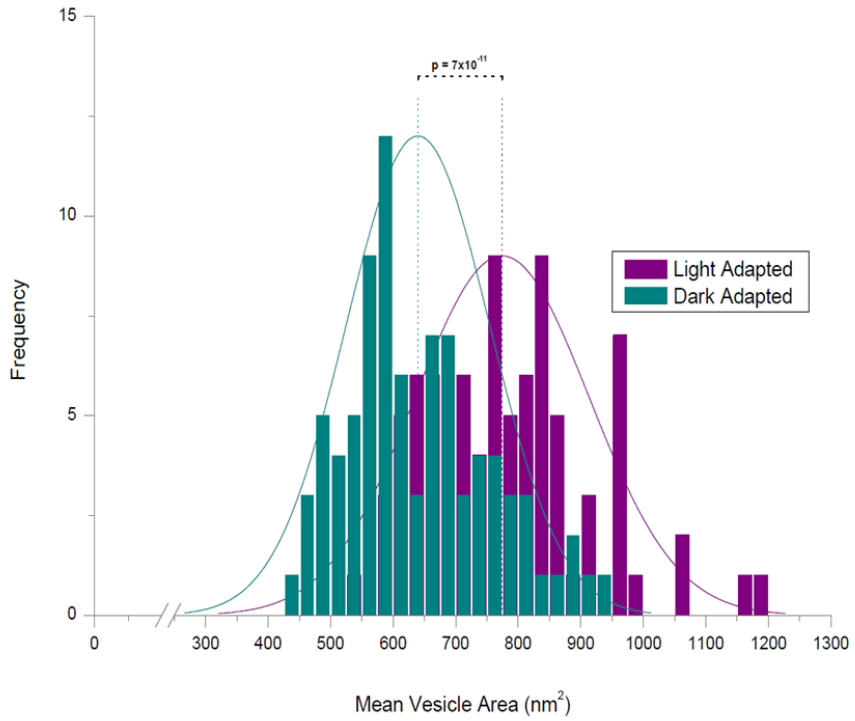

Fig. 4-6 – Final dataset. Histogram representation of vesicle data in Fig. 4-3. Light- and dark-adapted synaptic vesicle populations show distinct population means and distributions based upon synaptic vesicle area (df = 172, n = 174).

Moreover, by the same two-tailed, two sample Student's T-Test for equal variances, the dark and light adapted mean vesicle areas from the full dataset also proved to be significantly different (**Fig 4-6;** n = 174, df = 172, $p = 7 \times 10^{-11}$). Statistical analyses of vesicle numbers was not carried out for reasons alluded to in the section introduction and will be further discussed in depth later.

4.3.4 High Pressure Freezing & Automatic Freeze Substitution

Achieving good relative contrast and organelle integrity are tantamount to faithful analysis of imaged cellular components. To this aim, I utilised High Pressure Freezing (HPF) and Automatic Freeze Substitution (AFS) to better the aforementioned characteristics of future imaged synaptic terminals (**Fig. 4-7**). The theoretical limitations of cryofixation suggest that the beneficial effects of freezing drop off with increased specimen size. This is unless samples are frozen at high pressure, (Moor et al., 1980), and relevant cryoprotectants are used (Thijssen; Van Went; Van Aelst, 1998). These and other pre-requisites gave rise to the need for considerable protocol optimisation and troubleshooting.

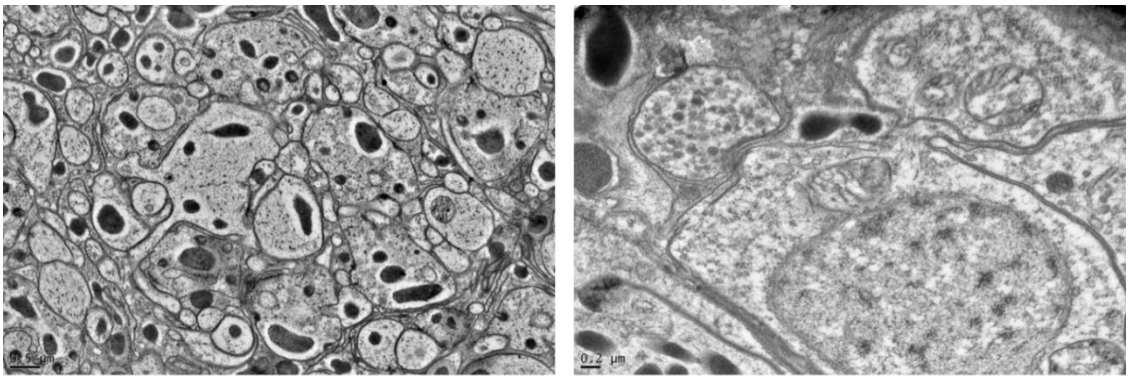

Fig. 4-7 – Example test images from initial HPF/AFS trials without light control:

Left – Example lamina cartridge ultrastructure. HPF/AFS-derived images show enhanced contrast and ultrastructure preservation is much better than for traditional aldehyde-based fixation (see Fig. 4-6).

Right – Example vesicles and axon bundles, at a pre-lamina stage. At present, achieving preservation of the visual lamina has been inconsistent. Further optimisation of the HPF and AFS protocols is necessary.

Starting with the rapid freezing and AFS of *Drosophila* retinae (Mun et al., 2005), I tested the effects of various protocol modifications upon the integrity of *Drosophila* half-head tissue samples. Such variations were deemed necessary based upon observations on the consistency of embedding made during cutting, image-based observations of contrast, freezing artefacts and cartridge integrity.

Modifications included the ratio of Acetone and Poly/Bed resin during infiltration, changed from 2:1 to 50:50 due to poor embedding. This resulted in spontaneous collapse of sections cut from the resin block. Further changes were made in the amount of OsO_4 used in the AFS cocktail for lipid staining, (Collin, 1974; Collin et al., 1973); and the type of cryoprotectant used; changed from 1-Hexadecene to Heptane (Thijssen; Van Went; Van Aelst, 1998).

4.4 Discussion

Previous electrophysiological investigation has shown that presynaptic photoreceptor responses are tightly linked via synaptic transmission to post-synaptic LMC responses (Li, 2011). In parallel, microvillar quantum bumps (Song et al., 2012) and light-induced photoreceptor voltage changes (Juusola & Hardie 2001), have been shown to adapt dynamically to varying environmental light conditions. Since the mechanisms by which photoreceptors both receive and encode information are modified by experience-driven external input, it is a reasonable assumption to make that these presynaptic processes should translate into synaptic adaptations also. This given, using transmission electron microscopy (T.E.M.) in association with traditional aldehyde-based fixation, standard alcohol dehydration and an LED-driven light/dark adaptation protocol, I have attempted to

quantify changes in synaptic vesicle size, occurring as a result of changes in light intensity in R1-R6 photoreceptor terminals.

To address the inherent subjectivity of the vesicle selection process, a substantial optimisation of the selection process had to precede the analysis. In standard practice, it is usual to select organelles for analysis on the basis of their adherence to a rigid set of characteristics, i.e. a typical profile, size, depth, etc… This set of criteria helps to ensure that, due to the inevitable generation of image artefacts caused by the dehydration and fixation steps, only subjects that fall within 'ideal' parameters are selected for analysis.

During selection optimisation, it became apparent that a large number of obvious synaptic vesicles were being rejected, often 100s per image, and that the majority of these rejected vesicles were those that potentially could indicate important differences between the populations (**Figs 4-2, 4-3** & **4-4**). Taking this into consideration, alongside the accommodation of signs of typically observed image artefacts (e.g. non-round vesicle profiles or non-standard sample depth) I decided to employ a less stringent selection process. This was based around the use of a non-traditional methodology which allowed the acceptance of elliptical vesicle profiles, overlapping vesicle profiles and lower contrast objects (see section 4.2.4 for more details). To offset this relaxation in vesicle acceptance I decided to measure their size using the internal diameter as an outer boundary. This helped to ensure that I did not over-estimate vesicle diameters during measurement. Additionally, all optimisation and subsequent selection was carried out in a blinded fashion, with images being both generated and encoded by a third party.

Such intrinsic subjectivity of selection means that large numbers of samples must be analysed, 174 synaptic terminals in this case. This in turn requires that very small p-values must be attained in order to achieve statistical significance, and counter their dilution by an increasing sample size. The means of 30355 synaptic vesicles were recorded and analysed

across all imaged terminals, resulting in a highly significant difference between light and dark adapted conditions ($p = 7 \times 10^{-11}$); with light-adapted terminals showing larger and more numerous vesicles than those in dark-adapted flies (**Fig. 4-5** & **4-6**). Our initial hypothesis had stated that synaptic vesicle diameter/area/volume, and therefore efficacy, should increase or decrease as a result of light decrements or increments, respectively. This was assumed to optimise the temporal resolution and information carrying capacity of *Drosophila* photoreceptors in line with the aforementioned electrophysiological data. However, the conventional E.M. data presented here suggest the opposite.

In support of our findings, different diameter synaptic vesicles (31 nm in R1-6, 44.45 nm in R7/R8) have previously been observed for the same neurotransmitter type (Takemura et al., 2008). These preliminary, blind analyses of electron micrographs shown here confirm this, showing an approximate >20% increase in mean vesicle area across all terminals quantified for a given condition.

To further validate these results we sent 10 random images for each condition to the third party responsible for blinding the study. These images were analysed and compared using separate criteria, ultimately producing a similarly relevant significant result ($p = 0.01$).

An aside to these findings is the physical relationship between the generation of synaptic vesicles and the amount of available plasma membrane. Vesicle recycling rates determine the amount of available plasma membrane, and thus impose restrictions upon the size and number of synaptic vesicles generated per synaptic event (Heuser, 1973). According to this view, and in line with our original hypothesis, changes in vesicle diameter/area/volume should be accompanied by changes in the number of vesicles in other words, for images where vesicles possess larger profiles there should be lower total numbers of vesicles, whilst the converse should be true for images where vesicle profiles are smaller. Somewhat

controversially these initial analyses do not correlate with these assumptions, instead showing results contrary to prior expectation.

Furthermore, due to ubiquitously poor image quality, I was unable to confirm the validity of the numbers of synaptic vesicles recorded in this study. As such, I have relinquished the opportunity to conduct any in-depth statistical analysis on synaptic vesicle number data acquired during this study so far.

These preliminary findings appear potentially contradictory to the electrophysiological LMC voltage analysis (Li, 2011), which suggests that the amplitude of their bump-like histamine responses decreases with increasing brightness. However, my results show that exposure to a saturating broadband light stimulus results in an increase in vesicle area and may increase vesicle numbers also. Should these results be a true reflection of the mode of neurotransmission at the synapse, this may necessitate the expression of an unknown mode of regulation that serves to change the distribution of post-synaptic responses. This is because larger vesicular quanta are expected to generate larger post-synaptic bumps.

Such regulation may manifest in several ways. Perhaps there is a selective, diffusion-based filtering of synaptic content, shaping post-synaptic exposure to released Histamine. Alternatively, *Ort* receptor kinetics may be modified, producing decreasing bump responses in the face of a saturating stimulus. Or maybe the increase in synaptic size is a consequence of dual-packaging and release of multiple neurotransmitters, leading to dual-gating of post-synaptic *Ort* receptors. One interesting consideration may be that post-synaptic receptors may display a ‘refractoriness’, whose time-course matches the stochasticity and level of histamine input. Song et al., (2012, 2014), elucidate a mechanism in Drosophila photoreceptors, whereby the number of available microvilli (photon sampling units) is regulated by their intrinsic refractoriness occurring after photon absorption. As large numbers of photons may be involved, the refractory period prevents saturation allowing

the sampling unit pool to be refreshed. Post-synaptic receptor activation could employ such a mechanism allowing similar dynamic optimisation for varying levels of input.

There are other findings, which lend support to the notion that modified receptor function may be responsible for this discrepancy. In dissociated L1/L2 LMCs, the potency of Histamine at the *Ort* receptor has been shown to be greatly reduced in Ort^{P306} receptor mutants (Gengs et al., 2002). Such mutants show altered photoreceptor voltage dynamics, responding with similar amplitudes, but faster and with a greater SNR at saturating light intensities (Zheng et al., 2006). These dynamics are suggestive of enhanced synaptic feedbacks acting upon photoreceptor output. Moreover, Ort^{P306} mutants show reduced adaptability in both photoreceptor and LMC outputs (Nikolaev et al., 2009). It would be interesting to carry out these electron microscopic analyses upon such Ort^{P306} flies, to test whether LMC-derived feedback is responsible for alteration to synaptic vesicle dynamics. Another such experiment would be to see whether the expression of *Kir2.1* in R1-R6 photoreceptors might result in reductions in synaptic vesicle size. The *Kir2.1* channel is a human inwardly-rectifying K^+ channel, whose expression can be genetically induced in neurons of a variety of organisms for the purpose of causing hyperpolarisation (Johns et al., 1999). Expression of this channel would mimic dark-adaptation through the enforcement of a constitutive hyperpolarisation, and could be used to test the voltage-dependence of these synaptic phenomena.

The *Drosophila* eye expresses two different Histamine-gated chloride channel sub-units, *HisCl-α1* and *HisCl-α2* (Gisselmann et al., 2002; Zheng et al., 2002). Each sub-unit, when expressed in *Xenopus* oocytes, appears to possess different functional characteristics. The α2 sub-unit shows dual sensitivities to both Histamine and GABA when expressed in homomeric channels (Gisselmann et al., 2004), responding with a much greater sensitivity to Histamine. Conversely, Histamine shows lower potency at the α1 sub-unit, when

expressed in a homomeric fashion, alongside an absence of a response to GABA (Zheng et al., 2002). Gisselmann et al. (2004) also suggests that α1 and α2 sub-units, when expressed together in heteromeric channels, show a vastly greater sensitivity to Histamine. These findings were confirmed in Pantazis et al. (2008), who further showed that LMC voltage responses develop an enhanced latency when HisCl1 (α2 sub-unit) is mutated, the converse to what appears to be so for the α1 subunit (Nikolaev et al., 2009). The α1 sub-unit, expressed in homomeric channels, is also known as *Ort*. Perhaps in a similar fashion to Glutamatergic NMDA receptors in vertebrates (Philpot et al., 2007), there may be an activity-dependent regulation in the ratio of such α1/ α2 sub-units. This may contribute to homeostatic control of post-synaptic responses to increasing Histamine release.

From the current data, it appears that the relationship between pre-synaptic photoreceptor voltage, synaptic vesicle size and post-synaptic LMC responses is not a simple one, and what these findings actually mean certainly remains to be seen. This ambiguity manifests in some part due to the 'quality' of the images generated; which becomes confounding as a result of bad contrast and definition, both of which are tantamount to efficient vesicle identification, selection and quantification. To attain better preparation integrity, image definition and consistency, we aim now to use T.E.M. and similar adaptational protocols in conjunction with High Pressure Freezing and Automatic Freeze Substitution (HPF/AFS). These techniques, in recent times, have been revitalising the study of synaptic transmission. Specifically, they have helped to challenge previous assumptions related to synaptic vesicle dynamics by allowing simultaneous millisecond optogenetic control of synaptic function. When coupled with instantaneous sample freezing, they have elucidated the temporal time scale of endo- and exo-cytotic processes that had previously been unresolvable (Watanabe et al., 2014, 2013a, 2013b).

With regards to use of the latter technique in this context, as the preparation (*Drosophila* half-heads) must be fixed inside the confines of the high pressure freezer, unlike during conventional processing, we are currently unable to continuously light-adapt the specimen once it is loaded into the relevant specimen carrier. As a result of this complication, we are attempting to produce a light stimulation preparation holder (see Watanabe et al., 2013; Nägerl et al., 2014), which would allow simultaneous light stimulation and freezing, along with a very precise temporal control of the adapting stimulus. Moreover, current protocols are not optimised for using such a large preparation, as they tend to be based upon the use of samples that adhere to the theoretical size limits for maximal benefits of high pressure freezing (≈200 µm at 210 MPa - Studer et al. 2008). Given these factors, several aspects of the protocol must be optimised further for this technique to work. These include, for example, the type of cryoprotectant used; i.e. Hexadecene, which is insoluble in Acetone at low temperatures (Hohenberg et al. 1994; Thijssen; Van Went; Van Aelst 1998), and therefore may affect the infiltration of acetone, stains and other AFS cocktail components during freeze substitution. Additionally, the initial ratio of Acetone to Poly/Bed resin appears to adversely affect the solidity of the resin block during cutting.

Despite the necessity for considerable tuning, and the potential for some inconsistency due to environmental factors, the ability to use HPF/AFS will allow the generation of images that are more faithful to actual morphology. This will bring about the realisation of specific light stimulation and visualisation of synaptic events at a temporal scale not afforded by other techniques.

5 Ca^{2+}-activated K^+ Ion Channels and the Behavioural Response

5.1 Introduction

Neurotransmission and its immediate consequences require homeostatic regulation. Such mechanisms curb the functional tendency towards excessive amplification of excitation or inhibition during correlative stimulus-evoked pre- and post-synaptic activity, such as Long Term Potentiation or Long Term Depression, respectively (Abbott and LeMasson, 1993; Miller and MacKay, 1994). Such bi-directional synaptic gain regulation can have several implications, not least upon adaptability (Li, 2011), information processing (Niven et al., 2003b), metabolic cost (Niven et al., 2003a) and toxicity (Franklin et al., 1992). Due to the inherent robustness of neuronal homeostasis, modification of ion currents through the manipulation of channel expression can result in normal-like neuronal outputs (Golowasch et al., 1999; Marder and Goaillard, 2006; Prinz et al., 2004). But the effects of manipulation and intrinsic homeostasis can be difficult to separate and interpret.

Ca^{2+}-activated K^+ ion channels can shape action potentials and dampen neuronal excitability. Their expression has been evolutionarily conserved (Abou Tayoun et al., 2011; Grimes et al., 2009; Klöcker et al., 2001), as has their function, with K^+ extrusion serving to re-balance positive ionic charges across the plasma membrane and affecting the after- and hyper-polarisation phases of generated action potentials.

In *Drosophila*, the *SK* Ca^{2+}-activated K^+ channel (*dSK*) and the *Slowpoke* BK channel (pore-forming α subunit, *dSlo*) show similar expression patterns in the optic lamina and retina (Abou Tayoun et al., 2011; Becker et al., 1995), though each channel displays its own defining gating and kinetics (Faber and Sah, 2003; McManus, 1991; Park, 1994). *dSK*

channels are small conductance channels, which are activated solely by Ca^{2+}, whilst *dSlo*-containing BK channels show a large conductance and are both voltage- and Ca^{2+}-gated.

Drosophila only has one copy of each gene for each of these channel sub-types, which in theory should make study of them more tractable. However the *dSlo* gene is subject to variable gene splicing in a tissue-specific fashion (Bohm et al., 2000; Yu et al., 2006), giving rise to functional differences (Lagrutta et al., 1994). To add to this complicated scenario, there are several known *dSlo* null alleles, which may generate functional effects upon both, muscular and neuronal systems (Atkinson et al., 2000; Brenner et al., 2000).

Following on from the findings in Abou Tayoun et al. (2011), in as yet unpublished data from the Juusola laboratory, *dSK*, $dslo^4$, $dslo^{18}$ and *dSK;;*$dslo^4$ double mutant R1-R6 resting potentials were shown to be more positive than in wild-type flies, and all showed a lower membrane resistance. In each case, the findings suggested a lower activation threshold. Differences in visual performance were also reflected in R1-R6 voltage responses; with wild-type, *dSK*, $dslo^4$ and *dSK;;*$dslo^4$ double mutants showing faster rising times in bright light than $dslo^{18}$, whilst all mutants responded with a lower latency than wild-type flies.

In this chapter, by using optomotor assay, I set out to determine whether disruption to the function of *dslo* and/or *dSK* channels, and therefore a change in the feedback contribution of *Drosophila* LMC's upon photoreceptor synapses, can be indicated in the behavioural performance of flies tethered in a traditional flight simulator. In the same set up as explained in Chapter 1, I used spectrally-broadband fast (180^o/s) and slow (45^o/s) grating rotations in an open-loop configuration to ascertain if differences in the optomotor torque response correlated with previous electrophysiological data.

The data here suggest that the channel perturbations may be subject to descending homeostatic control that helps stabilise behaviour but drives fly vision to slightly different

perceptual regimes. This is because *dSK*;;*dslo*^{4} double mutants, *dslo*^{4} and also *dslo*^{18} hybrid flies showed fast and large responses to slow grating rotations that appear to be comparable in size to wild-type Canton-S optomotor responses in both conditions where responses are smaller with fast grating rotation, and larger for slow rotation; these findings also mirror current electrophysiological data. However, the opposite was evident for *dSK* mutants alone, showing enhanced responses to fast rotation stimuli and reduced responses for slow grating rotations, ultimately indicating a predisposition towards a decreased activation threshold.

5.2 Methods

5.2.1 Drosophila Genetics

5.2.1.1 Stocks

dSK^{-} mutant flies were generated as described in Abou Tayoun et al. (2011), whilst *dslo4*$^{-}$ mutants were gifted by Nigel Atkinson, University of Texas, Austin (Atkinson et al., 1991).

dslo4 is a null allele of the *dslo* gene, in which dysfunction is implicated in mutant neural and muscular phenotypes (Atkinson et al., 2000). Muscular dysfunction results in aberrant spike generation and irregularity in flight muscle action potentials (Elkins et al., 1986), thus impairing flight. The neural phenotype has been behaviourally characterised previously using the 'sticky feet' assay, where after exposure to a heat blast, or light flash, flies will fail to escape and will 'cling' to a given surface when pushed.

Ash2^{18} is a mutant allele of the *Ash2* gene, located directly adjacent to *dslo* (Adamson and Shearn, 1996) and normally required for maintaining relevant genetic regulation during leg

and haltere patterning in the *Drosophila* embryo (LaJeunesse and Shearn, 1995). Co-expression of $Ash2^{18}$ with *dslo* in a transheterozygous hybrid ($dslo^{18}$) results in a 20 kb deletion in the *dslo* C1-C2 promotor region, which confers a knock-out of *dslo* expression specifically in the *Drosophila* CNS (Atkinson et al., 2000). Such a knock-out 'rescues' the muscular phenotype (Atkinson et al., 2000; Brenner et al., 2000) whilst retaining the neural mutation. $dslo^{18}$ hybrid flies were also a gift from Nigel Atkinson.

From each genotype, I used 3-7 day old, female flies throughout the experiments. All flies were raised on standard plant-based media.

5.2.1.2 Flight Simulator

Optomotor experiments were predominantly carried out as described in Chapter 1, however two different types of rotational stimulus were used in order to test the ability of mutant flies to respond normally to stimuli of different speeds. Stimuli of 45^{o}/s and 180^{o}/s were programmed in MATLAB and applied at the flight simulator. Stimuli were illuminated by spectrally broadband light and had the same time-course and stimulus pattern, as used in previous standard optomotor experiments.

5.3 Results

Here I have used the traditional *Drosophila* flight simulator to determine whether behavioural change may come about through the genetic manipulation of *dSK* and/or *dslo* Ca^{2+}-activated K^{+} Ion Channels. Statistics were calculated on the total mean response (T-Test), and the variance for the period 2.5-3 s (one-way ANOVA), i.e. the peak optomotor

response to anti-clockwise grating rotation, so as to ascertain the effects of inter-subject variability.

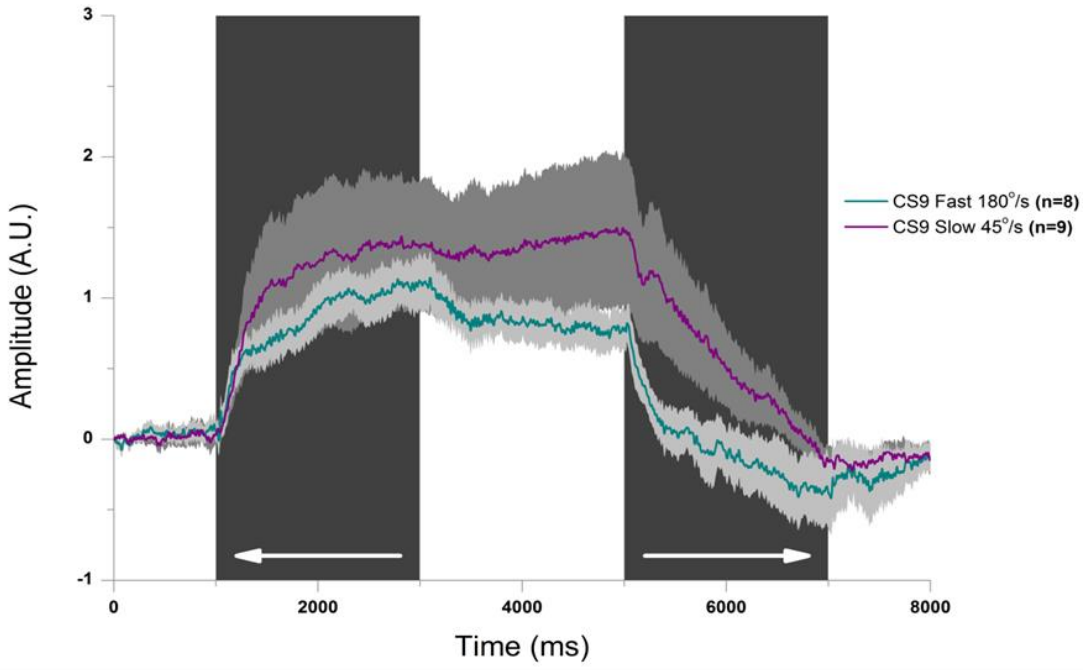

Fig. 5-1- Wild-type, Canton-S mean optomotor responses to fast (teal) and slow (purple) grating rotations. Canton-S flies appear to prefer the slower stimulus, though show a larger population variation for this rotational speed.

In opposition to Canton-S (**Fig. 5-1**), but corroborating the electrophysiology; where time-to-peak and response half-widths suggested a quickening of the photoreceptor response in bright conditions, *dSK* mutant flies showed larger responses to fast, 180°/s grating rotations (unpublished - T-Test, p=0.05).

Aside from catastrophic problems with their breeding and rearing, it became apparent after the observation of >20 flies that *dslo*^{4} mutants were also unable to fly consistently (**Fig. 3a**). Insufficient numbers were gathered to allow any statistical analysis. This failure to produce essential behaviours in robust fashion was attributed to the 'muscular' phenotype observed in *dslo* null mutants (see Atkinson et al. 2000 and Brenner et al. 2000). Such phenomena will be discussed at length later.

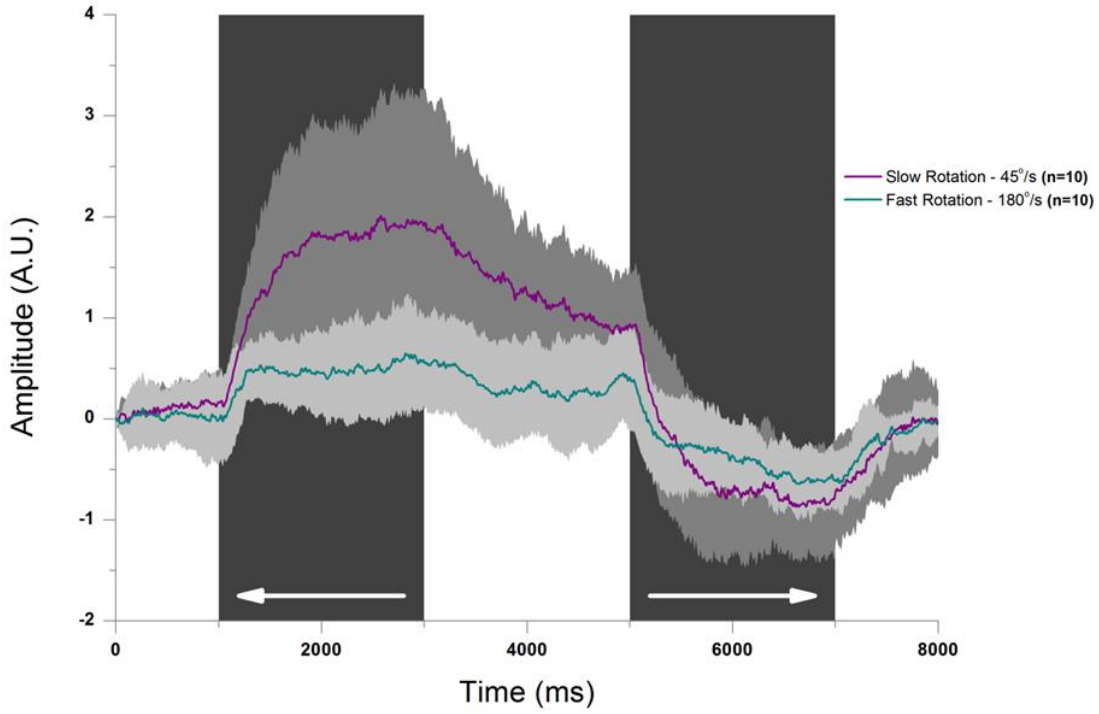

Fig. 5-2 - dSK;;dslo^4 double mutant mean optomotor responses to fast (teal) and slow (purple) grating rotations. As with Canton-S, the double mutant appears to prefer slower stimulus rotation, though again, shows very large variances in the population.

dSK;;dslo^4 double mutant flies did fly consistently and were shown to behave in a similar fashion to wild-type Canton-S flies (**Fig. 5-1** & **5-2**); they responded more strongly to slow 45°/s grating rotations than fast (n = 20, T-Test p = 0.01). For such double mutants, mean optomotor responses to fast 180°/s rotation were significantly different to wild-type (T-Test, p = 0.006), suggesting a deficiency in the ability to respond to high-frequency information. In contrast, differences in peak response variance were not found (one-way ANOVA, p = 0.45), implying that flies of each genotype responded in a relatively stereotypical fashion.

Conversely, when comparing *dSK;;dslo*^{4} and wild-type flies during slow 45°/s rotation, such inter-subject variability appeared statistically divergent (one-way ANOVA, p = 0.03), whilst mean responses did not (T-Test, p=0.58). To counteract the muscular phenotype, I used flies where *dslo* expression was rescued in the flight muscles, but retained in a

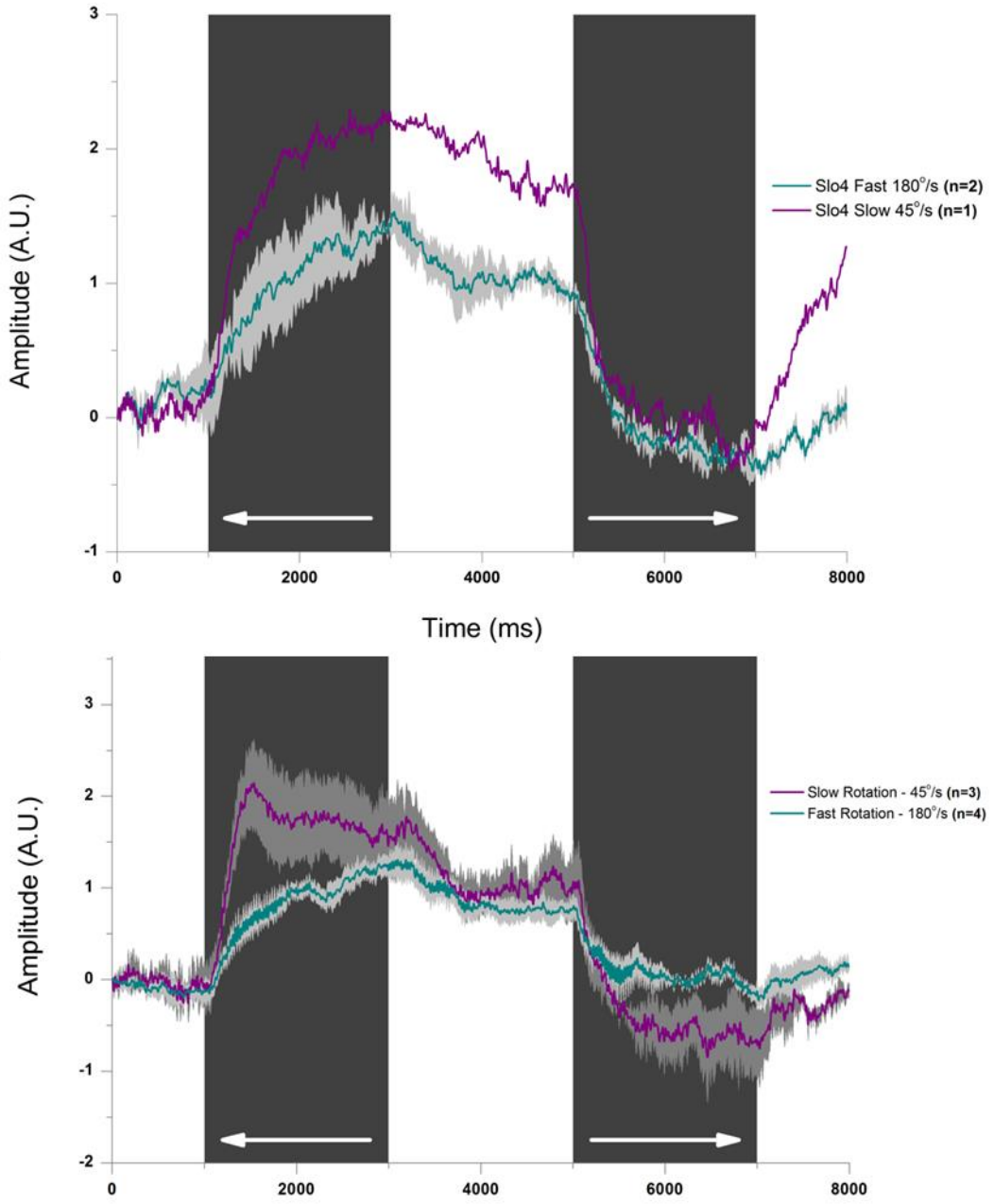

Fig. 5-3:

a) dslo^{4} mutant mean optomotor responses to fast (teal) and slow (purple) grating rotations. Such flies were unwell and gathering averaged responses became impossible, hence the low n numbers.

b) Rescued dslo^{18} mutant mean optomotor responses to fast (teal) and slow (purple) grating rotations. A lack of time prevented the gathering of more data for this figure.

dysfunctional state in neuronal cells. Known as *dslo*^{18}, such flies were easier to assay for optomotor responses, despite being equally as difficult to breed and raise (**Fig. 5-3b**). Numbers are as yet insufficient for proper statistical analysis, but preliminary optomotor data from such flies appear to correlate well with wild-type responses, with responses looking fast and strong to slow 45^{o}/s grating rotation as compared visually to fast 180^{o}/s motion.

5.4 Discussion

The data outlined in this chapter and other, aforementioned unpublished data, allude to the fact that, despite major alterations to the voltage function of *Drosophila* photoreceptors, robust and often wild-type like behavioural and electrophysiological responses can be generated by *dSK* and/or *dslo* mutants. Perhaps their involvement in photoreceptor homeostasis is not critical but synergistic and facilitatory, and therefore their respective and combined absence may be manageable at a cost, either by upregulation of the expression of their counterpart or by other underlying mechanisms, e.g. existence of a compensatory K^{+}/Cl^{-} leak conductance.

From previous data it can be inferred that wild-type *Drosophila* should generate stronger optomotor responses to slow grating rotation than to fast rotation (Blondeau and Heisenberg, 1982). *dSK*$^{-}$ flies showed atypical behaviour in this respect, as compared to wild-type Canton-S flies; responding more strongly to fast 180^{o}/s grating rotation but conversely with slow 45^{o}/s grating rotation. This preference for faster stimulation is further reflected in the apparent excitability of *dSK*$^{-}$ photoreceptors; i.e. faster voltage responses with a short time-to-peak, membrane resistance and high resting potential also (Abou Tayoun et al., 2011). *dSK*$^{-}$ LMC's show larger voltage responses at lower light levels, as

compared to Canton-S. They also show short time-to-peak response times, further suggesting a hyper-excitability.

Double, *dSK;;dslo*^{4} mutants almost seemed to mimic wild-type dynamics, but statistical differences suggest that this is not a simple story. Mean total responses to fast 180^{o}/s rotation are significantly different, with wild-type performing slightly better. In contrast, mean total responses to slow 45^{o}/s rotation were statistically similar, whilst response variation at peak response values for each individual fly was largely different. These data suggest that such flies are unable to respond to higher frequency information as well as wild-type; a suggestion that is again corroborated by the electrophysiology, with lower information capacities being observed at increasing light levels (unpublished data) and the presence of a delayed and sustained LMC voltage response.

dslo^{4} mutant flies appeared to possess the potential for producing responses in the image of their wild-type counterparts. However, muscular and neuronal co-morbidities and a lack of time have hindered further study. The *dslo*^{4} mutation is one of several *slowpoke* null mutants that show a dual phenotype, affecting both muscular and neuronal function in homozygotic mutants (Atkinson et al., 2000; Brenner et al., 2000). These papers highlight both a discrepancy in flight behaviour and the presence of a prolonged startle-type response known as the “sticky-feet phenotype”, both resulting from the homozygotic expression of one of several *dslo* null mutations.

What is not mentioned in these papers are the problems associated with breeding and raising these flies, with Atkinson et al. (2000) actually stating that flies are “healthy and fecund”. In our experience, *Drosophila* larvae between the 1st and 3rd instar stages tended to burrow into the media and remain there through pupariation, ultimately requiring manual extraction to prevent their death. Upon rescue and subsequent hatching, many 1-3 day old flies would also die, seemingly getting stuck at the bottom of a vial if left

unsupervised. Even if manual rescue of stuck, adult flies was achieved, the wings of such flies were often damaged, thus preventing their use in the flight simulator. These confounding characteristics of the relevant mutations often compounded with time constraints, meaning that I was incapable of generating sufficient behavioural data before the completion of my research timeframe.

For any analysis of the effects of *dslo* mutation to be relevant it is imperative that the muscular phenotype is rescued, as an inability to produce the relevant motor actions due to faulty biomechanics would invalidate any argument that behavioural differences are derived from visual dysfunction. As such, despite *dSK;;dslo*^{4} double mutant flies being apparently healthy and that a full set of data was acquired from these double mutants, the presence of the un-rescued homozygotic *dslo*^{4} mutation means that conclusions based upon visual impairment cannot be made faithfully.

dslo^{18} flies are transheterozygotic mutants flies that contain a second mutation appended to the *dslo*^{4} promotor region, which can be used to 'rescue' the muscular *dslo*^{4} phenotype. This mutation, *Ash2*^{18}, induces a break in the *dslo*^{4} neuronal promotor (see Chapter 3 methods for details), resulting in failed CNS expression of *dslo*^{4} whilst retaining its expression in muscular tissue. Such hybrid mutants were easier to assay for optomotor responses and appeared to reflect a wild type-like preference for slow grating rotation. However, such flies were also as difficult to breed and raise as homozygotic *dslo*^{4} flies, which meant that it was not possible to generate sufficient optomotor data for statistical analysis here either.

Comprehensive study of the *dslo*^{18} transheterozygote will be necessary to ensure faithful investigation of the visual effects of *dslo* mutation in this context. To follow the effects of *dslo* mutation through structure and function, it will be necessary to use intracellular electrophysiology, structural imaging and behavioural assay in a similar program to that

employed towards dSK and *dslo*^{4} mutants. Furthermore, expression of the transheterozygote in a double mutant *dSK;;dslo*^{18} construct and subsequent assay will also be necessary.

Likewise, although Abou Tayoun et al. (2011) show that *dSK* expression is "enriched" in the *Drosophila* optic lamina, the *dSK* gene is also known to be expressed in other adult organs; e.g. at 'moderate' levels in the adult heart, where its mutation has been suggested to affect adult heart rates (Sénatore et al., 2010). The specific role of dSK in such organs is not well characterised, but it is generally believed to universally function by opposing activity-driven Ca^{2+} loads, occurring in many excitable cell types. Whilst extra- or intra-cellular electrophysiology and structural studies may possess an inherent regional or cellular specificity, in a behavioural context where causal processes are not amenable to observation, it would be prudent to find a way of further localising expression of the mutant construct in the *Drosophila* eye before drawing definitive conclusions.

If taken alongside the electrophysiology, the behavioural data often appears confusing, as the specific characteristics may not follow intuitively. Certainly, dSK^{-} mutants seem hyper-excitable both in terms of their photoreceptor voltage time-to-peak response, response half-widths and their behaviour, but their information rates are wild type-like in bright conditions (Abou Tayoun et al., 2011). In un-rescued double mutant *dSK*;;*dslo*^{4} flies, there are some similar electrophysiological discrepancies that translate into impaired information rates in bright conditions, but their behavioural responses mimic wild-type dynamics, responding to slower grating rotations more strongly than to fast. Current *dslo*^{18} data suggests that photoreceptor voltage response half-widths are more compact than wild-type in brightening conditions and that their resting potentials are much more negative. Despite this, their information rates do not appear statistically significant when compared

to wild-type, and whilst being an incomplete dataset, behavioural responses also appear to mimic wild-type characteristics.

From these initial comparisons it is impossible to paint a clear picture without further specification and investigation, however it is reasonable to assume that unknown homestatic regulatory processes serve to maintain wild-type like behavioural function in dSK;;dSlo double mutants and are likely to function in other mutant derivatives. Ca^{2+}-driven voltages in excitable cells are well known to be subject to homeostatic regulation, e.g. in *Drosophila* through the function *Slowpoke* (Lee et al., 2008), *SK* (Abou Tayoun et al., 2011) and *Shaker* K^{+} channels (Niven et al., 2003a, 2003b). As such, the potentially deleterious effects occurring due to channel mis-expression or mutation could well be managed and compensated for homeostatically, perhaps through upregulation of the expression of synergistic ion channels, or alternatively the suppression of antagonistic components such as intracellular Ca^{2+} release and influx and/or Ca^{2+} persistence at the synapse. Despite not knowing the exact mechanism of regulation employed here, it is however, possible to see that behavioural responses can continue to be robust, appearing to resist changes in visual information processing capabilities that arise from mutation/expression-derived deleterious effects upon the proclivity and timing of photoreceptor responses.

6 Dietary Polyunsaturated Fatty Acids and the Optomotor Response

6.1 Introduction

In *Drosophila* eyes, light from the environment is channelled through the optics to the retinal surface using conduits known as Rhabdomeres. Along their length, these light guides (Kirschfeld and Snyder, 1976) contain ≈30,000 specialised microvilli, each possessing the necessary phototransduction machinery (Song et al., 2012). This PLC-mediated, $G\alpha_q$ GPCR phototransduction cascade is reasonably well characterised (for reviews see Hardie & Raghu 2001; Montell 2012). However, upon activation of Rhodopsin, exactly how light information is converted to the photoreceptor voltage response, through action of PLC upon PIP_2, is currently not fully understood.

Previous data has suggested that PIP_2 depletion and the resultant acidification is capable of activating the TRP/TRPL ion channels responsible for producing the light response (Huang et al., 2010). Other work has shown that mechanical forces are capable of activating TRP/TRPL channels and that PIP_2 depletion generates changes in membrane tension, leading to reduced membrane contractility in *Drosophila* photoreceptors (Hardie and Franze, 2012). Whilst further evidence advocates the idea that dietary restriction of Polyunsaturated Fatty Acids (PUFA's) and reinstatement of specific PUFA types are able to modify and rescue the light response, respectively (Chyb et al., 1999).

Drosophila are unable to synthesise PUFAs biologically thus must acquire them through their diet. Randall et al. (2015) suggests that a dietary absence of PUFAs not only reduces photoreceptor contractility, but that it leads to slowing of the photoreceptor voltage response and to slowing of behaviourally-relevant visual perception, as indicated here by the *Drosophila* optomotor response. The paper also shows that for 3rd-generation dietary-

deficient flies, supplementation of the PUFA – Linolenic Acid in the diet (18:3 LNA) is able to rescue these phenotypes under certain conditions.

In addition to showing a close relationship between the electrophysiology and behaviour, together with the aforementioned works, these data serve to show a link between diet and behaviour in *Drosophila* through the biophysical actions and biological function of a class of molecule. These data further support a model of *Drosophila* phototransduction where PIP_2 depletion, acidification, and perhaps the action of DAG metabolites are responsible for activation of TRP/TRPL channels, ultimately directing vision and visual behaviour.

6.2 Methods

6.2.1 Drosophila Genetics

6.2.1.1 Stocks

Wild-type red eyed Oregon Red flies (ROR) were used for control and dietary variance experiments.

6.2.1.2 Diet

Flies kept on a yeast-based diet (YF-Diet) and control flies were reared and fed as per Randall et al. (2015), and were kept on their relative diets for three generations before use. YF-Diet food consisted of; 100 ml tap water, 1 g of agar, 8 g of baker's yeast, 5 g of sucrose, 5 ml of nipagin (2.9%), and 25 mg of β-carotene. Rescue flies (LNA-Rescue) were raised on

an YF-Diet but in their 3rd generation were supplemented with 50 µl/ml of Linolenic Acid (18:3 LNA) before use in the flight simulator.

6.2.2 Flight Simulator

Experiments were carried out on 3-7 day old, female flies reared as previously mentioned, and in the same way as outlined in Chapter 5.

6.3 Results

Here, I recorded open loop *Drosophila* optomotor torque responses using a traditional flight simulator, as described in Chapters 1 and 3. Statistics were carried out on the mean response of each individual fly, for times that corresponded to the peak response, i.e. 2.5-3 s (one-way ANOVA).

6.3.1 Wild-type Oregon Red

In **Fig. 6-1**, red-eyed Oregon Red (ROR) flies responded in a statistically similar fashion to both fast (180 °/s, n = 8) and slow (45 °/s, n = 10) grating rotations despite appearing considerably different by eye (n = 18, one-way ANOVA on the mean variance for the period 2.50-3.00 s, p = 0.177).

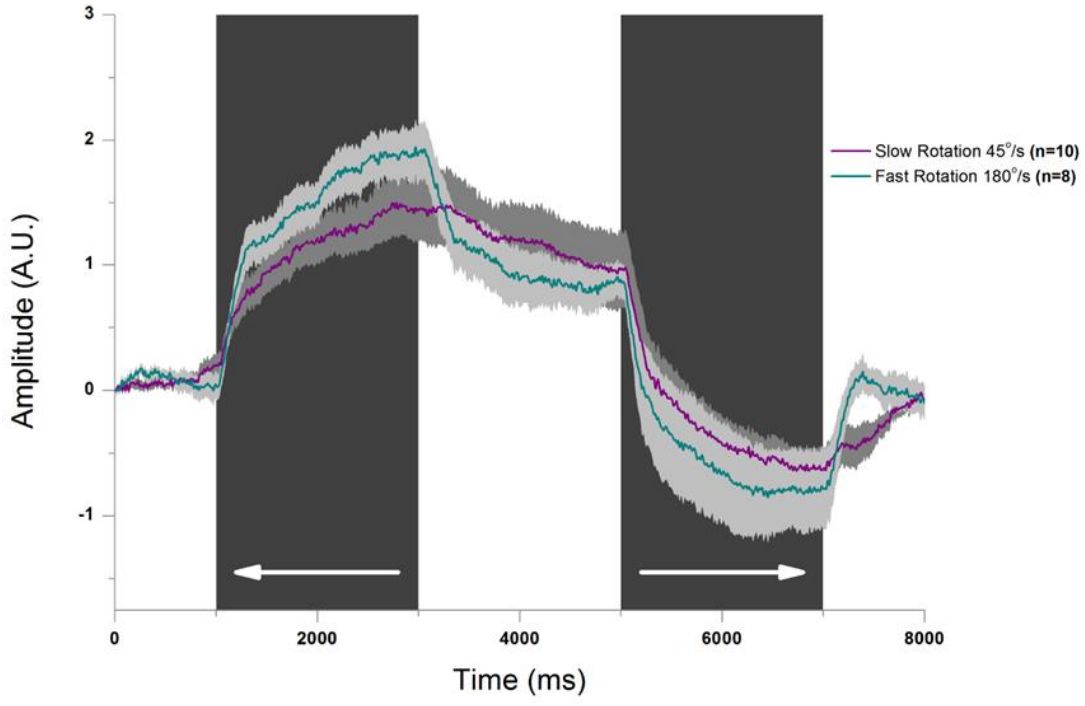

Fig. 6-1- Wild-type, red-eyed Oregon Red (ROR) mean optomotor responses to fast (teal) and slow (purple) grating rotation with broadband illumination. ROR flies prefer fast stimulus rotations, which contrasts with the Canton-S findings in Chapter 5. Here, little variation is seen in either population.

6.3.2 Slow 45°/s Grating Rotation

For slower stimuli (**Fig. 6-2**), where grating bars spend more time in a given region of the visual field, YF-Diet flies showed an appreciably reduced optomotor response as compared with wild-type ROR flies (n = 20, one-way ANOVA, p = 0.05).

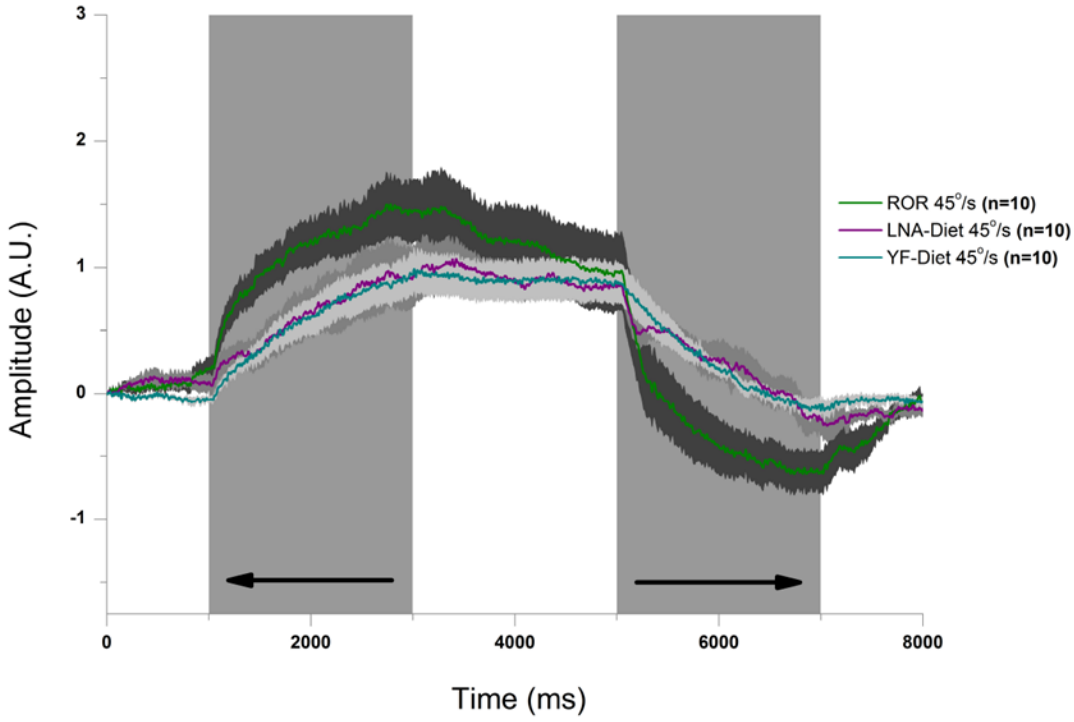

Fig. 6-2 – Mean optomotor responses to slow grating rotation with broadband illumination; from ROR (green), LNA-Diet (purple) and YF-Diet flies (teal). Despite the re-introduction of Linolenic Acid into the diet, there is no significant difference between rescue LNA-diet and YF-Diet flies for slow stimulus rotations, and neither perform as the wild-type ROR control.

However, when evaluating the apparent similarities between LNA-Diet and YF-Diet flies (**Fig. 6-2**), comparison of their response variance showed that such flies were indeed statistically indistinguishable (n = 20, one-way ANOVA, p = 0.90).

Surprisingly, despite appearing substantially different by eye, the responses of LNA-Diet rescue flies, also compared to wild-type, were equally as indistinct (n = 20, one-way ANOVA, p = 0.15).

6.3.3 Fast 180°/s Grating Rotation

When facing a much faster rotational speed (**Fig. 6-3**), a scenario in which flies must be able to respond to higher frequency visual information, YF-Diet flies were much less able to

follow the stimulus, as compared with wild-type ROR flies (n = 18, one-way ANOVA p = 3 x 10^{-6}).

LNA-Diet 'rescue' flies (n = 20, one-way ANOVA p = 0.0001), were also able to respond better than the PUFA-restricted YF-Diet flies.

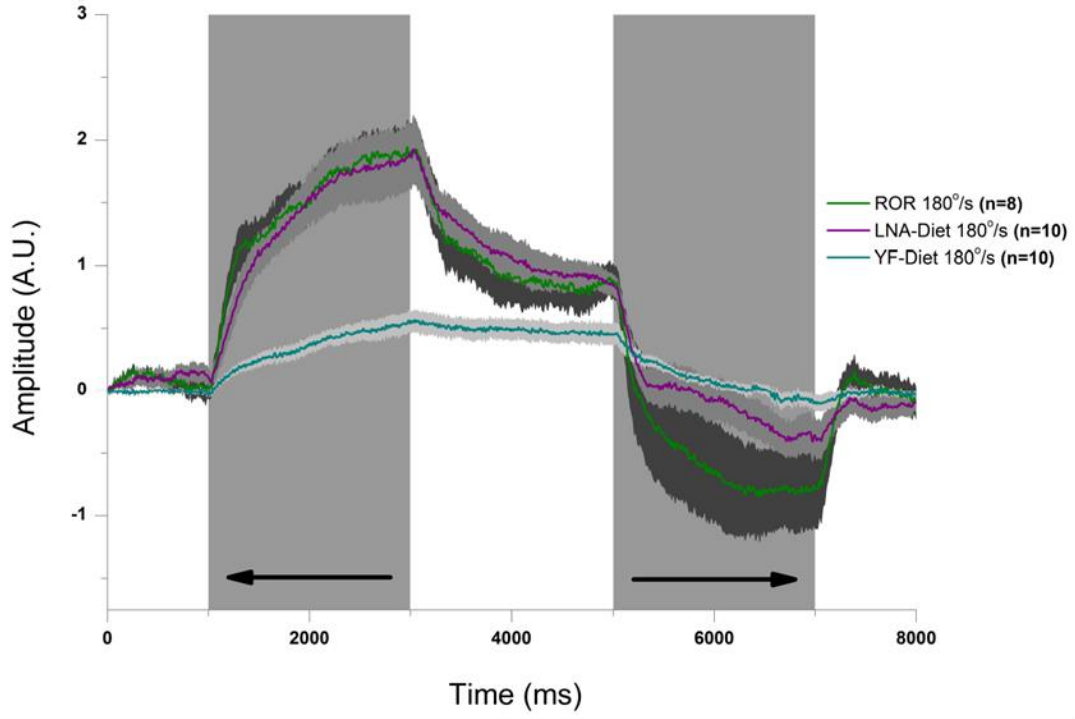

Fig. 6-3 – Mean optomotor responses to fast grating rotation with broadband illumination; from ROR (green), LNA-Diet (purple) and YF-Diet flies (teal). Rescue YF-Diet flies perform equally as well as ROR flies during fast stimulus rotations. Re-introduction of Linolenic Acid into the diet is associated with an increased ability to respond to a stimulus of a higher frequency.

Furthermore, such LNA-Diet flies were equally as capable as ROR flies, suggesting a complete rescue of the behavioural phenotype in this context (n = 18, one-way ANOVA p = 0.841).

6.4 Discussion

Carvalho et al., (2012) showed that changes in the lipid composition of the *Drosophila* diet alters the proportionality of phospholipids in the *Drosophila* head and retina, which appears to correlate with changes in quantum bump timing and phototransduction that affect visual performance and ultimately behaviour (Randall et al., 2015). They go on to suggest that such dietary modification affects the mechanical properties of the photoreceptor membrane, previously indicated in TRPL channel gating (Hardie and Franze, 2012), and that such effects are still present in phototransduction mutants. Here I have attempted to ascertain whether assay of the *Drosophila* optomotor response can be used to support the idea that restriction of dietary PUFA intake can lead to changes in visual information processing that translate further into behavioural dysfunction.

My investigation used 3rd generation flies that had been deprived of all PUFA content in their diet (YF-Diet), along with wild-type, red-eyed Oregon Red flies (ROR) and flies whose diet had been supplemented solely with Linolenic Acid (LNA-Diet); a PUFA whose dietary re-instatement correlated with a significant rescue of quantum bump and photoreceptor voltage response properties, i.e. response time-to-peak, latency, SNR and information transfer rate.

Behaviourally, wild-type ROR flies performed equally well during fast, 180 ^{o}/s and slow, 45 ^{o}/s grating rotation (**Fig. 6-1**); with optomotor responses not appearing to be statistically significant, despite seeming distinct by eye (**Fig. 6-4**). In light of previous findings suggesting that wild-type *Drosophila* respond more strongly to slow stimulation than to fast (Blondeau and Heisenberg, 1982), it is potentially surprising to see that ROR flies seem to respond more robustly to fast grating rotation. However, inter-subject variation at slow speeds may account for this finding.

ROR flies outperformed YF-Diet flies during both fast and slow stimulation (**Figs 6-2, 6-3** & **6-4**). Reflecting the loss of high frequency information in photoreceptor voltage responses to naturalistic stimulation, YF-Diet flies generated poor responses to fast grating rotations, whilst responding more strongly to slow stimulation. Contrastingly, LNA-Diet rescue flies showed stronger responses to fast rotations, performing with similar efficacy to YF-Diet flies during slow grating rotation (**Figs 6-2, 6-3** & **6-4**).

It makes sense that longer latency bump responses, as shown for YF-Diet flies in Randall et al. (2015), will take longer to integrate and photoreceptors will accordingly take longer to surpass their refractoriness (Song et al., 2012). Such protraction of the photoreception process may lead to the generation of a delayed but sustained photoreceptor voltage response, also shown in Randall et al. (2015), ultimately leading to a retardation of the ability to process faster visual input and impairing subsequent visuo-motor coupling.

Given such robust rescue of visual function in the fast rotation condition, and seeing as LNA-Diet flies appear capable of encoding higher frequency stimulus components when presented with a naturalistic light time series, it was unexpected that only ROR flies could statistically outperform YF-Diet flies at slow rotation speeds, despite appearing statistically similar to LNA-Diet flies (**Fig. 6-4**).

Again, such a finding may simply arise from examples of inter-subject variability present between samples for LNA-Diet flies at slow rotation speeds. Thus, LNA-Diet flies may well outperform YF-Diet flies with different subjects.

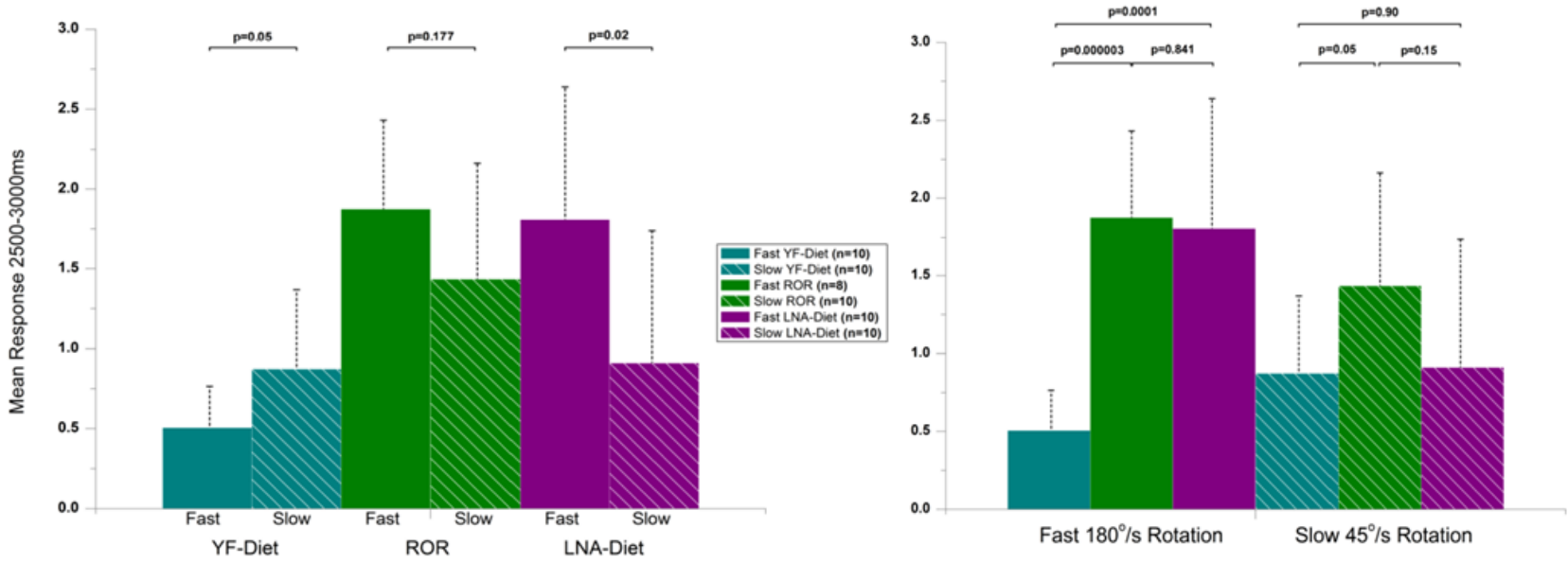

Fig. 6-4 – Mean optomotor responses to fast and slow grating rotation with broadband illumination, for the first peak activity period between 2500-3000ms, with SD – (bars); from ROR (green), LNA-Diet (purple) and YF-Diet flies (teal):

a) Compared within themselves. Both YF-Diet and LNA-Diet show differences between their own responses to fast and slow stimuli.

b) Compared against each other. However, only the rescue LNA-Diet flies are capable of performing similarly to wild-type ROR flies during fast stimulus rotation.

On the other hand, the lipidomic analysis conducted in Randall et al. (2015) shows diet-specific alterations to the prevalence of lipids with different saturation states in the head of *Drosophila*. From such analyses, it is apparent that the relationship between the depletion and rescue of these different PIP_2 species, in flies raised on the PUFA-deprived YF-Diet or the LNA-supplemented diet respectively, is not a linear one; with some species considerably increasing in relative abundance as a result of a decline in others. It may be possible that in the rescue, LNA-Diet flies, such remaining species still highlight a relative imbalance in a necessary proportionality of relevant PIP_2 species, leading to an inability to support approximately normal behaviour at slow rotational speeds or stimulation rates. Thus, YF- and LNA-Diet flies may well behave similarly for slow stimulus paradigms, perhaps because supplementation of Linolenic Acid alone is insufficient to fully restore membrane deficiencies.

To investigate this further, it may be helpful to test for changes in photoreceptor and LMC voltage responses that occur both as a function of diet and changes in light intensity. Such future electrophysiological assay, coupled with additional dietary modifications and variations of optomotor stimulus speed at the flight simulator, might help further elucidate the effects of diet upon the temporal representation of visual information and its relevance to optomotor behaviour.

7 Concluding Remarks:

The *Drosophila* optomotor response is a robust and easily reproducible method by which researchers can ascertain the behavioural relevance of visual-biological components. Moreover, the assay is inexpensive and does not require any highly sophisticated equipment. The optomotor response is generated through the integration of sensory information and motor function, thus can be used to provide an indirect measure of the fidelity of complex visuo-motor neuronal circuit function.

This thesis primarily uses the optomotor response and examples the wide range of visual-behavioural function that it can be used to investigate; from the effects of nutrition on visual behaviour, to the behavioural consequences of failed/altered feedback regulation and the contribution of complex inter-cellular connectivity to the communication of behaviourally-relevant visual information. Each subset of processes co-operates biologically at some level and these contributions have been shown here to be reflected in the fly's behavioural performance.

Furthermore, I have shown that the technique can be used to echo the findings of more direct and reductionist techniques such as electrophysiology, making a case for its use to build a wide-reaching and more holistic picture of the effects of investigation upon visual-behavioural function. So despite being simplistic and decades old, the assay can be an elegant method in the gamut of techniques used to study vision in *Drosophila*.

The use of Electron Microscopy has been of utmost importance to elucidating structural detail in all manner of scientific subjects and for countless purposes within the spectrum of scientific fields. Its ubiquity however, comes with its own set of foibles derived from processing effects, such as subtle morphological changes and protracted fixation durations.

As already evidenced by the work from Eric Jorgensen's laboratory (Watanabe et al., 2013a, 2013b, 2014), the use of High Pressure Freezing with simultaneous light stimulation, combined with subsequent Automatic Freeze Substitution, is going to revolutionise research aimed at the study of membrane trafficking and synaptic transmission. Adapting this technique to study synaptic vesicle dynamics in larger preparations will soon help provide more accurate representations of how adaptive states may be translated through the synapse, from light-driven photoreceptor voltage responses into adapting voltage responses in the post-synaptic LMCs. Future experiments may further exploit developing optogenetic tools, perhaps allowing more precise imaging of activity-dependent changes in synaptic morphology.

Supplementary Figures

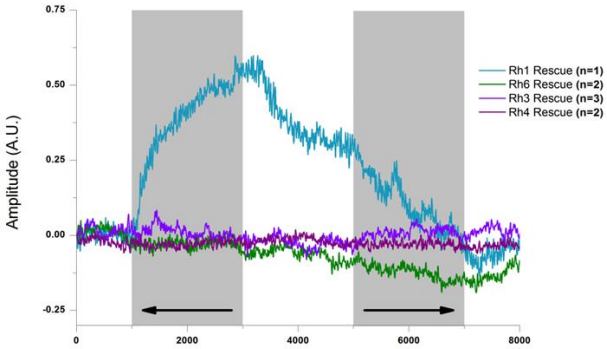

Supp. Fig. 1 – Optomotor responses of Rh1, Rh3, Rh4 & Rh6 norpA rescue flies, each with painted ocelli. 45 °/s grating rotation, illuminated by broadband light (≈380-900nm).

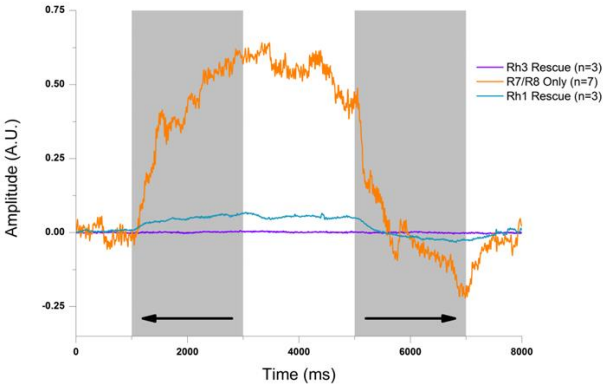

Supp. Fig. 2 – Optomotor responses of Rh1 and Rh3 norpA rescue flies, compared against flies with only R7 & R8 function remaining, all with painted ocelli. 45 °/s grating rotation, illuminated by UV light (≈350-405nm).

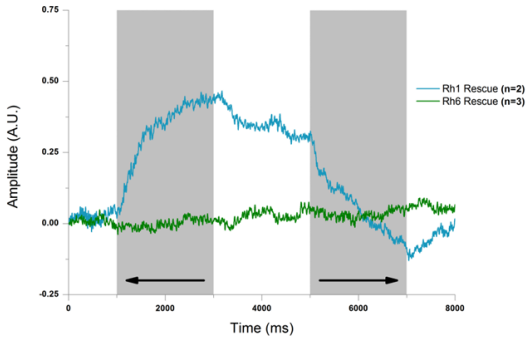

Supp. Fig. 3 – Optomotor responses of Rh1 and Rh6 norpA rescue flies, each with painted ocelli. 45 °/s grating rotation, illuminated by amber light (≈560-620nm).

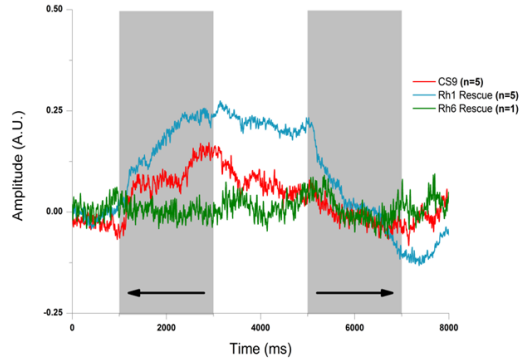

Supp. Fig. 4 – Optomotor responses of Rh1 and Rh6 norpA rescue flies, compared against Canton-S flies, all with painted ocelli. 45 °/s grating rotation, illuminated by red light (≈590-670nm).

Bibliography

Abbott, L.F., LeMasson, G., 1993. Analysis of Neuron Models with Dynamically Regulated Conductances. Neural Comput. 5, 823–842. doi:10.1162/neco.1993.5.6.823

Abou Tayoun, A.N., Li, X., Chu, B., Hardie, R.C., Juusola, M., Dolph, P.J., 2011. The Drosophila SK channel (dSK) contributes to photoreceptor performance by mediating sensitivity control at the first visual network. J. Neurosci. 31, 13897–910. doi:10.1523/JNEUROSCI.3134-11.2011

Adamson, A.L., Shearn, A., 1996. Molecular genetic analysis of Drosophila ash2, a member of the trithorax group required for imaginal disc pattern formation. Genetics 144, 621–33.

Alderson, T., 1965. Chemically Induced Delayed Germinal Mutation in Drosophila. Nature 207, 164–167. doi:10.1038/207164a0

Atkinson, N., Robertson, G., Ganetzky, B., 1991. A component of calcium-activated potassium channels encoded by the Drosophila slo locus. Science (80-.). 253, 551–555. doi:10.1126/science.1857984

Atkinson, N.S., Brenner, R., Chang, W. m, Wilbur, J., Larimer, J.L., Yu, J., 2000. Molecular Separation of Two Behavioral Phenotypes by a Mutation Affecting the Promoters of a Ca-Activated K Channel. J. Neurosci. 20, 2988–93.

Auerbach, C., 1949. Chemical Mutagenesis. Biol. Rev. 24, 355–391. doi:10.1111/j.1469-185X.1949.tb00580.x

Bartolomé-Martín, D., Ramírez-Franco, J., Castro, E., Sánchez-Prieto, J., Torres, M., 2012. Efficient synaptic vesicle recycling after intense exocytosis concomitant with the accumulation of non-releasable endosomes at early developmental stages. J. Cell Sci. 125, 422–34. doi:10.1242/jcs.090878

Bausenwein, B., Dittrich, a. P.M., Fischbach, K.F., 1992. The optic lobe of Drosophila melanogaster: II. Sorting of retinotopic pathways in the medulla. Cell Tissue Res. 267, 17–28. doi:10.1007/BF00318687

Becker, M.N., Brenner, R., Atkinson, N.S., 1995. Tissue-specific expression of a Drosophila calcium-activated potassium channel. J. Neurosci. 15, 6250–9.

Benzer, S., 1967. Behavioural Mutants of Drosophila Isolated by Countercurrent Distribution. Proc. Natl. Acad. Sci. U. S. A. 58, 1112–9.

Bird, M.J., 1951. Chemical Mutagenesis. Drosoph. Inf. Serv. 25, 100.

Blondeau, J., Heisenberg, M., 1982. The three-dimensional optomotor torque system of Drosophila melanogaster - Studies on wildtype and the mutant optomotor-blindH31. J. Comp. Physiol. ??? A 145, 321–329. doi:10.1007/BF00619336

Bloomquist, B.T., Shortridge, R.D., Schneuwly, S., Perdew, M., Montell, C., Steller, H., Rubin, G., Pak, W.L., 1988. Isolation of a putative phospholipase c gene of drosophila, norpA, and its role in phototransduction. Cell 54, 723–733. doi:10.1016/S0092-8674(88)80017-5

Bohm, R.A., Wang, B., Brenner, R., Atkinson, N.S., 2000. Transcriptional control of Ca(2+)-activated K(+) channel expression: identification of a second, evolutionarily conserved, neuronal promoter. J. Exp. Biol. 203, 693–704.

Braitenberg, V., 1967. Patterns of projection in the visual system of the fly. I. Retina-lamina projections. Exp. Brain Res. 3, 271–298. doi:10.1007/BF00235589

Brembs, B., Heisenberg, M., 2001. Conditioning with compound stimuli in Drosophila melanogaster in the flight simulator. J. Exp. Biol. 204, 2849–2859.

Brenner, R., Yu, J.Y., Srinivasan, K., Brewer, L., Larimer, J.L., Wilbur, J.L., Atkinson, N.S., 2000. Complementation of Physiological and Behavioral Defects by a Slowpoke Ca2+ - Activated K+ Channel Transgene. J. Neurochem. 75, 1310–1319. doi:10.1046/j.1471-4159.2000.751310.x

Byzov, A.L., Shura-Bura, T.M., 1986. Electrical feedback mechanism in the processing of signals in the outer plexiform layer of the retina. Vision Res. 26, 33–44. doi:10.1016/0042-6989(86)90069-6

Carvalho, M., Sampaio, J.L., Palm, W., Brankatschk, M., Eaton, S., Shevchenko, A., 2012. Effects of diet and development on the Drosophila lipidome. Mol. Syst. Biol. 8, 600. doi:10.1038/msb.2012.29

Castro, J.P., Carareto, C.M.A., 2004. Drosophila melanogaster P Transposable Elements: Mechanisms of Transposition and Regulation. Genetica 121, 107–118. doi:10.1023/B:GENE.0000040382.48039.a2

Ceccarelli, B., Hurlbut, W.P., Mauro, A., 1973. Turnover of transmitter and synaptic vesicles at the frog neuromuscular junction. J. Cell Biol. 57, 499–524.

Ceccarelli, B., Hurlbut, W.P., Mauro, A., 1972. Depletion of vesicles from frog neuromuscular junctions by prolonged tetanic stimulation. J. Cell Biol. 54, 30–8.

Chou, W.-H., Hall, K.J., Wilson, D.B., Wideman, C.L., Townson, S.M., Chadwell, L. V, Britt, S.G., 1996. Identification of a Novel Drosophila Opsin Reveals Specific Patterning of the R7 and R8 Photoreceptor Cells. Neuron 17, 1101–1115. doi:10.1016/S0896-6273(00)80243-3

Chyb, S., Raghu, P., Hardie, R.C., 1999. Polyunsaturated fatty acids activate the Drosophila light-sensitive channels TRP and TRPL. Nature 397, 255–9. doi:10.1038/16703

Collin, R., 1974. Staining and fixation of unsaturated membrane lipids by osmium tetroxide Crystal structure of a model osmium(VI) di-ester. Biochim. Biophys. Acta - Gen. Subj. 354, 152–154. doi:10.1016/0304-4165(74)90064-6

Collin, R., Griffith, W.P., Phillips, F.L., Skapski, A.C., 1973. Staining and fixation of unsaturated membrane lipids by osmium tetroxide: c rystal structure of a model osmium (VI) intermediate. Biochim. Biophys. Acta - Gen. Subj. 320, 745–747. doi:10.1016/0304-4165(73)90157-8

Cowman, A.F., Zuker, C.S., Rubin, G.M., 1986. An opsin gene expressed in only one photoreceptor cell type of the Drosophila eye. Cell 44, 705–710. doi:0092-8674(86)90836-6 [pii]

Crompton, D.E., Griffin, A., Davies, J.A., Miklos, G.L.G., 1992. Analysis of a cDNA from the neurologically active locus shaking-B (Passover) of Drosophila melanogaster. Gene 122, 385–386. doi:10.1016/0378-1119(92)90233-F

Curtis, H.J., Cole, K.S., 1940. Membrane action potentials from the squid giant axon. J. Cell. Comp. Physiol. 15, 147–157. doi:10.1002/jcp.1030150204

Delgado, R., Bacigalupo, J., 2009. Unitary recordings of TRP and TRPL channels from isolated Drosophila retinal photoreceptor rhabdomeres: activation by light and lipids. J. Neurophysiol. 101, 2372–9. doi:10.1152/jn.90578.2008

Delgado, R., Muñoz, Y., Peña-Cortés, H., Giavalisco, P., Bacigalupo, J., 2014. Diacylglycerol Activates the Light-Dependent Channel TRP in the Photosensitive Microvilli of Drosophila melanogaster Photoreceptors. J. Neurosci. 34, 6679–86. doi:10.1523/JNEUROSCI.0513-14.2014

Elkins, T., Ganetzky, B., Wu, C.F., 1986. A Drosophila mutation that eliminates a calcium-dependent potassium current. Proc. Natl. Acad. Sci. U. S. A. 83, 8415–9.

Estacion, M., Sinkins, W.G., Schilling, W.P., 2001. Regulation of Drosophila transient receptor potential-like (TrpL) channels by phospholipase C-dependent mechanisms. J. Physiol. 530, 1–19.

Faber, E.S.L., Sah, P., 2003. Calcium-activated potassium channels: multiple contributions to neuronal function. Neuroscientist 9, 181–94.

Feiler, R., Bjornson, R., Kirschfeld, K., Mismer, D., Rubin, G.M., Smith, D.P., Socolich, M., Zuker, C.S., 1992. Ectopic expression of ultraviolet-rhodopsins in the blue photoreceptor cells of Drosophila: visual physiology and photochemistry of transgenic animals. J. Neurosci. 12, 3862–3868.

Fischbach, K.-F.-F., Dittrich, A.P.M.P., 1989. The optic lobe of Drosophila melanogaster. I: A. Golgi analysis of wild-type structure. Cell Tissue Res 258, 441–475. doi:doi: 10.1007/BF00218858

Franceschini, N., Kirschfeld, K., Minke, B., 1981. Fluorescence of photoreceptor cells observed in vivo. Science (80-.). 213, 1264–1267. doi:10.1126/science.7268434

Franklin, J.L., Fickbohm, D.J., Willard, A.L., 1992. Long-term regulation of neuronal calcium currents by prolonged changes of membrane potential. J. Neurosci. 12, 1726–35.

Fryxell, K.J., Meyerowitz, E.M., 1987. An opsin gene that is expressed only in the R7 photoreceptor cell of Drosophila. EMBO J. 6, 443–51.

Gandhi, S.P., Stevens, C.F., 2003. Three modes of synaptic vesicular recycling revealed by single-vesicle imaging 423, 607–613.

Gegenfurtner, K.R., Hawken, M.J., 1996. Interaction of motion and color in the visual pathways. Trends Neurosci. 19, 394–401. doi:10.1016/S0166-2236(96)10036-9

Gengs, C., Leung, H.-T., Skingsley, D.R., Iovchev, M.I., Yin, Z., Semenov, E.P., Burg, M.G., Hardie, R.C., Pak, W.L., 2002. The target of Drosophila photoreceptor synaptic transmission is a histamine-gated chloride channel encoded by ort (hclA). J. Biol. Chem. 277, 42113–42120.

Gisselmann, G., Plonka, J., Pusch, H., Hatt, H., 2004. Unusual functional properties of homo- and heteromultimeric histamine-gated chloride channels of Drosophila melanogaster: Spontaneous currents and dual gating by GABA and histamine. Neurosci. Lett. 372, 151–156. doi:10.1016/j.neulet.2004.09.031

Gisselmann, G., Pusch, H., Hovemann, B.T., Hatt, H., 2002. Two cDNAs coding for histamine-gated ion channels in D. melanogaster. Nat. Neurosci. 5, 11–2. doi:10.1038/nn787

Goldsmith, T.H., Barker, R.J., Cohen, C.F., 1964. Sensitivity of Visual Receptors of Carotenoid-Depleted Flies: A Vitamin A Deficiency in an Invertebrate. Science (80-.). 146, 65–67. doi:10.1126/science.146.3640.65

Golowasch, J., Casey, M., Abbott, L.F., Marder, E., 1999. Network stability from activity-dependent regulation of neuronal conductances. Neural Comput. 11, 1079–96.

Gonzalez-Bellido, P.T., Wardill, T.J., Juusola, M., 2011. Compound eyes and retinal information processing in miniature dipteran species match their specific ecological demands. Proc. Natl. Acad. Sci. U. S. A. 108, 4224–4229. doi:10.1073/pnas.1014438108

Götz, K.G., 1968. Flight Control in Drosophila by Visual Perception of Motion. Kybernetik 4, 199–&. doi:10.1007/bf00272517

Götz, K.G., 1964. Optomotorische Untersuchung des visuellen systems einiger Augenmutanten der Fruchtfliege Drosophila. Kybernetik 2, 77–92. doi:10.1007/BF00288561

Grace, A.A., Llinás, R., 1985. Morphological artifacts induced in intracellularly stained neurons by dehydration: Circumvention using rapid dimethyl sulfoxide clearing. Neuroscience 16, 461–475. doi:10.1016/0306-4522(85)90018-1

Graham, F.L., van der Eb, A.J., 1973. A new technique for the assay of infectivity of human adenovirus 5 DNA. Virology 52, 456–467. doi:10.1016/0042-6822(73)90341-3

Graham, J., Gerard, R.W., 1946. Membrane potentials and excitation of impaled single muscle fibers. J. Cell. Comp. Physiol. 28, 99–117. doi:10.1002/jcp.1030280106

Granit, R., 1938. Processes of adaptation in the vertebrate retina in the light of recent photochemical and electrophysiological research. Doc. Ophthalmol. 1. doi:10.1007/BF00196424

Granseth, B., Odermatt, B., Royle, S.J., Lagnado, L., 2009. Comment on "The dynamic control of kiss-and-run and vesicular reuse probed with single nanoparticles". Science 325, 1499; author reply 1499. doi:10.1126/science.1176007

Grimes, W.N., Li, W., Chávez, A.E., Diamond, J.S., 2009. BK channels modulate pre- and postsynaptic signaling at reciprocal synapses in retina. Nat. Neurosci. 12, 585–92. doi:10.1038/nn.2302

Hamdorf, K., Hochstrate, P., Höglund, G., Moser, M., Sperber, S., Schlecht, P., 1992. Ultra-violet sensitizing pigment in blowfly photoreceptors R1-6; probable nature and binding sites. J. Comp. Physiol. A 171. doi:10.1007/BF00194108

Harata, N.C., Aravanis, A.M., Tsien, R.W., 2006. Kiss-and-run and full-collapse fusion as modes of exo-endocytosis in neurosecretion. J. Neurochem. 97, 1546–1570. doi:10.1111/j.1471-4159.2006.03987.x

Hardie, R.C., 2001. Phototransduction in Drosophila melanogaster. J. Exp. Biol. 3409, 3403–3409.

Hardie, R.C., 1979. Electrophysiological analysis of fly retina. I: Comparative properties of R1-6 and R 7 and 8. J. Comp. Physiol. ? A 129, 19–33. doi:10.1007/BF00679908

Hardie, R.C., 1977. Electrophysiological Properties of R7 and R8 in Dipteran Retina. Zeitschrift für Naturforsch. C 32, 887–890. doi:10.1515/znc-1977-9-1038

Hardie, R.C., Franze, K., 2012. Photomechanical responses in Drosophila photoreceptors. Science 338, 260–3. doi:10.1126/science.1222376

Hardie, R.C., Kirschfeld, K., 1983. Ultraviolet sensitivity of fly photoreceptors R7 and R8: Evidence for a sensitising function. Biophys. Struct. Mech. 9, 171–180. doi:10.1007/BF00537814

Hardie, R.C., Peretz, A., Suss-Toby, E., Rom-Glas, A., Bishop, S.A., Selinger, Z., Minke, B., 1993. Protein kinase C is required for light adaptation in Drosophila photoreceptors. Nature 363, 634–7. doi:10.1038/363634a0

Hardie, R.C., Raghu, P., 2001. Visual transduction in Drosophila. Nature 413, 186–193. doi:10.1038/35093002

Hardie, R.C., Raghu, P., 1998. Activation of heterologously expressed Drosophila TRPL channels: Ca2+ is not required and InsP3 is not sufficient. Cell Calcium 24, 153–163. doi:10.1016/S0143-4160(98)90125-7

Hardie, R.C.C., Martin, F., Cochrane, G.W.W., Juusola, M., Georgiev, P., Raghu, P., 2002. Molecular basis of amplification in Drosophila phototransduction: roles for G protein, phospholipase C, and diacylglycerol kinase. Neuron 36, 689–701. doi:10.1016/S0896-6273(02)01048-6

He, L., Xue, L., Xu, J., McNeil, B.D., Bai, L., Melicoff, E., Adachi, R., Wu, L.-G., 2009. Compound vesicle fusion increases quantal size and potentiates synaptic transmission. Nature 459, 93–97. doi:10.1038/nature07860

Heide, G., Götz, K.G., 1996. Optomotor control of course and altitude in Drosophila melanogaster is correlated with distinct activities of at least three pairs of flight steering muscles. J. Exp. Biol. 199, 1711–26.

Heisenberg, M., Buchner, E., 1977. The role of retinula cell types in visual behavior of Drosophila melanogaster. J. Comp. Physiol. A Sensory, Neural, Behav. Physiol. 117, 127–162. doi:10.1007/BF00612784

Heisenberg, M., Wolf, R., 1988a. Reafferent control of optomotor yaw torque inDrosophila melanogaster. J. Comp. Physiol. A 163, 373–388. doi:10.1007/BF00604013

Heisenberg, M., Wolf, R., 1988b. Reafferent Control of Optomotor Yaw Torque in Drosophila melanogaster. J. Comp. Physiol. A Sensory, Neural, Behav. Physiol. 163, 373–388. doi:10.1007/bf00604013

Heisenberg, M., Wolf, R., 1984. Vision in Drosophila. Genetics of microbehaviour. Springer Verlag.

Heisenberg, M., Wolf, R., 1979. On the Fine Structure of Yaw Torque in Visual Flight Orientation of Drosophila melaogaster. J. Comp. Physiol. A Sensory, Neural, Behav. Physiol. 130, 113–130.

Henderson, S.R., Reuss, H., Hardie, R.C., 2000. Single photon responses in Drosophila photoreceptors and their regulation by Ca2+. J. Physiol. 524 Pt 1, 179–194. doi:10.1111/j.1469-7793.2000.00179.x

Heuser, J.E., 1973. Evidence for Recycling of Synaptic Vesicle Membrane During Transmitter Release At the Frog Neuromuscular Junction. J. Cell Biol. 57, 315–344. doi:10.1083/jcb.57.2.315

Hiesinger, P.R., Zhai, R.G., Zhou, Y., Koh, T.-W.W., Mehta, S.Q., Schulze, K.L., Cao, Y., Verstreken, P., Clandinin, T.R., Fischbach, K.-F.F., Meinertzhagen, I. a., Bellen, H.J., 2006. Activity-Independent Prespecification of Synaptic Partners in the Visual Map of Drosophila. Curr. Biol. 16, 1835–1843. doi:10.1016/j.cub.2006.07.047

Hohenberg, H., Mannweiler, K., Muller, M., 1994. High-pressure freezing of cell suspensions in cellulose capillary tubes. J. Microsc. 175, 34–43. doi:10.1111/j.1365-2818.1994.tb04785.x

Holst, E., Mittelstaedt, H., 1971. The principle of reafference: Interactions between the central nervous system and the peripheral organs. PC Dodwell (Ed. Trans.), Percept. Process. Stimul. Equiv. pattern Recognit. 41–72.

Horridge, G.A., Mimura, K., 1975. Fly Photoreceptors. I. Physical Separation of Two Visual Pigments in Calliphora Retinula Cells 1-6. Proc. R. Soc. B Biol. Sci. 190, 211–224. doi:10.1098/rspb.1975.0088

Howard, J., Blakeslee, B., Laughlin, S.B., 1987. The Intracellular Pupil Mechanism and Photoreceptor Signal: Noise Ratios in the Fly Lucilia cuprina. Proc. R. Soc. B Biol. Sci. 231, 415–435. doi:10.1098/rspb.1987.0053

Hu, K.G., Stark, W.S., 1980. The roles of Drosophila ocelli and compound eyes in phototaxis. J. Comp. Physiol. ??? A 135, 85–95. doi:10.1007/BF00660183

Huang, J., Liu, C.-H., Hughes, S.A., Postma, M., Schwiening, C.J., Hardie, R.C., 2010. Activation of TRP channels by protons and phosphoinositide depletion in Drosophila photoreceptors. Curr. Biol. 20, 189–97. doi:10.1016/j.cub.2009.12.019

Huber, A., Schulz, S., Bentrop, J., Groell, C., Wolfrum, U., Paulsen, R., 1997. Molecular cloning of Drosophila Rh6 rhodopsin: the visual pigment of a subset of R8 photoreceptor cells 1The cDNA sequence of the Drosophila Rh6 gene has been submitted to the EMBL data library under accession number Z86118.1. FEBS Lett. 406, 6–10. doi:10.1016/S0014-5793(97)00210-X

Jagadish, S., Barnea, G., Clandinin, T.R., Axel, R., 2014. Identifying functional connections of the inner photoreceptors in Drosophila using Tango-Trace. Neuron 83, 630–44. doi:10.1016/j.neuron.2014.06.025

Jarvilehto, M., Zettler, F., 1971. Localized intracellular potentials from pre- and postsynaptic components in the external plexiform layer of an insect retina. Z. Vgl. Physiol. 75, 422–440. doi:10.1007/BF00630561

Johns, D.C., Marx, R., Mains, R.E., O'Rourke, B., Marban, E., 1999. Inducible Genetic Suppression of Neuronal Excitability. J. Neurosci. 19, 1691–1697.

Johnson, E.C., Pak, W.L., 1986. Electrophysiological study of Drosophila rhodopsin mutants. J. Gen. Physiol. 88, 651–73.

Juusola, M., 1994. Measuring complex admittance and receptor current by single electrode voltage-clamp. J. Neurosci. Methods 53, 1–6.

Juusola, M., French, A.S., Uusitalo, R.O., Weckström, M., 1996. Information processing by graded-potential transmission through tonically active synapses. Trends Neurosci. 19, 292–297.

Juusola, M., Hardie, R.C., 2001. Light adaptation in Drosophila photoreceptors: I. Response dynamics and signaling efficiency at 25 degrees C. J. Gen. Physiol. 117, 3–25.

Juusola, M., Hardie, R.C., 2001. Light adaptation in Drosophila photoreceptors: II. Rising temperature increases the bandwidth of reliable signaling. J. Gen. Physiol. 117, 27–42.

Juusola, M., Uusitalo, R.O., Weckström, M., 1995a. Transfer of graded potentials at the photoreceptor-interneuron synapse. J. Gen. Physiol. 105, 117–148. doi:10.1085/jgp.105.1.117

Juusola, M., Uusitalo, R.O., Weckström, M., 1995b. Transfer of graded potentials at the photoreceptor-interneuron synapse. J. Gen. Physiol. 105, 117–148.

Juusola, M., Weckström, M., Uusitalo, R.O., Korenberg, M.J., French, A.S., 1995c. Nonlinear models of the first synapse in the light-adapted fly retina. J. Neurophysiol. 74, 2538–2547.

Kamermans, M., Fahrenfort, I., 2004. Ephaptic interactions within a chemical synapse: hemichannel-mediated ephaptic inhibition in the retina. Curr. Opin. Neurobiol. 14, 531–41. doi:10.1016/j.conb.2004.08.016

Kamermans, M., Fahrenfort, I., Schultz, K., Janssen-Bienhold, U., Sjoerdsma, T., Weiler, R., 2001. Hemichannel-mediated inhibition in the outer retina. Science 292, 1178–80. doi:10.1126/science.1060101

Karess, R.E., Rubin, G.M., 1984. Analysis of P transposable element functions in Drosophila. Cell 38, 135–146. doi:10.1098/rstb.1984.0123

Kaufman, P.D., Rio, D.C., 1992. P element transposition in vitro proceeds by a cut-and-paste mechanism and uses GTP as a cofactor. Cell 69, 27–39. doi:10.1016/0092-8674(92)90116-T

Kidwell, M.G., Kidwell, J.F., Sved, J.A., 1977. Hybrid Dysgenesis in DROSOPHILA MELANOGASTER: A Syndrome of Aberrant Traits Including Mutation, Sterility and Male Recombination. Genetics 86, 813–33.

Kirschfeld, K., 1979. The function of photostable pigments in fly photoreceptors. Biophys. Struct. Mech. 5, 117–128. doi:10.1007/BF00535442

Kirschfeld, K., 1967. Die projektion der optischen umwelt auf das raster der rhabdomere im komplexauge von Musca. Exp. Brain Res. 3. doi:10.1007/BF00235588

Kirschfeld, K., Feiler, R., Franceschini, N., 1978. A photostable pigment within the rhabdomere of fly photoreceptors no. 7. J. Comp. Physiol. A 125, 275–284. doi:10.1007/BF00656606

Kirschfeld, K., Feiler, R., Hardie, R., Vogt, K., Franceschini, N., 1983. The sensitizing pigment in fly photoreceptors. Biophys. Struct. Mech. 10, 81–92. doi:10.1007/BF00535544

Kirschfeld, K., Franceschini, N., 1969. Ein Mechanismus zur Steuerung des Lichtflusses in den Rhabdomeren des Komplexauges von Musca. Kybernetik 6, 13–22. doi:10.1007/BF00288624

Kirschfeld, K., Franceschini, N., Minke, B., 1977. Evidence for a sensitising pigment in fly photoreceptors. Nature 269, 386–390. doi:10.1038/269386a0

Kirschfeld, K., Snyder, A.W., 1976. Measurement of a photoreceptor's characteristic waveguide parameter. Vision Res. 16, 775–IN5. doi:10.1016/0042-6989(76)90188-7

Klöcker, N., Oliver, D., Ruppersberg, J.P., Knaus, H.G., Fakler, B., 2001. Developmental expression of the small-conductance Ca(2+)-activated potassium channel SK2 in the rat retina. Mol. Cell. Neurosci. 17, 514–20. doi:10.1006/mcne.2000.0956

Klyachko, V. a, Jackson, M.B., 2002. Capacitance steps and fusion pores of small and large-dense-core vesicles in nerve terminals. Nature 418, 89–92. doi:10.1038/nature00852

Kononenko, N.L., Haucke, V., 2015. Molecular mechanisms of presynaptic membrane retrieval and synaptic vesicle reformation. Neuron 85, 484–96. doi:10.1016/j.neuron.2014.12.016

Krapp, H.G., Hengstenberg, R., 1996. Estimation of self-motion by optic flow processing in single visual interneurons. Nature 384, 463–6. doi:10.1038/384463a0

Krishnan, S.N., Frei, E., Schalet, A.P., Wyman, R.J., 1995. Molecular basis of intracistronic complementation in the Passover locus of Drosophila. Proc. Natl. Acad. Sci. U. S. A. 92, 2021–5.

Krishnan, S.N., Frei, E., Swain, G.P., Wyman, R.J., 1993. Passover: A gene required for synaptic connectivity in the giant fiber system of Drosophila. Cell 73, 967–977. doi:10.1016/0092-8674(93)90274-T

Kumar, J.P., Ready, D.F., 1995. Rhodopsin plays an essential structural role in Drosophila photoreceptor development. Development 121, 4359–4370.

Lagrutta, A., Shen, K.Z., North, R.A., Adelman, J.P., 1994. Functional differences among alternatively spliced variants of Slowpoke, a Drosophila calcium-activated potassium channel. J. Biol. Chem. 269, 20347–51.

LaJeunesse, D., Shearn, A., 1995. Trans-regulation of thoracic homeotic selector genes of the Antennapedia and bithorax complexes by the trithorax group genes: absent, small, and homeotic discs 1 and 2. Mech. Dev. 53, 123–139. doi:10.1016/0925-4773(95)00430-0

Laski, F. a, Rio, D.C., Rubin, G.M., 1986. Tissue specificity of Drosophila P element transposition is regulated at the level of mRNA splicing. Cell 44, 7–19. doi:10.1016/0092-8674(86)90480-0

Laughlin, S.B., Howard, J., Blakeslee, B., 1987. Synaptic limitations to contrast coding in the retina of the blowfly Calliphora. Proc. R. Soc. Lond. B. Biol. Sci. 231, 437–467. doi:10.1098/rspb.1987.0054

Lee, J., Ueda, A., Wu, C.-F., 2008. Pre- and post-synaptic mechanisms of synaptic strength homeostasis revealed by slowpoke and shaker K+ channel mutations in Drosophila. Neuroscience 154, 1283–96. doi:10.1016/j.neuroscience.2008.04.043

Li, X., 2011. Information Processing and Distribution in the Fly early Visual System. University of Sheffield.

Ling, G., Gerard, R.W., 1949. The normal membrane potential of frog sartorius fibers. J. Cell. Comp. Physiol. 34, 383–396. doi:10.1002/jcp.1030340304

Liu, L., Wolf, R., Ernst, R., Heisenberg, M., 1999. Context generalization in Drosophila visual learning requires the mushroom bodies. Nature 400, 753–6. doi:10.1038/23456

Loveless, A., 1958. Increased Rate of Plaque-type and Host-range Mutation following Treatment of Bacteriophage in vitro with Ethyl Methane Sulphonate. Nature 181, 1212–1213. doi:10.1038/1811212a0

Marder, E., Goaillard, J.-M., 2006. Variability, compensation and homeostasis in neuron and network function. Nat. Rev. Neurosci. 7, 563–74. doi:10.1038/nrn1949

Masai, I., Okazaki, A., Hosoya, T., Hotta, Y., 1993. Drosophila retinal degeneration A gene encodes an eye-specific diacylglycerol kinase with cysteine-rich zinc-finger motifs and ankyrin repeats. Proc. Natl. Acad. Sci. U. S. A. 90, 11157–61.

McCann, G.D., 1972. Spectral and Polarization Sensitivity of the Dipteran Visual System. J. Gen. Physiol. 59, 534–558. doi:10.1085/jgp.59.5.534

McManus, O.B., 1991. Calcium-activated potassium channels: Regulation by calcium. J. Bioenerg. Biomembr. 23, 537–560. doi:10.1007/BF00785810

Meinertzhagen, I. a, O'Neil, S.D., 1991. Synaptic organization of columnar elements in the lamina of the wild type in Drosophila melanogaster. J. Comp. Neurol. 305, 232–263. doi:10.1002/cne.903050206

Miller, K.D., MacKay, D.J.C., 1994. The Role of Constraints in Hebbian Learning. Neural Comput. 6, 100–126. doi:10.1162/neco.1994.6.1.100

Miller, G. V., Hansen, K.N., Stark, W.S., 1981. Phototaxis in Drosophila: R1–6 input and interaction among ocellar and compound eye receptors. J. Insect Physiol. 27, 813–819. doi:10.1016/0022-1910(81)90073-1

Misra, S., Buratowski, R.M., Ohkawa, T., Rio, D.C., 1993. Cytotype control of Drosophila melanogaster P element transposition: Genomic position determines maternal repression. Genetics 135, 785–800.

Montell, C., 2012. Drosophila visual transduction. Trends Neurosci. 35, 356–63. doi:10.1016/j.tins.2012.03.004

Montell, C., Jones, K., Hafen, E., Rubin, G., 1985. Rescue of the Drosophila phototransduction mutation trp by germline transformation. Science 230, 1040–3.

Montell, C., Jones, K., Zuker, C., Rubin, G., 1987. A second opsin gene expressed in the ultraviolet-sensitive R7 photoreceptor cells of Drosophila melanogaster. J. Neurosci. 7, 1558–66.

Moor, H., Bellin, G., Sandri, C., Akert, K., 1980. The influence of high pressure freezing on mammalian nerve tissue. Cell Tissue Res. 209. doi:10.1007/BF00237626

Morante, J., Desplan, C., 2008. The Color-Vision Circuit in the Medulla of Drosophila. Curr. Biol. 18, 553–565. doi:10.1016/j.cub.2008.02.075

Muller, H.J., 1927. Artificial Transmutation of the Gene. Science 66, 84–7. doi:10.1126/science.66.1699.84

Mun, J.Y., Kim, M.C., Eum, J.H., Studer, D., HAN, S.S., 2005. Modified Plunge Freezing Method Applied to Retinal Cells of Drosophila melanogaster for the Ultrastructure Close to the Living State. Microsc. Microanal. 11, 1182–1183. doi:10.1017/S1431927605500941

Nägerl, U.V., Triller, A. (Eds.), 2014. Nanoscale Imaging of Synapses, Neuromethods. Springer New York, New York, NY. doi:10.1007/978-1-4614-9179-8

Nastuk, W.L., Hodgkin, A.L., 1950. The electrical activity of single muscle fibers. J. Cell. Comp. Physiol. 35, 39–73. doi:10.1002/jcp.1030350105

Nelson, S.B., Turrigiano, G.G., 2008. Strength through Diversity. Neuron 60, 477–482. doi:10.1016/j.neuron.2008.10.020

Niemeyer, B.A., Suzuki, E., Scott, K., Jalink, K., Zuker, C.S., 1996. The Drosophila Light-Activated Conductance Is Composed of the Two Channels TRP and TRPL. Cell 85, 651–659. doi:10.1016/S0092-8674(00)81232-5

Nikolaev, A., Zheng, L., Wardill, T.J., O'Kane, C.J., de Polavieja, G.G., Juusola, M., 2009. Network Adaptation Improves Temporal Representation of Naturalistic Stimuli in Drosophila Eye: II Mechanisms. PLoS One 4, e4306. doi:10.1371/journal.pone.0004306

Niven, J.E., Vahasoyrinki, M., Juusola, M., 2003a. Shaker K(+)-channels are predicted to reduce the metabolic cost of neural information in Drosophila photoreceptors. Proc Biol Sci 270 Suppl , S58–61. doi:10.1098/rsbl.2003.0010

Niven, J.E., Vahasoyrinki, M., Kauranen, M., Hardie, R.C., Juusola, M., Weckstrom, M., 2003b. The contribution of Shaker K+ channels to the information capacity of Drosophila photoreceptors. Nature 421, 630–634. doi:10.1038/nature01384

O'Tousa, J.E., Baehr, W., Martin, R.L., Hirsh, J., Pak, W.L., Applebury, M.L., 1985. The Drosophila ninaE gene encodes an opsin. Cell 40, 839–850. doi:10.1016/0092-8674(85)90343-5

Ogden, D., 1994. Microelectrode Techniques: The Plymouth Workshop Handbook, 2nd Editio. ed. Company of Biologists.

Palmer, A.E., Qin, Y., Park, J.G., McCombs, J.E., 2011. Design and application of genetically encoded biosensors. Trends Biotechnol. 29, 144–152. doi:10.1016/j.tibtech.2010.12.004

Pantazis, A., Segaran, A., Liu, C.-H., Nikolaev, A., Rister, J., Thum, A.S., Roeder, T., Semenov, E., Juusola, M., Hardie, R.C., 2008. Distinct roles for two histamine receptors (hclA and hclB) at the Drosophila photoreceptor synapse. J. Neurosci. 28, 7250–7259.

Papatsenko, D., Sheng, G., Desplan, C., 1997. A new rhodopsin in R8 photoreceptors of Drosophila: evidence for coordinate expression with Rh3 in R7 cells. Development 124, 1665–73.

Park, Y.B., 1994. Ion selectivity and gating of small conductance Ca(2+)-activated K+ channels in cultured rat adrenal chromaffin cells. J. Physiol. 481 (Pt 3, 555–70.

Parsons, M.M., Krapp, H.G., Laughlin, S.B., 2010. Sensor fusion in identified visual interneurons. Curr. Biol. 20, 624–8. doi:10.1016/j.cub.2010.01.064

Pearn, M.T., Randall, L.L., Shortridge, R.D., Burg, M.G., Pak, W.L., 1996. Molecular, Biochemical, and Electrophysiological Characterization of. Biochemistry 271, 4937–4945. doi:10.1074/jbc.271.9.4937

Pellicer, A., Robins, D., Wold, B., Sweet, R., Jackson, J., Lowy, I., Roberts, J., Sim, G., Silverstein, S., Axel, R., 1980. Altering genotype and phenotype by DNA-mediated gene transfer. Science (80-.). 209, 1414–1422. doi:10.1126/science.7414320

Phelan, P., Stebbings, L.A., Baines, R.A., Bacon, J.P., Davies, J.A., Ford, C., 1998. Drosophila Shaking-B protein forms gap junctions in paired Xenopus oocytes. Nature 391, 181–4. doi:10.1038/34426

Philpot, B.D., Cho, K.K.A., Bear, M.F., 2007. Obligatory Role of NR2A for Metaplasticity in Visual Cortex. Neuron 53, 495–502. doi:10.1016/j.neuron.2007.01.027

Prinz, A.A., Bucher, D., Marder, E., 2004. Similar network activity from disparate circuit parameters. Nat. Neurosci. 7, 1345–52. doi:10.1038/nn1352

Raghu, P., Colley, N.J., Webel, R., James, T., Hasan, G., Danin, M., Selinger, Z., Hardie, R.C., 2000. Normal phototransduction in Drosophila photoreceptors lacking an InsP(3) receptor gene. Mol. Cell. Neurosci. 15, 429–45. doi:10.1006/mcne.2000.0846

Raghu, P., Usher, K., Jonas, S., Chyb, S., Polyanovsky, A., Hardie, R.C., 2000. Constitutive Activity of the Light-Sensitive Channels TRP and TRPL in the Drosophila Diacylglycerol Kinase Mutant, rdgA. Neuron 26, 169–179. doi:10.1016/S0896-6273(00)81147-2

Randall, A.S., Liu, C.-H., Chu, B., Zhang, Q., Dongre, S.A., Juusola, M., Franze, K., Wakelam, M.J.O., Hardie, R.C., 2015. Speed and sensitivity of phototransduction in Drosophila depend on degree of saturation of membrane phospholipids. J. Neurosci. 35, 2731–46. doi:10.1523/JNEUROSCI.1150-14.2015

Reuss, H., Mojet, M.H., Chyb, S., Hardie, R.C., 1997. In Vivo Analysis of the Drosophila Light-Sensitive Channels, TRP and TRPL. Neuron 19, 1249–1259. doi:10.1016/S0896-6273(00)80416-X

REYNOLDS, E.S., 1963. The use of lead citrate at high pH as an electron-opaque stain in electron microscopy. J. Cell Biol. 17, 208–12.

Rio, D.C., Laski, F. a, Rubin, G.M., 1986. Identification and immunochemical analysis of biologically active Drosophila P element transposase. Cell 44, 21–32. doi:10.1016/0092-8674(86)90481-2

Rubin, G.M., Spradling, A.C., 1982. Genetic transformation of Drosophila with transposable element vectors. Science 218, 348–53.

Ruck, P., 1962. On Photoreceptor Mechanisms of Retinula Cells on JSTOR [WWW Document]. Biol. Bull.

Ryan, T. a, Smith, S.J., Reuter, H., 1996. The timing of synaptic vesicle endocytosis. Proc. Natl. Acad. Sci. U. S. A. 93, 5567–5571. doi:10.1073/pnas.93.11.5567

Schaffner, W., 1980. Direct transfer of cloned genes from bacteria to mammalian cells. Proc. Natl. Acad. Sci. U. S. A. 77, 2163–7.

Schnaitmann, C., Garbers, C., Wachtler, T., Tanimoto, H., 2013. Color discrimination with broadband photoreceptors. Curr. Biol. 23, 2375–82. doi:10.1016/j.cub.2013.10.037

Sénatore, S., Rami Reddy, V., Sémériva, M., Perrin, L., Lalevée, N., 2010. Response to mechanical stress is mediated by the TRPA channel painless in the Drosophila heart. PLoS Genet. 6, e1001088. doi:10.1371/journal.pgen.1001088

Shaw, S.R., Fröhlich, A., Meinertzhagen, I.A., Fröhlich, A., Meinertzhagen, I.A., 1989. Direct connections between the R7/8 and R1-6 photoreceptor subsystems in the dipteran visual system. Cell Tissue Res. 257, 295–302. doi:10.1007/BF00261833

Smith, D., Ranganathan, R., Hardy, R., Marx, J., Tsuchida, T., Zuker, C., 1991. Photoreceptor deactivation and retinal degeneration mediated by a photoreceptor-specific protein kinase C. Science (80-.). 254, 1478–1484. doi:10.1126/science.1962207

Smith, J.E., Reese, T.S., 1980. Use of aldehyde fixatives to determine the rate of synaptic transmitter release. J. Exp. Biol. 89, 19–29.

Song, Z., Juusola, M., 2014. Refractory sampling links efficiency and costs of sensory encoding to stimulus statistics. J. Neurosci. 34, 7216–37. doi:10.1523/JNEUROSCI.4463-13.2014

Song, Z., Postma, M., Billings, S. a., Coca, D., Hardie, R.C., Juusola, M., 2012. Stochastic, adaptive sampling of information by microvilli in fly photoreceptors. Curr. Biol. 22, 1371–1380. doi:10.1016/j.cub.2012.05.047

Spradling, A.C., Stern, D.M., Kiss, I., Roote, J., Laverty, T., Rubin, G.M., 1995. Gene disruptions using P transposable elements: an integral component of the Drosophila genome project. Proc. Natl. Acad. Sci. U. S. A. 92, 10824–30.

Stark, W.S., Carlson, S.D., 1986. Ultrastructure of capitate projections in the optic neuropil of Diptera. Cell Tissue Res. 246, 481–486.

Steinert, J.R., Kuromi, H., Hellwig, A., Knirr, M., Wyatt, A.W., Kidokoro, Y., Schuster, C.M., 2006. Experience-Dependent Formation and Recruitment of Large Vesicles from Reserve Pool. Neuron 50, 723–733. doi:10.1016/j.neuron.2006.04.025

Strausfeld, N.J., 1971. The organization of the insect visual system (Light microscopy). Zeitschrift für Zellforsch. und Mikroskopische Anat. 121, 377–441. doi:10.1007/BF00337640

Strausfeld, N.J., Lee, J.-K., 2009. Neuronal basis for parallel visual processing in the fly. Vis. Neurosci. 7, 13. doi:10.1017/S0952523800010919

Strauss, R., Renner, M., Götz, K., 2001. Task-specific association of photoreceptor systems and steering parameters in Drosophila. J. Comp. Physiol. - A Sensory, Neural, Behav. Physiol. 187, 617–632. doi:10.1007/s003590100234

Stryer, L., Hurley, J.B., Fung, B.K.-K., 1981. Transducin: an amplifier protein in vision. Trends Biochem. Sci. 6, 245–247. doi:10.1016/0968-0004(81)90089-X

Studer, D., Humbel, B.M., Chiquet, M., 2008. Electron microscopy of high pressure frozen samples: bridging the gap between cellular ultrastructure and atomic resolution. Histochem. Cell Biol. 130, 877–89. doi:10.1007/s00418-008-0500-1

Südhof, T.C., Rizo, J., 2011. Synaptic vesicle exocytosis. Cold Spring Harb. Perspect. Biol. 3, a005637. doi:10.1101/cshperspect.a005637

Takemura, S.-Y., Lu, Z., Meinertzhagen, I.A., 2008. Synaptic circuits of the Drosophila optic lobe: the input terminals to the medulla. J. Comp. Neurol. 509, 493–513.

Theobald, J.C., Ringach, D.L., Frye, M.A., 2010. Dynamics of optomotor responses in Drosophila to perturbations in optic flow. J. Exp. Biol. 213, 1366–1375. doi:10.1242/jeb.037945

Thijssen; Van Went; Van Aelst, 1998. Heptane and isooctane as embedding fluids for high-pressure freezing of Petunia ovules followed by freeze-substitution. J. Microsc. 192, 228–235. doi:10.1046/j.1365-2818.1998.00385.x

Tomlinson, A., 2012. The origin of the Drosophila subretinal pigment layer. J. Comp. Neurol. 520, 2676–82. doi:10.1002/cne.23063

Trujillo-Cenóz, O., 1965. Some aspects of the structural organization of the intermediate retina of dipterans. J. Ultrastruct. Res. 13, 1–33. doi:10.1016/S0022-5320(65)80086-7

Uusitalo, R.O., Juusola, M., Kouvalainen, E., Weckström, M., 1995. Tonic transmitter release in a graded potential synapse. J. Neurophysiol. 74, 470–473.

Uusitalo, R.O., Weckström, M., 2000. Potentiation in the first visual synapse of the fly compound eye. J. Neurophysiol. 83, 2103–12.

Vogt, K., 1983. Is the Fly Visual Pigment a Rhodopsin? Zeitschrift für Naturforsch. C 38, 329–333. doi:10.1515/znc-1983-3-428

Vroman, R., Klaassen, L.J., Kamermans, M., 2013. Ephaptic communication in the vertebrate retina. Front. Hum. Neurosci. 7, 612. doi:10.3389/fnhum.2013.00612

Wardill, T.J., List, O., Li, X., Dongre, S., McCulloch, M., Ting, C.-Y., O'Kane, C.J., Tang, S., Lee, C.-H., Hardie, R.C., Juusola, M., 2012. Multiple Spectral Inputs Improve Motion Discrimination in the Drosophila Visual System. Science (80-.). 336, 925–931. doi:10.1126/science.1215317

Wardill, T.J., List, O., Li, X., Dongre, S., McCulloch, M., Ting, C.-Y.Y., O'Kane, C.J., Tang, S., Lee, C.-H.H., Hardie, R.C., Juusola, M., 2012. Multiple spectral inputs improve motion discrimination in the Drosophila visual system. Supp. Science (80-.). 336, Supplement. doi:10.1126/science.1215317

Watanabe, S., Liu, Q., Davis, M.W., Hollopeter, G., Thomas, N., Jorgensen, N.B., Jorgensen, E.M., 2013a. Ultrafast endocytosis at Caenorhabditis elegans neuromuscular junctions. Elife 2, e00723. doi:10.7554/eLife.00723

Watanabe, S., Rost, B.R., Camacho-Pérez, M., Davis, M.W., Söhl-Kielczynski, B., Rosenmund, C., Jorgensen, E.M., 2013b. Ultrafast endocytosis at mouse hippocampal synapses. Nature 504, 242–7. doi:10.1038/nature12809

Watanabe, S., Trimbuch, T., Camacho-Pérez, M., Rost, B.R., Brokowski, B., Söhl-Kielczynski, B., Felies, A., Davis, M.W., Rosenmund, C., Jorgensen, E.M., Watanabe, S., Trimbuch, T., Camacho-pe, M., 2014. Clathrin regenerates synaptic vesicles from endosomes. Nature 515, 228–233. doi:10.1038/nature13846

Weckström, M., Kouvalainen, E., Juusola, M., 1992. Measurement of cell impedance in frequency domain using discontinuous current clamp and white-noise-modulated current injection. Pflugers Arch. Eur. J. Physiol. 421, 469–472.

Williams, H., Noble, J., 2007. Homeostatic plasticity improves signal propagation in continuous-time recurrent neural networks. Biosystems 87, 252–259. doi:10.1016/j.biosystems.2006.09.020

Wolf, R., Heisenberg, M., 1990. Visual control of straight flight in Drosophila melanogaster. J. Comp. Physiol. A 167. doi:10.1007/BF00188119

Yamaguchi, S., Wolf, R., Desplan, C., Heisenberg, M., 2008. Motion vision is independent of color in Drosophila. Proc. Natl. Acad. Sci. U. S. A. 105, 4910–5. doi:10.1073/pnas.0711484105

Yu, J.Y., Upadhyaya, A.B., Atkinson, N.S., 2006. Tissue-specific alternative splicing of BK channel transcripts in Drosophila. Genes. Brain. Behav. 5, 329–39. doi:10.1111/j.1601-183X.2005.00164.x

Zhang, Q., Li, Y., Tsien, R.W., 2009. The dynamic control of kiss-and-run and vesicular reuse probed with single nanoparticles. Science 323, 1448–53. doi:10.1126/science.1167373

Zheng, L., de Polavieja, G.G., Wolfram, V., Asyali, M.H., Hardie, R.C., Juusola, M., 2006. Feedback network controls photoreceptor output at the layer of first visual synapses in Drosophila. J. Gen. Physiol. 127, 495–510. doi:10.1085/jgp.200509470

Zheng, L., Nikolaev, A., Wardill, T.J., O'Kane, C.J., Polavieja, G.G. de, Juusola, M., de Polavieja, G.G., Juusola, M., 2009. Network Adaptation Improves Temporal Representation of Naturalistic Stimuli in Drosophila Eye: I Dynamics. PLoS One 4, e4307. doi:10.1371/journal.pone.0004307

Zheng, Y., Hirschberg, B., Yuan, J., Wang, A.P., Hunt, D.C., Ludmerer, S.W., Schmatz, D.M., Cully, D.F., 2002. Identification of two novel Drosophila melanogaster histamine-gated

chloride channel subunits expressed in the eye. J. Biol. Chem. 277, 2000–2005. doi:10.1074/jbc.M107635200

Zuker, C.S., Cowman, A.F., Rubin, G.M., 1985. Isolation and structure of a rhodopsin gene from D. melanogaster. Cell 40, 851–858. doi:10.1016/0092-8674(85)90344-7

Zuker, C.S., Montell, C., Jones, K., Laverty, T., Rubin, G.M., 1987. A rhodopsin gene expressed in photoreceptor cell R7 of the Drosophila eye: homologies with other signal-transducing molecules. J. Neurosci. 7, 1550–7.

Appendix – Published Manuscripts

1. **Wardill, T.J., List, O., Li, X., Dongre, S., McCulloch, M., Ting, C.-Y., O'Kane, C.J., Tang, S., Lee, C.-H., Hardie, R.C., Juusola, M., 2012.** Multiple Spectral Inputs Improve Motion Discrimination in the Drosophila Visual System. **Science (80-.). 336, 925–931.**

2. **Randall, A.S., Liu, C.-H., Chu, B., Zhang, Q., Dongre, S.A., Juusola, M., Franze, K., Wakelam, M.J.O., Hardie, R.C., 2015.** Speed and sensitivity of phototransduction in Drosophila depend on degree of saturation of membrane phospholipids. **J. Neurosci. 35, 2731–46.**